EXTRACTION OF ALUMINIUM FROM COAL FLY ASH USING A TWO-STEP ACID LEACH PROCESS

Alan Shemi

A dissertation submitted to the faculty of Engineering and the Built Environment, University of Witwatersrand, Johannesburg, in fulfillment of the requirements for the degree of Master of Science in Engineering

DECLARATION

I declare that this dissertation is my own unaided work. It is being submitted to the degree of Master of Science in Engineering to the University of the Witwatersrand, Johannesburg. It has not been submitted before for any other degree or examination in any other University.

Alan Shemi

14th Day of May 2013

ABSTRACT

Hydrometallurgical extraction technologies provide a process route for resource recovery of valuable metals from both primary as well as secondary resources. In this study, the possibility of treating coal fly ash (CFA), a residue formed as a result of coal combustion in coal-fired power plants, was investigated. Eskom CFA contains significant amounts of alumina typically, 26-31%, in two dissimilar phases, namely amorphous and crystalline mullite, which may be processed separately. Due to its high silica content, however, CFA cannot be treated through the Bayer process route. Therefore, a leach-sinter-leach process was formulated that employed a two-step acid leach technique to extract alumina from CFA using sulphuric acid.

In the preliminary test work, the effect of parameters on CFA leaching characteristics was investigated. From the experimental results, appropriate factor levels were found to be 6M acid concentration, 6 hours leaching time, 75°C temperature and 1:4 solid to liquid ratio. Calcium sulphate precipitate formation was found to inhibit aluminium extraction and activation energy-based kinetic results showed that aluminium extraction from CFA was a product diffusion layer controlled mechanism.

By leaching the CFA, and using design of experiments (DOE) and response surface methodology strategy for screening and optimization of significant factors, it was found that temperature and leaching time significantly influence the aluminium extraction process. The theoretical optimum conditions established from the statistically based optimization model, for a maximum aluminium extraction of 23.9%, was found to be a temperature of 82°C and a leaching time of 10.2 hrs.

Using the optimum conditions, the first stage leaching was done, followed by sintering at 1150°C for 180 minutes to liberate the mullite phase aluminium and then second stage leaching. An aluminium extraction of 24.8%, representing 89.3% extraction from the CFA amorphous phase, was obtained from first stage leaching. The second stage leaching yielded an aluminium extraction of 84.3%. A combination of the two leaching stages gave a total aluminium extraction of 88.2%.

This work has shown that by employing a leach-sinter-leach method based on a two-step acid leach technique, CFA can be optimally leached.

PUBLICATIONS AND PRESENTATIONS

This work has produced some publications.

Journal Publications

1. Shemi, A., Mpana, R.N., Ndlovu, S., van Dyk, L.D., Sibanda, V., Seepe, L., 2012. Alternative techniques for extracting alumina from coal fly ash. Minerals Engineering 34, pp. 30-37.

Conference Proceedings

1. Shemi, A., Ndlovu, S., Sibanda, V., van Dyk, L.D., 2012. Extraction of alumina from coal fly ash: Identification and Optimization of Influential Factors: Anglo American Hydrometallurgy Symposium, University of Cape Town, South Africa, 29th July – 1st August, 2012.

2. Shemi, A., Ndlovu, S., Sibanda, V., van Dyk, L.D., Mpana, R.N., Seepe, L., 2011. Coal fly ash as an alternative source of smelter grade alumina: A comparison of aluminium extraction techniques. The 6th International Conference of the African Materials Research Society, Victoria Falls, Zimbabwe, 11th – 16th December 2011.

3. Sibanda, V., Ndlovu, S., van Dyk, L.D., Shemi, A., Mpana, R.N., 2011. Alternative techniques for extracting alumina from coal fly ash: Conference of metallurgists (COM) 2011, Montreal Canada, 2nd – 5th October 2011.

DEDICATION

Dedicated to

my lovely wife, Alice and three children, Ettric, Lerato and Elvin for their understanding and support

ACKNOWLEDGEMENTS

I wish to express my special gratitude to my supervisor Prof. S. Ndlovu, for the many inspirational discussions, insight and technical guidance throughout this work. My sincere gratitude goes to my co-supervisors Dr. V. Sibanda and Dr. L. VanDyk for their many helpful suggestions and technical support.

Kendal Power Plant, a division of Eskom (RSA), is gratefully acknowledged for the coal fly ash used in this study.

The National Research Foundation of South Africa and Carnegie are gratefully acknowledged for their financial contribution to the research.

Birkenmayer (Pty) Ltd is gratefully acknowledged for helping with the pelletization of coal fly ash.

While many other persons have contributed either directly or indirectly to this work, I should like to mention some of them by name: Dr. M. Bwalya, Geoffrey Simate, Bruce Mothibedi and Steyn Herman, many thanks for their continued interest and support.

Finally, special thanks to the Metals Extraction and Recovery Research Group (MERG) for team work.

Table of Contents

LIST OF FIGURES

LIST OF FIGURES (CONTINUED)

LIST OF TABLES

LIST OF TABLES (CONTINUED)

CHAPTER ONE

INTRODUCTION

1.1 Introduction

Coal fly ash (CFA), formed as a result of coal combustion in coal-fired power plants, typically contains about 26-31% alumina (Al_2O_3), possibly second only to bauxite in alumina content. Bauxite, a naturally occurring alumina ore, contains about 30-60% (Authier-Martin et al., 2001) alumina and is the chief source for aluminium in the world. Although South Africa has no exploitable high grade bauxite ore deposits, it has readily available aluminium smelters and feedstock is sourced from countries abroad like Australia. The potential of developing other alternative sources of alumina such as CFA would provide a significant source of raw material for the local smelters. This would cut down on alumina import costs and has the potential to unlock large tonnage of previously unavailable raw material.

Coal-combustion-based electric power is the major source of electricity generation in South Africa and Eskom is the main power utility and the chief producer of CFA (Maleka et al., 2010). There are 15 coal-fired power stations in the country that generate about 89.1% of Eskom's electric power capacity. In similar fashion, CFA is produced in millions of tonnes every year, world-wide, from the burning of pulverized coal to heat boilers, which in turn drive generators to produce electricity. In 2001(Landman, 2003), it was estimated that 27 million tonnes of CFA was generated by Eskom alone and the trend is going upwards. Current available CFA stock is estimated at not less than 500 million tonnes. As long as the main source of electric-power is coal-combustion-based, South Africa's generation of CFA is inevitable and is bound to increase with increase in demand for electricity.

CFA disposal has increasingly become an environmental concern. Most of the CFA produced from the power plants is being disposed of in controlled landfills or waste containment facilities. Only a small portion, about 20%, of CFA collected in South Africa is re-used for productive purposes and this is primarily for construction-related applications (Landman, 2003). By contrast, other industrialized countries have had much higher utilization rates in construction and

non-construction related applications: Germany, 80%; France, 65%; and the United Kingdom, 55%.

South African CFA contains metals as both major and minor constituents and is capable of becoming an inexpensive secondary source of metals, thus serving as a national resource and alleviating the waste-disposal problem. This, coupled with the increasing landfill costs, stricter implementation and enforcement of environmental legislation, has caused the scientific community to focus on finding innovative methods of CFA utilization. Processing the ash for metals recovery would have the following benefits, (1) significantly reduce volume of ash for disposal thus realizing savings on disposal and landfill costs, (2) lessen the potential for environmental damage, (3) supplement alumina feedstock, therefore, generating revenue from aluminium production and (4) stimulate entrepreneurial activity and boost economic growth.

CFA from Eskom power plants typically contains: SiO_2 (56.1wt %), Al_2O_3 (30.52wt %), Fe_2O_3 (0.4wt %), FeO (3.25wt %), CaO (5.03wt %), TiO_2 (1.67wt %). Alumina (Al_2O_3) is present as the second major constituent after silica (SiO_2) and is therefore amenable to metallurgical and chemical processes of recovery such as acid or base leaching, precipitation, solvent extraction, crystallization and calcination. The mineralogy of CFA (**Table 1.1**) consists of two alumina phases; the non-crystalline amorphous phase and the crystalline mullite phase (Nayak and Chitta, 2009; Matjie et al., 2005). Mullite is a solid solution compound of alumina and silica with a chemical formula as $3Al_2O_3{\cdot}2SiO_2$ (Duval et al., 2008) whereas the amorphous phase is not a single compound defined by one chemical formula. The amorphous phase in CFA is a mixture of metal oxides one of which is aluminium oxide (Loubser and Verryn, 2008).

Table 1.1 Mineralogical analysis of Eskom CFA

CFA	Phase (wt %)	Al_2O_3 (wt %)
Amorphous	52.9	27.8
Hematite	0.8	-
Magnetite	1.65	-
Mullite	30.68	72.2
Quartz	13.97	-

The crystalline mullite phase is acid-insoluble and aluminium in this phase cannot easily be recovered whilst the non-crystalline amorphous phase is acid-soluble and aluminium can thus easily be recovered by direct acid leaching (Nayak and Chitta, 2009; Kelmers et al., 1982). Acid leaching routes for processing CFA or alumina bearing clays are generally preferred mainly because they allow good solubilization of alumina and have an advantage that silica is substantially insoluble in acid (Nayak and Chitta, 2009; Shcherban et al., 1995) unlike alkaline routes. Both alumina phases, crystalline mullite and amorphous, are alkaline-soluble but the high silica solubility in alkaline solutions is a major problem (Matjie et al., 2005) with high silica materials like CFA.

Leaching of CFA using an inorganic acid like sulphuric acid is achieved by proton attack. The hydronium ion displaces the metal cation from the ash particle matrix, thus inducing the dissolution of metals according to the following reactions:

$$CaO + Al_2O_{3(s)} + 8H^+_{(aq)} + SO_4^{2-}{}_{(aq)} \rightarrow 2Al^{3+}_{(aq)} + CaSO_{4(s)} + 4H_2O_{(l)} \qquad (1.1)$$

$$CaO{\cdot}Al_2O_3{\cdot}2SiO_{2(s)} + 8H^+_{(aq)} + SO_4^{2-}{}_{(aq)} \rightarrow 2Al^{3+}_{(aq)} + CaSO_{4(s)} + 2SiO_{2(s)} + 4H_2O_{(l)} \qquad (1.2)$$

The non-acid soluble phases of the ash plus calcium sulphate precipitate are retained as residue and the resultant aluminium sulphate leach liquor is separated for purification and recovery of alumina.

Leaching processes such as sulphuric acid leaching of CFA can be described in the framework of heterogeneous non-catalytic reactions in conjunction with the shrinking core model. The model assumes that the reaction products and/or inert matter that remain in the solid phase form a layer of ash that encapsulates the unreacted core (Jinping et al., 2007). In their leaching kinetic model, Seidel and Zimmels (1998) attribute low aluminium extraction to the formation of a calcium sulphate barrier on the surface and within pores of CFA particles during metal dissolution. They postulate that the precipitate causes resistance to the mass transfer of reactants and products thus inhibiting alumina dissolution.

Recent developments on the acid leaching of CFA have focused on sinter-based processes to try and optimize the extraction of the aluminium in the mullite phase. An example of such a process is the lime-sinter process where a mixture of CFA, a lime source and carbon are sintered to form a clinker containing soluble calcium aluminate (Matjie et al., 2005). The clinker is reduced to coarse powder and the soluble compounds dissolved in a sulphuric acid solution.

The sintering process is based on the concept that the recovery of minerals from CFA requires methods that will thermally attack and break the crystalline mullite phase ($3Al_2O_3{\cdot}2SiO_2$) to make leaching effective (Matjie et al., 2005; Murtha and Burnet, 1983). While this is true, however, it is important to remember that not all the alumina is contained in the mullite phase. CFA is partly mullite and partly amorphous phase with most of the alumina concentrated in the mullite phase and the balance in the amorphous phase (Nayak and Chitta, 2009; Kelmers et al., 1982; Matjie et al., 2005). The mullite phase, being insoluble in inorganic acids such as HNO_3, HCl and H_2SO_4, requires pre-treatment by sintering methods in order to make leaching more effective (post-sinter leaching). The amorphous phase, being acid-soluble, however, requires no pre-treatment before leaching (pre-sinter leaching). Pre-sinter acid leaching is known to extract aluminium with yields of up to 24 - 30% (Matjie et al., 2005; Seidel and Zimmels, 1998) while post-sinter leaching has shown that CFA could be leached under atmospheric conditions with

aluminium extractions of up to 85% (Matjie et al., 2005). This shows that pre-conditioning of CFA is vital to the high extraction of aluminium.

It is important to note that there are two alumina phases in CFA that play a major role in alumina dissolution kinetics, the amorphous and the crystalline mullite phases. Therefore, the total recovery of alumina from CFA must be attributed to both phases (Nayak and Chitta, 2009). However, heating both phases as practiced in the current lime-sinter process may not be necessary as the amorphous phase in CFA is acid-soluble and does not need heat application to achieve metal dissolution. The two phases may thus be processed separately. This may optimize extraction as well as increase the efficiency of energy utilization as heating in the lime-sinter process is energy intensive. A flow diagram of the proposed process for alumina extraction using a pre-sinter and post-sinter (two-step acid leach) process is presented in **Figure 1.1**.

This research, therefore, is focused on using the two-step acid leach process namely the pre-sinter and post-sinter leach method to establish the optimum extraction of aluminium from the amorphous and crystalline mullite phases of CFA.

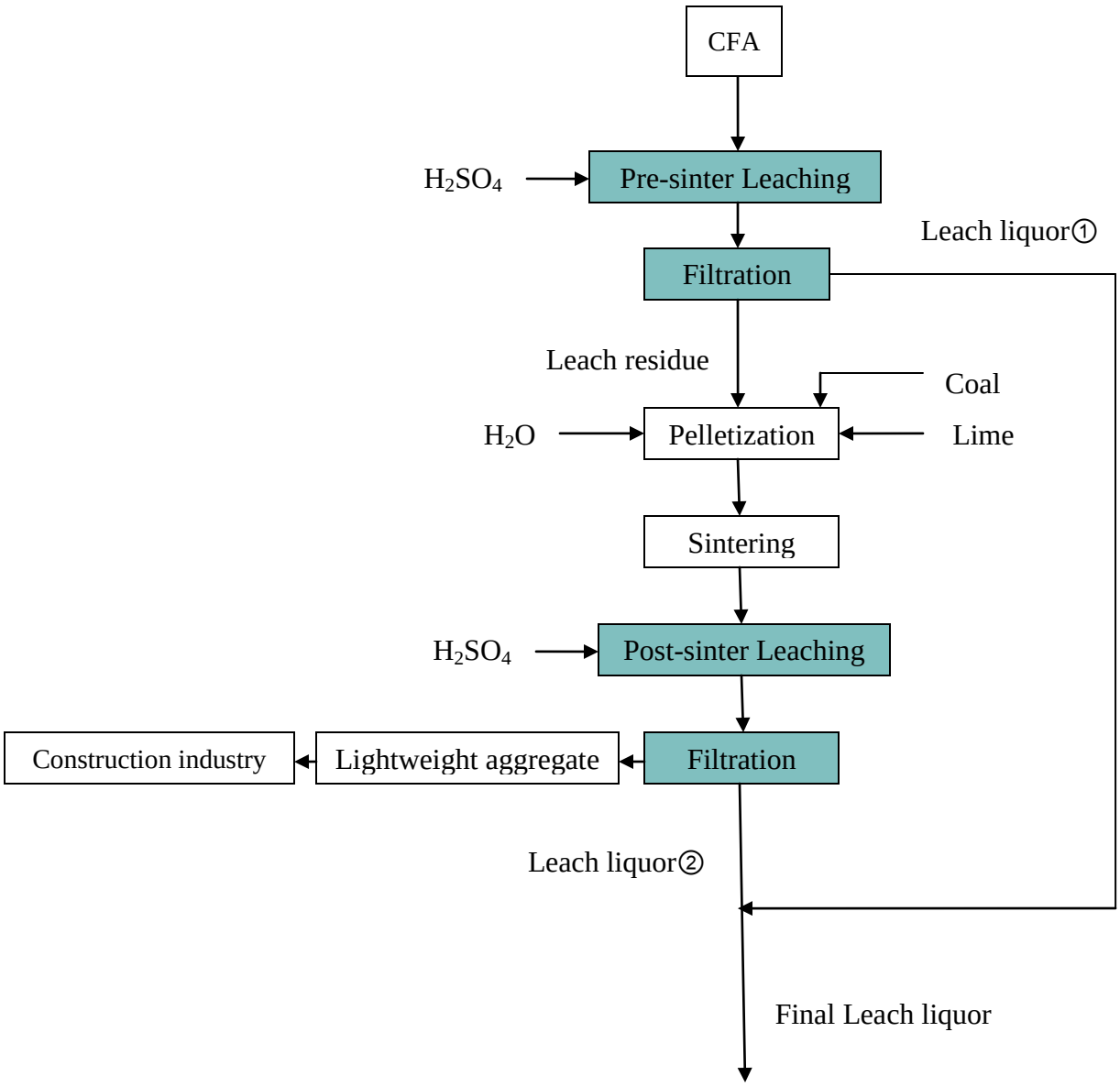

Figure1.1 A flow diagram of the proposed pre-sinter and post-sinter (two-step acid leach) process for extracting alumina from CFA.

1.2 Problem Statement

Although the acidic and alkaline single-step leaching of CFA and other alumina bearing materials has been a subject of much study in recent years, information on the separate leaching of the two CFA alumina phases is non-existent. It is theorized that the two dissimilar alumina phases present in CFA, amorphous and mullite, when leached separately, using sulphuric acid in a two-step acid leach process, will lead to optimum aluminium extraction from both phases. This is the fundamental conceptual theory and value proposition upon which this research is based.

1.3 Objectives

The aim of this study is to develop a pre-sinter and post-sinter two-step acid leach process for the extraction of aluminium from CFA using sulphuric acid. The two-step acid leach extraction process makes use of an inorganic acid, a sinter step and two leaching stages.

The specific objectives are:

- To investigate the extent of aluminium extraction from CFA using sulphuric acid.
- To investigate parameters that promote alumina dissolution in CFA using pre-sinter and post-sinter leaching processes.
- To investigate the physical and chemical properties of CFA during leaching so as to understand the response of the ash to the beneficiation process.

1.4 Research Methodology

The research methodology for this study involved the following major tasks: Literature review, experimental design, laboratory testing, and laboratory test data analysis, drawing conclusions from results, recommendations and documentation.

1.5 Dissertation Lay out

This section provides a snapshot of the chapters and sections that are covered in this dissertation. This dissertation comprises eight chapters. Each chapter begins with a short introduction that highlights the areas that will be covered in various sections of the chapter. A summary and

conclusion is provided at the end of each chapter to focus the reader on what has been covered and also guide the reader to subsequent chapters. The schematic representation of the layout is summarized in the flowchart in **Figure 1.2**.

Chapter 1 *Introduction:* This chapter provides the motivation for the research, the problem statement, and the overall objectives of the study.

Chapter 2 *Literature Review:* This chapter sets out to review related literature on the extraction of alumina from CFA. The chapter includes general knowledge on CFA mineralogy and source; the current metallurgical and chemical extraction processes.

Chapter 3 *Experimental Design:* This chapter describes the materials and methods used in the study.

Chapters 4-7: These chapters describe laboratory tests and discussion of the findings.

Chapter 8 *Conclusions and Recommendations:* This chapter concludes the dissertation with a summary of the findings and recommendations.

References to all articles used in the study are provided at the end of the dissertation. An appendix section provides relevant laboratory test results and other important data.

1.6 Summary

In this introductory chapter, the background, problem statement and study objectives were discussed. This was followed by a short description of the research methodology and dissertation layout. The next chapter discusses literature review.

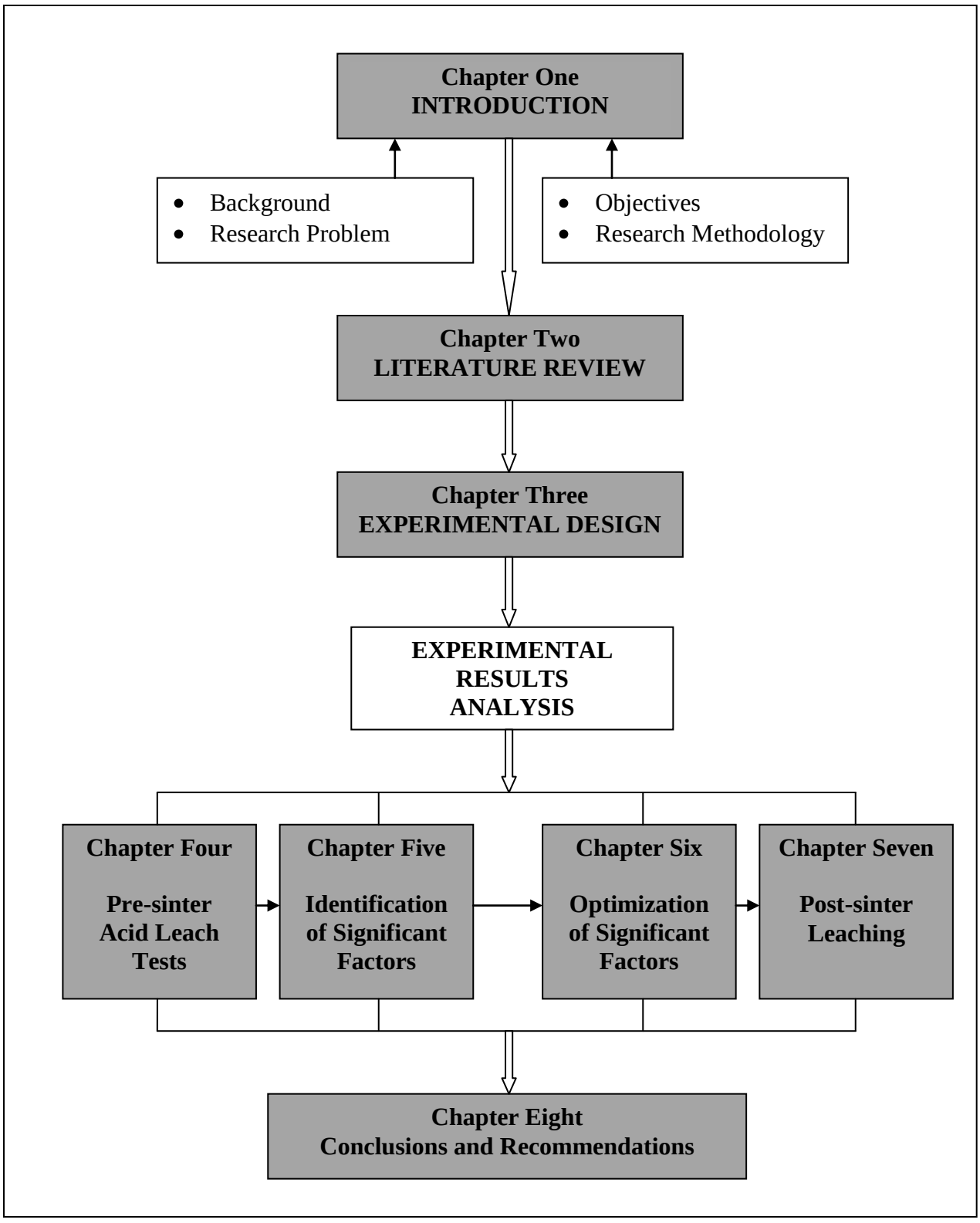

Figure 1.2 Dissertation layout

CHAPTER TWO

LITERATURE REVIEW

2.1 General Introduction

Aluminium is the most abundant metallic element in the earth's crust (8.3% by weight) and the third most abundant of all elements after oxygen and silicon (Earnshaw and Greenwood, 1997). It occurs in nature in the form of aluminium oxide (Al_2O_3) and other combined forms such as bauxite ore. Commercial processing of bauxite through the Bayer process involves conversion of the hydrated aluminium oxide in the ore to smelter grade alumina. The process includes leaching the ore with hot sodium hydroxide to form sodium aluminate solution ($Na[Al(OH)_4]$) from which aluminium trihydrate ($Al[OH]_3$) is precipitated then calcinated to form aluminium oxide (Al_2O_3). The alumina (Al_2O_3) is then smelted via the Hall-Heroult electrolytic process to produce pure aluminium metal (Habashi, 2005). Aluminium is the most widely used non-ferrous metal in the world (Aluminium, 2012).

Production of primary aluminium in South Africa thrives on alumina feedstock imported from countries abroad such as Australia. Although South Africa does not have commercially exploitable bauxite deposits it has pre-mined CFA reserves and readily available aluminium smelters. These ashes contain significant amounts of alumina and present an alternative to bauxite. The four types, or ranks, of coal from which fly ash may be generated include anthracite, bituminous, sub-bituminous, and lignite (Maleka et al., 2010). These coals differ in terms of calorific value, chemical composition and ash content because of their different geological origins.

The aim of this literature review is to give a general overview of CFA mineralogy and its source including past and present processing methods. The importance of selecting a route for processing CFA based on its chemical characteristics and subsequent preference towards sulphuric acid leaching by solubilizing alumina through proton attack (Nayak and Chitta, 2009; Shcherban et al., 1995) is highlighted.

2.1.1 Aluminium

Aluminum (Al) is a silver-white metal with a face-centered cubic crystalline structure; electronic configuration, $1s^2 2s^2 2p^6 3s^2 3p^1$; atomic number, 13; valence, +3; atomic mass, 26.9815g; specific gravity, 2.6989 at 20°C; melting point, 660°C and boiling point, 2467°C. Aluminium is amphoteric (having the characteristics of an acid and a base) and can react with mineral acids to form soluble salts and hydrogen.

Due to its unique physical and chemical properties, aluminium has become the most widely used metal after iron. Some of its metallurgical properties include high strength-to-weight ratio, resistance to corrosion, non-toxicity, catalytic properties, good thermal and electrical conductivity and strength retention under extreme cold without becoming brittle.

Among secondary resources, CFA is a potential alternative source of alumina for the production of aluminium metal. The main markets for aluminium are non-ferrous and ferrous (less than 1% iron) alloys which are used in applications such as building and construction, transportation, consumer durables and electrical applications. Powdered aluminium is also used in paint, and in pyrotechnics such as rocket fuels and thermite. Furthermore, aluminium is used to form compounds such as aluminium sulphate used in the manufacture of paper, in water purification and sewage treatment, in leather tanning and as a mordant in a fire extinguisher (Thompson, 1995; Van and Kent, 1967).

2.2 Coal Fly Ash Source and Mineralogy

CFA is produced from three types of coal-fired boiler furnaces used in the electric utility industry – dry-bottom boiler furnaces, wet-bottom boiler furnaces and cyclone furnaces. The dry-bottom boiler furnace is the most common type. The burning of pulverized coal in the aforementioned furnaces generates two types of ash – bottom ash which collects at the bottom of the boiler and fly ash which is carried off in flue gas and is collected by electrostatic precipitators, bag houses or mechanical collection devices such as cyclones. Fly ash represents about 80% of all the ash that leaves the furnace (Babcock and Wilcox, 2007).

CFA formation and its physical and chemical characteristics are controlled by the type of coal, the boiler and its operating conditions, and post-combustion parameters (Kutchko and Kim, 2006). In a pulverized coal-fired boiler, the furnace combustion zone operating temperatures are typically in excess of 1400°C. At these temperatures, the mineral matter entrained over years within the coal, such as kaolinite, may oxidize, decompose, fuse, disintegrate or agglomerate (Kutchko and Kim, 2006; Shcherban et al., 1995). Evolution of CO_2 and H_2O gases from trapped volatile matter can cause the ash particles to expand to form hollow three-layer-structured cenospheres with an outer layer, middle layer and inner layer (Sakamoto et al., 2003; Landman, 2003).

The cenospheric ash particles owe their spherical structure to vapour and atmospheric pressure, surface tension and gravitational forces on the molten particle as it is forced up the furnace stack against gravity (Landman, 2003). The molten particles cool down rapidly in the post-combustion zone, maintaining their equilibrium shape. The rapid cooling in the post-combustion zone results in the formation of spherical particles. Some of the vaporized low boiling elements, for example alkali metal salts coalesce to form submicron particles. Vaporized compounds, most notably the polynuclear aromatic hydrocarbons and polycyclic aromatic hydrocarbons, adsorb onto the outer surface layer of the ash particle thus enriching it in carbon, potassium, sodium, calcium and magnesium (Kutchko and Kim, 2006; Landman, 2003). The middle layer is predominantly rich in sodium and the inner layer is rich in sodium, silicon and aluminium (Sakamoto et al., 2003).

Kaolinite decomposition in the furnace combustion zone results in the formation of mullite and polymorphous conversion of quartz into high temperature modification of silica according to the following reaction (Shcherban et al., 1995):

$$3[Al_2Si_2O_5(OH)_4] \rightarrow 3Al_2O_3{\cdot}2SiO_2 + 4SiO_2 + 6H_2O \qquad (2.1)$$

Kaolinite mullite silica

As a result of this reaction, most of the aluminium is concentrated in the crystalline mullite phase while the rest goes to the amorphous phase (Matjie et al., 2005). CFA is a heterogeneous substance and its mineralogy is closely related to the minerals entrained in the coal. The main

phases found in the ash include amorphous, mullite, quartz, magnetite, haematite and anhydrite (Loubser and Verryn, 2008). The non-amorphous phases make up the crystalline phase thus making CFA generally a two-phased material, amorphous and crystalline. The amorphous and crystalline phases contain approximately 28% and 72% alumina respectively. Recovery of alumina from these phases is based on the application of metallurgical and chemical processes.

2.3 Currently Existing CFA Processing Methods

The chemical composition of CFA is similar to bauxite ore. A comparison of the typical chemical composition of bauxite and Eskom CFA is presented in **Table 2.1**(Authier-Martin et al., 2001). Worth noting is the silica, ferric oxide and alumina content. CFA has higher silica, lower ferric oxide and within range alumina content compared to bauxite. Despite the high silica content, metallurgical means of processing can be applied to extract the significant amounts of alumina present in South African CFA.

Table 2.1 Typical chemical compositions of Bauxite and CFA (Authier-Martin et al., 2001)

Component	Bauxite	Eskom CFA
	wt%	wt%
SiO_2	< 0.5 – 10	46 – 60
Al_2O_3	30 – 60	26 – 31
Fe_2O_3	1 – 30	4 – 6
TiO_2	< 0.5 - 10	1.3 – 1.7
CaO	0.1 - 2.0	3 – 11
P_2O_5	0.02 - 1.0	0.3 – 1.1

Alumina recovery processes by hydrometallurgical means are broadly divided into two types, acidic and basic. The recovery of alumina from bauxite ore follows a basic route because of the ore's low silica content and high Fe insolubility in alkaline solutions. However, the silica content in South African CFA is high, typically 46 – 60%. If treated through the basic route, large volumes of co-dissolved silica would have to be removed from the alkaline solutions at the expense of aluminium. The difference in silica content is a major factor influencing the choice of a treatment route; notably, CFA has different processing requirements compared to bauxite. The high concentration of silica which is the primary gangue element in CFA, therefore, dictates the treatment process to be followed.

Several leaching methods for CFA processing have been extensively researched using a variety of routes that are acidic, alkaline or a combination of acidic and alkaline. The most important ones are discussed in the subsequent sections.

2.3.1 Bioleaching

Bioleaching involves the use of bacterial microorganisms to recover metals from primary ores or secondary sources. *Thiobacilli* species is the most common microorganism that is known to facilitate metal bioleaching reactions. These microorganisms utilize insoluble metal sulphides or sulphur as an energy source producing sulphuric acid - the main cell metabolite that indirectly leaches CFA particles. Seidel and co-workers (2001) conducted a study on the process of bioleaching of CFA by *Thiobacillus thiooxidans*. They investigated effects of CFA content in suspension on the growth of Thiobacillus and the subsequent bioleaching of aluminium and iron. In their work, calcium sulphate deposition in the bioleaching process was noticed to interfere with cell attachment to sulphur particles thus resulting in suppressed cell growth rates and adverse effect on cell performance (Seidel et al., 2001). They, however, overcame this hurdle by removal of the alkaline component (CaO) from CFA with hydrochloric acid prior to bioleaching (Seidel et al., 2001). Silica, which is usually present in high levels in CFA, was not noticed to interfere with the bioleaching process in any way. The authors reported an aluminium extraction close to 25% after 3 weeks of bioleaching time (Seidel et al., 2001). Bioleaching has advantages of low cost, mild process conditions and low energy demand or landfill space. However, slow

kinetics and insufficient selectivity with respect to specific metals, particularly aluminium, offset the advantages of the CFA bioleaching process (Seidel et al., 2001).

2.3.2 Alkaline Leaching

In basic leaching, solutions of NaOH or alkaline salts such as Na_2CO_3 are used, often under pressure to permit the use of elevated temperatures (Murtha and Burnet, 1983). The traditional Bayer process for the recovery of alumina from Bauxite involves the dissolution of alumina in sodium hydroxide. The process includes leaching the ore with hot sodium hydroxide to form sodium aluminate solution ($Na[Al(OH)_4]$) from which aluminium trihydrate ($Al[OH]_3$) is precipitated then calcinated to form aluminium oxide (Habashi, 2005). It is noted that although pressure leaching of CFA with alkaline solutions is quite selective for aluminium as Fe is almost insoluble in alkaline solutions, the simultaneous dissolution of SiO_2 is of concern and can only be removed at the expense of extracted aluminium (Shcherban et al., 1995; Burnet et al., 1984; Jackson, 1986). Removal of silicon species from aluminate solution prior to precipitation of $Al(OH)_3$ can become a major problem (Matjie et al., 2005) due to the formation of insoluble sodium aluminate silicates.

2.3.3 Acid Leaching of CFA

Introduction

For the extraction of aluminium from high silica non-bauxitic resources such as CFA, acid leaching processes are generally preferred because acid routes have the advantage that silica is substantially insoluble in acid (Nayak and Chitta, 2009; Shcherban et al., 1995) unlike alkaline routes. Processing of CFA using the acid route may be done directly or indirectly. Direct acid leaching requires no intervention before the leaching process. However, indirect acid leaching requires some material pre-conditioning prior to leaching. The pre-conditioning helps to achieve a modification of some chemical characteristics of the CFA alumina species in order to make it more responsive to the leaching process.

Lixiviants Used in Acid Leaching

A lixiviant is a liquid medium used to selectively extract the desired metal from the ore or mineral. It assists in rapid and complete leaching. The lixiviants which are important in the hydrometallurgical processes are either acidic or basic in nature. A brief review of the three commonly used acidic lixiviants is given here as knowledge of their characteristics is necessary for the selection of suitable conditions for acid leaching processes.

Hydrochloric Acid Hydrochloric acid, also known as muriatic acid, and spirit of salt, is a clear, colourless aqueous solution of hydrogen chloride gas. It is a highly corrosive, strong monoprotic mineral acid with many industrial uses (Lide, 2007). The boiling point of hydrochloric acid decreases with increasing molarity; at 2.9M, the boiling point is 103°C whilst at 12.4M, the boiling point is 48°C (Perry et al., 1984). Hydrochloric acid (20.2%) as a binary mixture of hydrochloric acid and H_2O has a constant-boiling azeotrope at 108.6°C (Lide, 2007; Perry et al., 1984); it forms corrosive acid mists at higher concentrations. Concentrated hydrochloric acid dissolves many metals, and forms oxidized metal chlorides and hydrogen gas, and it reacts with basic compounds such as calcium carbonate or calcium sulphate to form soluble chlorides. Hydrochloric acid is consumed in many mining operations for ore treatment, metal extraction, separation, purification, and water treatment (Earnshaw and Greenwood, 1997). The average cost of hydrochloric acid (36%) is $3,849/tonne (SD Fine-Chemicals, 2012).

Nitric Acid Nitric acid, also known as aqua fortis, and spirit of niter, is a highly corrosive, monoprotic, toxic and strong mineral acid with strong oxidizing characteristics (Housecroft, 2008). The acid is normally colourless, but tends to acquire a yellow cast due to the accumulation of oxides of nitrogen if long-stored. Nitric acid (68%) as a binary mixture of nitric acid and H_2O has a constant-boiling azeotrope at 121°C (Dean, 1992). Ordinary nitric acid has a concentration of 68% and when the concentration contains more than 86% nitric acid, it forms nitric acid fumes. Nitric acid is subject to thermal or light decomposition to form nitrous gas according to the following reaction (Housecroft, 2008):

$$4HNO_3 \rightarrow 2H_2O + 4NO_2 + O_2 \qquad (2.2)$$

The main important uses of nitric acid include the production of explosives, etching and dissolution of metals, especially as a component of aqua regia for the purification and extraction of gold, and in chemical synthesis (Thiemann, 2005). The average cost of nitric acid (60%) is $4,669/tonne (SD Fine-Chemicals, 2012).

Sulphuric Acid Sulphuric acid, also known as oil of vitriol, is a highly corrosive, diprotic and strong mineral acid; boiling point, 337°C. It is a colourless to slightly yellow viscous liquid which is soluble in water at all concentrations (Lide, 2007). The 98% grade is more stable in storage, and is the usual form of what is described as concentrated sulphuric acid. It has strong dehydrating and oxidizing properties at high concentrations (Housecroft, 2008). Sulphuric acid possesses different chemical properties and therefore has a wide range of applications some of which include metal extraction, chemical synthesis and production of copper sulphate solution used as electrolyte in copper electro-refining and electro-winning processes (Earnshaw and Greenwood, 1997). The average cost of sulphuric acid (98%) is $2,239/tonne (SD Fine-Chemicals, 2012).

Sulphuric acid was used in the acid leaching of CFA, because the acid is stable, easier to handle, cheap and allows good solubilization of alumina.

Direct Acid Leaching of CFA

Direct acid leaching methods are amongst the earliest attempts at extracting alumina from alumina bearing clays. These particular methods have, however, yielded low extraction rates, typically less than 50% (Nayak and Chitta, 2009; Nehari et al., 1999). Alumina extraction by direct acid leaching with sulphuric acid has been extensively researched by several workers (Matjie et al., 2005; Nayak and Chitta, 2009; Nehari et al., 1999; Jinping et al., 2007; Seidel et al., 1998; Gilliam et al., 1982; Phillips and Wills, 1982). The results reported show that direct leaching of CFA with sulphuric acid solution at low acid concentration and ambient temperature yielded poor alumina extraction.

Direct leaching work done by Seidel and Zimmels (1998) using sulphuric acid yielded an aluminium extraction of 30%. In their investigations, the researchers leached a 1% CFA suspension at a fixed pH of 0.8, for a period of 100 days under ambient temperature and atmospheric pressure conditions. They attributed the low alumina extraction to the formation of calcium sulphate. They postulated that the sulphate precipitate forms a barrier on the surface and within pores of CFA particles during metal dissolution causing resistance to mass transfer. In their attempt to overcome this problem, they pre-leached CFA with hydrochloric acid at a constant pH of 4 for 24hours after which it was leached with 0.5M sulphuric acid (or fixed pH of 1.5) at room temperature and atmospheric pressure for 4 days. They found that approximately 28% of the aluminium could be leached from a 10% suspension of conditioned CFA, while during the same period of time it was possible to leach only 20% from the unconditioned CFA sample. Their results showed that despite dissolving about 65% of the calcium from CFA, there was no significant improvement in alumina dissolution due to the pre-leaching process. Therefore, they concluded that conditioning the CFA by a pre-leaching process with hydrochloric acid only enhanced the leaching rates and shortened extraction time but the maximum aluminium extraction level remained unchanged.

Leaching at higher acid concentrations has, however, shown better results. Work done by Nayak and Chitta (2009) showed that alumina extractions of 2.66% to 84.17% could be achieved. The conditions employed involved placing the CFA mixture in a one-liter flask, constant stirring and boiling within the temperature range of 150 – 200°C at sulphuric acid concentrations ranging from 1.5M to 18M, solid to liquid ratios of 1:1 to 1:4 and a leaching time of 4 hrs. However, under these conditions, they had to contend with the evolution of acid fumes at higher levels of acid concentration due to acid boiling. They also had to constantly add water to avoid solidification of the mixture as well as maintain the desired solid to liquid ratio. Despite these efforts, the mixture finally became slurry and solidified due to the high evaporative loss of water. The solidified CFA mixture had to be extracted with hot distilled water and filtered using a suction pump.

Other direct acid leaching work conducted under relatively moderate conditions, showed low aluminium extraction efficiencies. Work done by Matjie and co-workers (2005) using a 6.12M

sulphuric acid solution at a solid to liquid ratio of 1:4 yielded alumina extraction efficiencies in the range of 12 – 24% even after 6 hours of leaching under reflux. However, their results were found to be in agreement with earlier work done by other researchers like Hansen and co-workers (1966). The authors reported that 80% of the alumina originally present in Sasol CFA is constituted in the mullite phase with the balance located in the amorphous glassy phase. They concluded that 20% alumina extraction efficiency by direct acid leaching is the achievable limit thus indicating that phase mineralogy has an effect on the leaching characteristics of CFA.

Indirect Acid Leaching of CFA

Although several processes have been proposed for the treatment of CFA by basic and acidic routes, none of the processes have found commercial industrial application because of high capital and operational costs, environmental concerns and technological outlay. However, acidic routes such as sulphuric acid leaching are generally accepted as easier to handle, cheaper, and of minimum environmental impact. The possibility to use indirect sulphuric acid leaching has long been investigated by several workers (McDowell and Seeley, 1981a; McDowell and Seeley, 1981b; Padilla and Sohn, 1985; Murtha and Burnet, 1983; Matjie et al., 2005) and has been found to have the potential of producing leachable phases from CFA. Indirect acid leaching processes are based on intervention measures such as sintering prior to leaching.

In their work, McDowell and Seeley (1981a) describe a method which comprises sintering a mixture of CFA and calcium sulphate prior to leaching. The mixture is sintered for a period of time sufficient to quantitatively convert the alumina into an acid-leachable form. They sintered a sample of CFA with 2 parts of $CaSO_4$ at 1450°C then leached the sintered product with concentrated sulphuric acid at a solid to liquid ratio of 1: 2.5 for 3 hours. The slurry was further diluted to a solid to liquid ratio of 1: 5 then leached with a 2M sulphuric acid for an extra 3 hours from which they achieved an aluminium extraction efficiency of 98%. However, while chemical leachability of the desired aluminium and other metal values was high even at temperatures greater than 1300°C, they reported that the sintered material was difficult to grind.

In a separate study, McDowell and Seeley (1981b) illustrate a method for recovering aluminium values from CFA which consists of sintering the CFA with a mixture of NaCl and Na_2CO_3 for a

period of time sufficient to convert the aluminium content of the CFA into an acid-soluble phase. They mixed three parts of a sinter medium consisting of 2 parts by weight NaCl, 1 part Na_2CO_3 and 1 part CFA. They heated the mixture under atmospheric conditions to a temperature of 400°C for 1 hour then raised and maintained the temperature at 900°C for 2 hours. The sintered product was cooled, ground to powder and then washed with hot water to separate the aluminium from the unreacted NaCl and Na_2CO_3 components followed by acid leaching with 1M nitric acid at a leaching temperature in the range of 85°C - 100°C. They found that greater than 90% and up to 99% of the aluminium could be recovered using their salt-soda-sinter method. However, in spite of the high extraction efficiencies, the high reagent consumption at a rate of 3 parts reagents (NaCl and Na_2CO_3) to 1 part CFA seems to outweigh the advantages of high alumina extraction.

The work by Phillips and Wills (1982) showed that alumina recoveries of 60-80% could be achieved on pre-calcined micaceous china clay (25-35% alumina) leached with nitric acid at atmospheric boiling point and pressure. Although the researchers did not specify or reveal any additives used in the pre-calcining process, they calcined the clay at an optimum temperature of 800°C. The sintered product was then leached with 7M nitric acid, in a 1 litre round bottomed flask fitted with a reflux condenser, a thermometer and a mechanical stirrer rotated at 250 rpm. The authors found that calcining beyond 800°C resulted in reduced aluminium extraction possibly due to either some structural collapse or solid state transition to silicon spinel, a mineral form which was more resistant to leaching with nitric acid.

In a lime-sulphur-carbon-sinter study, Murtha (1983) shows a method in which an addition of a small amount of sulphur and carbon to the lime-CFA sinter mixture was found to lower sintering temperatures resulting in an alumina extraction of almost 90%. The author added about 1-2 wt% sulphur and 1-2 wt% carbon to a mixture of about 1 part CFA and 2 parts $CaCO_3$. The sinter was then heated to about 1200°C to 1380°C for 1 hour to react the sulphur with calcium and alumina forming a clinker containing a calcium sulpho-aluminate compound. The sinter product was reduced to a coarse powder and then leached with a 3 wt% aqueous $NaCO_3$ solution at a solid to liquid ratio of 1:10, at 65°C for 10 minutes, thereby extracting alumina from CFA. However, despite the fast leaching kinetics of the process at a relatively low temperature, the high reagent consumption of sulphur, Na_2CO_3 and $CaCO_3$ could outweigh these advantages.

2.4 Sintering Process

According to Murtha (1983), there are mainly three types of sintering methods, used for alumina recovery, with several variations some of which include: lime-sinter, lime-soda sinter, lime-$CaSO_4$-sinter, lime-sulphur-carbon-sinter and salt-soda-sinter. Sinter processes involve high temperature chemical methods of attacking the refractory glass matrix of the ash particles. The conventional practice is to subject raw CFA, as a sinter feed, to high sintering temperatures, usually in excess of 1000^{o}C for a pre-determined period of time typically 30 - 180 minutes. The full procedure involves pelletization, sintering and post-sinter leaching.

2.4.1 Pelletization

In the lime-sinter process (Kelmers et al., 1982; Matjie et al., 2005), CFA is mixed with a carbon source such as coal and a lime source such as limestone or gypsum in the ratio of 5:4:1 then made into pellets of 4.5-5.5 mm size. Pelletizing is the process of compressing or molding a material into the shape of a pellet or ball. CFA is preferred in the form of pellets because the configuration of CFA pellets as packed spheres in the muffle furnace allows air to flow between the pellets. The spaces between the pellets decrease the resistance to the air that flows through the layers of material during the sintering process.

2.4.2 Sintering

The pellets are sintered at typical temperatures of 1000 - 1150 ^{o}C for 30 – 180 minutes (Murtha and Burnet, 1983). The main objective of the sintering step is to provide strong materials with a high crushing strength and also to transform the crystalline mullite phase rendering Al_2O_3 free for leaching. Sintering relies on solid-phase or liquid-phase reactions at points of localized melting between particles to break bonds and form new compounds without complete melting of the reactants (Murtha and Burnet, 1983).

In the chemical reaction assumed to take place first, the sinter reagent (limestone) decomposes according to the following reaction:

$$CaCO_3 \rightarrow CaO + CO_2 \qquad (2.3)$$

This is followed by the reaction of CaO with mullite and other alumina-containing species in the CFA to form anorthite and/ or gehlenite, as well as some combination with free silica to form calcium silicate (Shcherban et al., 1995). The following are some of the possible reactions that can occur:

$$3Al_2O_3{\cdot}2SiO_2 + 3CaO + 4SiO_2 \rightarrow 3(CaO{\cdot}Al_2O_3{\cdot}2SiO_2) \quad (2.4)$$

(Mullite) (Anorthite)

$$3Al_2O_3{\cdot}2SiO_2 + 6CaO + SiO_2 \rightarrow 3(2CaO{\cdot}Al_2O_3{\cdot}SiO_2) \quad (2.5)$$

(Mullite) (Gehlenite)

$$SiO_2 + 2CaO \rightarrow Ca_2SiO_4 \quad (2.6)$$

$$3Al_2O_3{\cdot}2SiO_2 + 5CaO \rightarrow Ca_2Si_2O_6 + 3(CaO{\cdot}Al_2O_3) \quad (2.7)$$

2.4.3 Post-sinter Leaching

The products formed in the sintering process are subsequently dissociated in a post-sinter acid leach step. Leaching conditions required in the post-sinter leaching step range from 3.06M to 6.12M H_2SO_4, 4 to 12 hours leaching time, 60 to 90°C leaching temperature and 1:3.5 to 1:5 solid to liquid ratio (Matjie et al., 2005). The following are possible reactions that take place:

$$CaO{\cdot}Al_2O_3{\cdot}2SiO_2 + 4H_2SO_4 \rightarrow Al_2(SO_4)_3 + CaSO_4 + 2SiO_2 + 4H_2O \quad (2.8)$$

$$2CaO{\cdot}Al_2O_3{\cdot}SiO_2 + 5H_2SO_4 \rightarrow Al_2(SO_4)_3 + 2CaSO_4 + SiO_2 + 5H_2O \quad (2.9)$$

$$CaO{\cdot}Al_2O_3 + 4H_2SO_4 \rightarrow Al_2(SO_4)_3 + CaSO_4 + 4H_2O \quad (2.10)$$

The dissolved metals such as Al, Fe, and Ti are then separated by solvent extraction or ion exchange. The lime-sinter process is known to extract alumina with recoveries of about 85% (Matjie et al., 2005). A solid product is then obtained by precipitation or crystallization often followed by calcination to yield metal oxides such as alumina (Al_2O_3). A flow diagram of the current lime-sinter process for alumina extraction is presented in **Figure 2.1**.

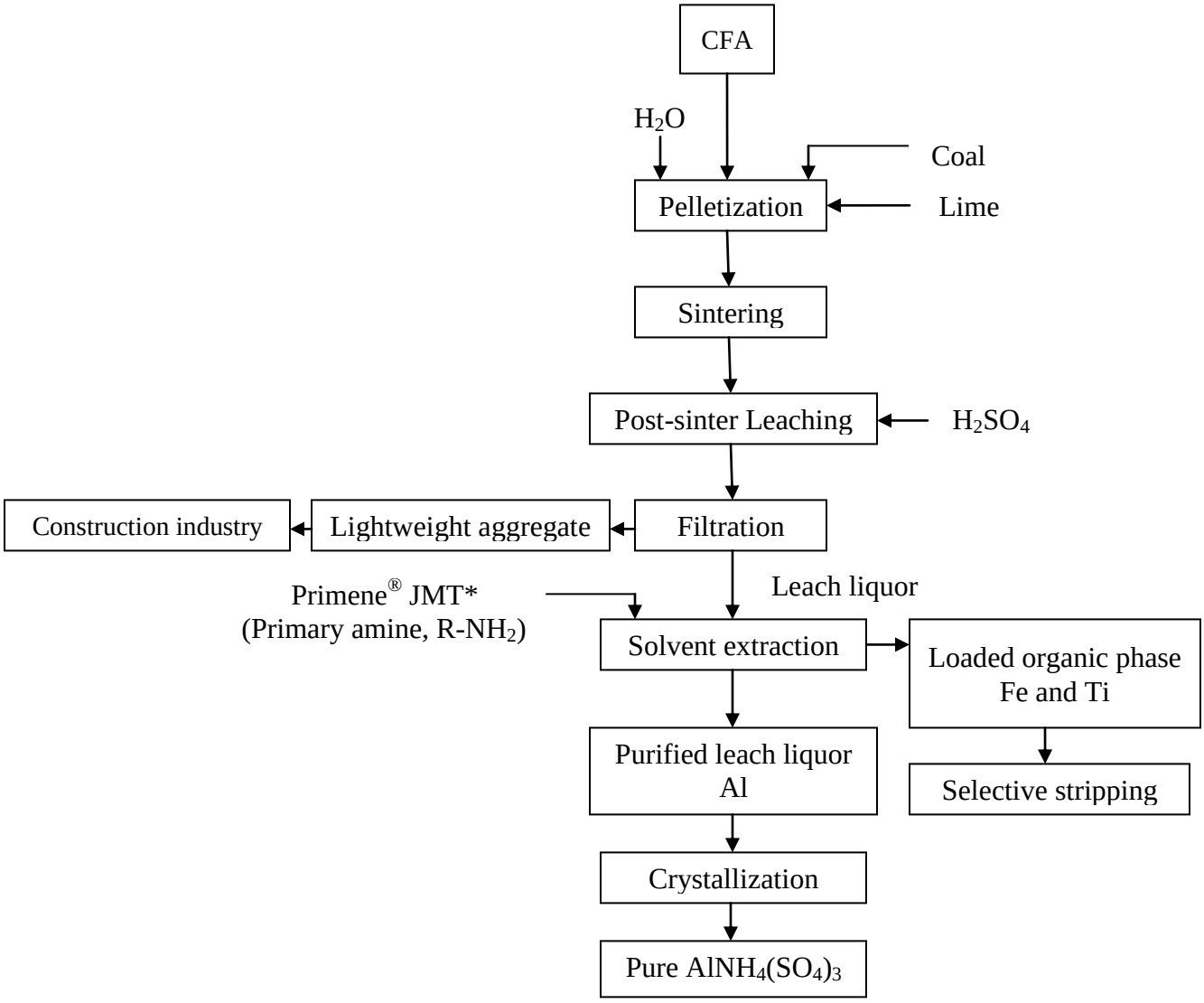

*JMT is a Trade Mark acronym for the Primene (primary amine containing 18-22 carbon atoms) manufactured by Rohm & Haas, (Saeed et al., 2009)

Figure 2.1 A flow diagram of the current lime-sinter process for extracting alumina from CFA (Matjie et al., 2005)

CFA pre-conditioning and post-sinter leaching conditions are important factors that affect the extraction efficiency and leachability of alumina. However, none of the foregoing works on alumina recovery deal with 'pre-sinter and post-sinter leaching' where the sintering and leaching response is expected to demonstrate different characteristics.

Noting that there are two alumina phases which have an effect on the leaching characteristics of CFA (Matjie et al., 2005; Nayak and Chitta, 2009) it is postulated that the two dissimilar alumina phases, amorphous and mullite, when leached separately, using sulphuric acid in a pre-sinter and post-sinter (two-step acid leach) process, will lead to optimum aluminium extraction from both phases. The acid-soluble amorphous phase can be leached out first, in a pre-sinter leaching step, followed by the sintering and post-sinter leaching of the mullite phase thus optimizing aluminium extraction.

In the pre-sinter and post-sinter (two-step acid leach) process, pre-sinter leaching has the potential to reduce fly ash residue weight resulting in reduced sinter feed thus saving on energy. Pre-sinter leaching can alter CFA morphology by exposing the mullite phase after the elimination of the amorphous phase thus increasing the mullite surface area available for contact and reaction in the subsequent sinter process. Furthermore, pre-sinter acid leaching reactions produce $CaSO_4$ as a by-product. The $CaSO_4$ formed in these reactions can be utilized as part of the pellet mixture. When used as an addition to limestone, $CaSO_4$ is known to lower sintering temperatures and also form a highly soluble calcium alumino sulphate phase, $4CaO{\cdot}3Al_2O_3{\cdot}SO_4$, which improves alumina extraction (Murtha and Burnet, 1983). A flow diagram of the proposed process for alumina extraction using a pre-sinter and post-sinter (two-step acid leach) process is presented in section 1.1, **Figure 1.1**.

2.5 The Kinetics of Leaching Processes

Leaching is a unit operation where separation is achieved by preferential dissolution of a solute in a solid base using a solvent (McCabe et al., 1993; Richardson et al., 2002). The leaching reaction involves the extraction of specific metals from their ore or metal bearing material by dissolving them in aqueous media. In other words, metals bound in minerals are transformed into metal ions that are released into aqueous media thus making them mobile. The leaching reaction

takes place at the interface between a solid and liquid phase, and sometimes gaseous phase (Gupta, 2003). Fluid-solid reactions are encountered in a variety of chemical processes (Wen, 1968). One such example is the extraction of metals from ores using acids (Levenspiel, 1972).

Mathematical modeling of fluid-solid systems is usually used to interpret experimental results and to gain insight into these reaction mechanisms. The shrinking core model has been widely used in the area of hydrometallurgy to model leaching systems (Gbor and Jia, 2004) like sulphuric acid leaching of CFA. Leaching processes such as acid leaching of CFA can be described in the framework of heterogeneous non-catalytic reactions in conjunction with the shrinking core model where the initial radius of the leached particles gradually decreases leaving a reacted layer around the unreacted core (Seidel and Zimmels, 1998; Wen, 1968).

The shrinking core model is based on the assumptions of pseudo-steady state diffusion and that the solid particle is spherical and reacts with the fluid isothermally (Gbor and Jia, 2004). Based on these assumptions the surface reaction of solid-fluid systems can be considered to consist of the following steps (Wen, 1968): (1) diffusion of the fluid reactants across the fluid film surrounding the solid, (2) diffusion of the fluid reactants through the porous solid layer (3) adsorption of the fluid reactants at the solid reactant surface, (4) chemical reaction with the solid surface, (5) desorption of the fluid products from the solid reaction surface, and (6) diffusion of the product away from the reaction surface through the porous solid media and through the fluid film surrounding the solid. Depending on which step is rate-controlling, three different types of reaction mechanisms may be obtained; diffusion control, product layer control and chemical reaction control. Since these steps take place consecutively, if any of the above steps is much slower than all the others, that step becomes the rate-determining-step (Wen, 1968). Therefore, identification of this step and the parameters that can influence it is very important. Equations governing these rate controlling regimes to express the reaction rates in terms of particle conversion or fractions reacted (Levenspiel, 1972) are presented in **Table 2.2.**

Table 2.2 Shrinking core models (Levenspiel, 1972)

Regime	Equation
Film diffusion control	$X = kt$
Chemical reaction control	$1 - (1 - x)^{1/3} = kt$
Ash diffusion control	$1 - 3(1 - x)^{2/3} + 2(1 - x) = kt$

x = fractional conversion; t = time (hours); k = rate constant (hr^{-1})

Activation energies of the leaching process

Reaction kinetics and rate controlling mechanisms for leaching processes may also be described in the framework of heterogeneous non-catalytic solid-liquid reactions in conjunction with activation energies. The magnitude of the activation energy can provide positive evidence for the rate controlling regimes (Habashi, 1968; Potgieter et al., 2006). Activation energies governing these rate controlling mechanisms are shown in **Table 2.3.**

Table 2.3 Activation energies for rate controlling mechanisms (Habashi, 1968; Potgieter et al., 2006)

Regime	Activation Energy
Product (Ash) diffusion control	< 20 $kJmol^{-1}$
Film diffusion control	20 - 50 $kJmol^{-1}$
Chemical reaction control	> 50 $kJmol^{-1}$

The method for calculating activation energies is the Arrhenius equation based reaction rate constant, ***k.***

The Arrhenius **Equation 2.11** gives a quantitative relation between the rate constant (***k)*** and temperature (**T**):

$$\boldsymbol{k = Ae^{\frac{-E_a}{RT}}} \qquad (2.11)$$

Where, ***A*** is the frequency factor or pre-exponential constant, $\boldsymbol{E_a}$ is the activation energy, ***T*** is the absolute temperature in Kelvin and ***R*** is the gas constant.

Taking natural logarithms on both sides, **Equation 2.11** becomes:

$$lnk = -\frac{\boldsymbol{E_a}}{RT} + lnA \qquad (2.12)$$

For a reaction at two known temperatures and/or rate constants, **Equation 2.12** takes the forms,

$$lnk_1 = lnA - \frac{\boldsymbol{E_a}}{RT_1} \qquad (2.13)$$

And

$$lnk_2 = lnA - \frac{\boldsymbol{E_a}}{RT_2} \qquad (2.14)$$

Subtracting **Equation 2.13** from **Equation 2.14**, the final equation (Chang, 2005; Segal, 1975; Laidler, 1984; Logan, 1982) is presented as:

$$lnk_2 - lnk_1 = \frac{\boldsymbol{E_a}}{R}\ \frac{1}{T_1} - \frac{1}{T_2} \qquad (2.15)$$

The activation energy ($\boldsymbol{E_a}$) can, therefore, be calculated using **Equation 2.15**. Alternatively, using **Equation 2.12**, the activation energy ($\boldsymbol{E_a}$) can be computed from the slope of the Arrhenius plot of ***lnk*** versus $\mathbf{T^{-1}}$**.**

It is clear, from **Equation 2.12**, that as the value of activation energy $\boldsymbol{E_a}$ decreases, the value of $\boldsymbol{k}$ increases and, therefore the reaction rate increases. This shows that low activation energies are indicative of fast reaction rates and vice versa.

2.6 Summary

Aluminium occurs in nature in the form of bauxite which is commercially used to extract aluminium metal using the Bayer process (Habashi, 2005). It was highlighted in this review that although South Africa does not have commercially exploitable bauxite deposits, it has pre-mined CFA reserves and readily available aluminium smelters.

CFA contains significant amounts of alumina but, it cannot be treated using the Bayer process route because it contains high amounts of silica, typically 46-60%. However, in the acidic route, silica is substantially insoluble and alumina can be extracted by pre-conditioning the CFA in order to form leachable alumina phases which are easily solubilized by sulphuric acid. This requires pre-sinter leaching of the CFA to leach out the easily leachable alumina from the amorphous phase first. The pre-sinter leaching step has advantages of exposing the acid-insoluble mullite phase for effective sintering and phase transformation prior to post-sinter leaching.

It was demonstrated that CFA contains two dissimilar alumina phases, amorphous and mullite, one of which does not need heat application to achieve metal dissolution. Therefore, in this review, the potential of using the pre-sinter and post-sinter (two-step acid leach) method was investigated and postulated to be a possible alumina recovery process. The next chapter discusses materials and analytical methods used in the study.

CHAPTER THREE

MATERIALS AND METHODS

3.1 Introduction

This chapter discusses the preparation of materials as well as the experimental and analytical methods used in the study.

3.2 Experimental

3.2.1 Coal Fly Ash

The CFA material used throughout this study was provided by Kendal Power Plant, a division of Eskom, South Africa. The CFA material was obtained in fine particle form and did not need further grinding. Representative samples used in all experiments were prepared using a riffler splitter (Model: 15A, Eriez Magnetics, South Africa).

The CFA was characterized by investigating the surface morphology, phase mineralogy, particle size and chemical analysis. The typical CFA morphology, mineralogical phases, particle size distribution (PSD) and chemical composition are presented in **Figure 3.1, Table 3.1, Figure 3.2** and **Table 3.2**, respectively. The particle size analysis was done by physically screening the samples using test sieves (Fritsch, Germany) of various screen sizes within the range of -38µm and +212µm. The CFA surface morphology analysis was carried out using a Scanning Electron Microscope (Model: Quanta-400F, FEI, USA). The CFA phase mineralogy analysis and the quantification of calcium sulphate ($CaSO_4$) in residue-CFA were carried out using an X-ray diffractometer (Model: X'Pert, PANalytical, Netherlands) operated with Co-Kα radiation generated at 40kV and 50mA. The chemical composition analysis was carried out using Wavelength Dispersive X-ray fluorescence (XRD) spectrometer (Model: Axios, PANalytical, Netherlands) operated with a Rhodium tube excitation source. Filtrates were analyzed for aluminium using Inductively Coupled Plasma-Optical Emission Spectrometry (ICP-OES) analyzer (Model: SPECTRO GENESIS, Spectro Analytical Instruments, Germany).

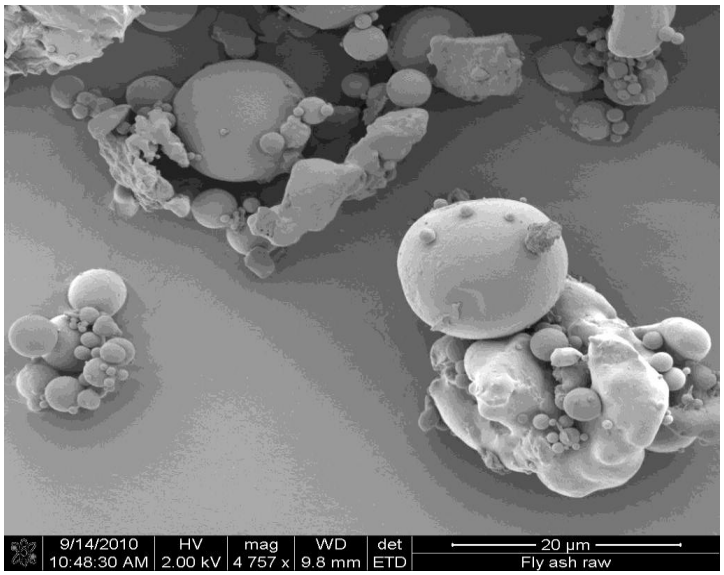

Figure 3.1 Surface morphology of Eskom CFA

Table 3.1 Mineralogical analysis of Eskom CFA

CFA	**Phase** (wt %)	**Al_2O_3** (wt %)
Amorphous	52.9	27.8
Hematite	0.8	-
Magnetite	1.65	-
Mullite	30.68	72.2
Quartz	13.97	-

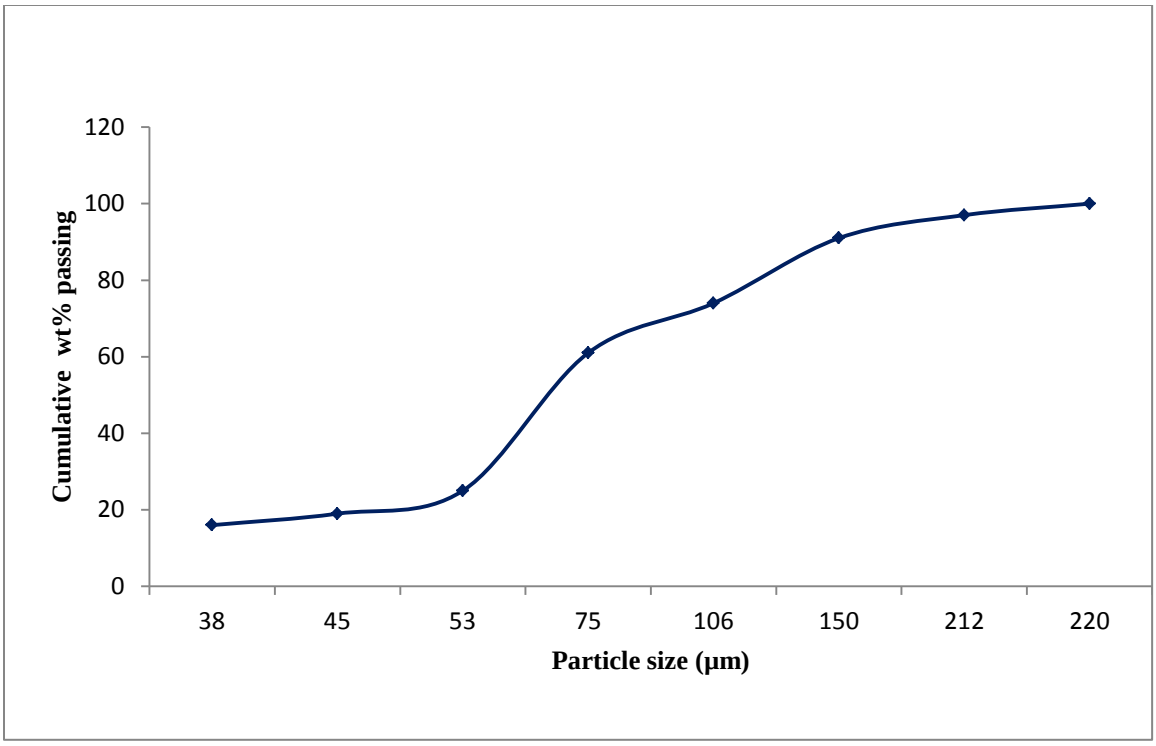

Figure 3.2 Particle size distribution (PSD) of Eskom CFA

Table 3.2 Chemical composition of Eskom CFA (wt %)

SiO_2	Al_2O_3	Fe_2O_3	FeO	MnO	MgO	CaO	Na_2O	K_2O	TiO_2	P_2O_5	Cr_2O_3	NiO	L.O.I
56.1	30.52	0.4	3.25	0.03	1.43	5.03	0.24	0.71	1.67	0.6	0.03	0.01	1.43

3.2.2 Reagents

All reagents used in this study were of analytical grade (AR). Analytical grade reagents are chemical substances of sufficient purity fit for laboratory and general use according to International standards (ASTM®, 2012; Grades of chemicals, 2008). The reagents used in this study were all purchased from Merck and Sigma Aldrich and were used as received. Distilled water, analytical grade sulphuric acid (98% w/w) and calcium carbonate were used in the experiments.

According to ELGA® LabWater (2009), distilled water is produced by a process that separates water from contaminants by changing the state of water from a liquid phase to a gas phase and

then back to a liquid phase. Each of these transitions provides an opportunity to separate water from contaminants thus producing very pure water. Deionized water is produced by a chemical process that uses ion-exchange resins which exchange hydrogen ions and hydroxide ions for dissolved minerals which then recombine to form water. Because the majority of water impurities are dissolved salts, deionization produces high purity water that is similar to distilled water. However, deionization does not significantly remove uncharged organic molecules, viruses or bacteria.

In this study, distilled water was found more suitable for laboratory use than deionized water.

3.2.3 Coal

Coal used in this study was obtained from Matla Collieries, South Africa. It was crushed and finely ground to 100% passing 212 µm (similar grind as CFA). The Thermo-gravimetric analysis (TGA) and chemical composition of the coal as obtained from the supplier stated that the moisture content is 4.32%, volatiles are 20.25%, the fixed carbon is 68.20%, the ash content is 7.23% and the Al content is 1.05%.

3.2.4 Design of Experiments

The main focus of this study was the identification and optimization of factors that significantly influence the aluminium extraction process. After identifying and optimizing these factors, they were used in all the leaching experiments. Therefore, a statistical Design of Experiments (DOE) method was employed as a research tool to accomplish the main objective of the study. The advantage of using DOE is that it provides for a simultaneous study of several process parameters which provide useful information (Czitrom, 1999; Barrentine, 1999). By using DOE, the estimates of the effects of each factor are more precise and the interaction between factors can be estimated systematically. Therefore, by using DOE there is experimental information in a large factor space which improves prediction of the response.

Screening of factors (Chapter 5) was done at the beginning so as to explore the possible influence of factors on the response (aluminium extraction) and to identify their appropriate

upper and lower limits. A full 2^4 factorial design was used in determining the influential factors. A statistical analysis of the experimental results was employed to evaluate the significance of the factors using the normal probability plot and Pareto analysis.

Normal probability plot of effects

The normal probability plot is a statistical method that is used to evaluate the significance of factors. In the assessment of effects from unreplicated factorials, occassionally real and meaningful higher-order interactions occur and therefore it is necessary to allow for selection (Box et al., 1978). However, cited by Simate and Ndlovu (2008), Daniel (1959)'s method by which effects are plotted on a normal probability plot often provides an effective way of helping with selection. This is the plot of the actual value of the effect estimates against their cumulative normal probabilities. If the effects had occurred simply as the result of random variation about a fixed mean, and the changes in levels of the independent variables had had no real effect at all on the response, then all the main effects and interactions would be distributed about zero (normal distribution). They would therefore plot on a normal probability plot as a straight line whereas significant effects will have a non-zero means and will not lie along the straight line. To see whether they do, the main effects are ordered in increasing order and plotted with an appropriate scale. The scale is obtained by employing the generalized equation (Box et al., 1978):

$$\boldsymbol{P = \ i - 0.5 \ * \frac{100}{m}} \qquad (3.1)$$

Where, m = total number of effects, P = Probability points, i = Order number

Pareto chart

Plotting the effects on a Pareto chart provides an alternative and equally effective way of helping with the selection of significant factors. The Pareto chart is based on an algorithm that produces a statistically-based acceptance limit of significance (Tague, 2004; Wilkinson, 2006). The level of significance is represented by horizontal bar graphs. The statistical technique, based on the Pareto principle of the 'vital few', is used for the selection of factors that produce a statistically significant overall effect.

The procedure involves plotting the actual value of the effects against their cumulative frequencies. Arranged in decreasing order, the values of effects on the x-axis are plotted against cumulative percent frequencies on the y-axis to form a curve. On the same graph, bar graphs of effects on the x-axis are arranged in decreasing order and plotted against percent frequencies on the y-axis. A line is drawn at the 80% mark on the y-axis parallel to the x-axis then dropped to the x-axis at the point of intersection with the curve. This point on the x-axis separates the significant effects from the non-significant effects (Quality guide, 2012).

Optimization

Optimization of factors (Chapter 6) was carried out after screening so as to predict the response values for all possible combinations of the significant factors within the experimental range and to identify the optimum point. The response surface methodology (RSM) was used in the optimization of significant factors. RSM is a collection of statistical and mathematical methods that are useful for modeling and analyzing problems. In this technique, the main objective is to optimize the response surface that is influenced by various process parameters. The RSM quantifies the relationship between the controllable input parameters and the response surface (Tripathy and Murthy, 2012). The design procedure for RSM (Simate et al., 2009; Tripathy and Murthy, 2012) used in this study had three stages as follows: (1) Designing and conducting of experiments (2) Deriving and developing a mathematical model (3) Finding the stationary points or optimal set of experimental parameters.

The optimization experiments were designed using the central composite rotatable design (CCRD) and the optimal set of parameters was determined mathematically. According to the NIST/SEMATECH e-Handbook of Statistical Methods (2012), a CCRD contains an imbedded factorial or fractional factorial design with centre points that is augmented with a group of 'star (axial)' points that allow estimation of curvature. If the distance from the centre of the design space to a factorial point ±1 unit for each factor, the distance from the centre of the design space to the star (axial) point is $\pm\alpha$ with $\alpha>1$. The precise value of α depends on certain properties desired for the design and on the number of factors involved. A CCRD with k factors has $2k$ star (axial) points. The star (axial) points establish new extreme values (low and high) for each factor in the design. This design has circular, spherical or hyper-spherical symmetry hence rotatable. To

maintain rotatability, the value of α depends on the number of experimental runs in the factorial portion of the CCRD.

For a full factorial, $\alpha = 2^{k(\frac{1}{4})}$ (3.2)

Where, $k = number\ of\ factors(variables)$

In the CCRD method the factorial designs were augmented with axial designs and a quadratic response surface model of the form (Simate et al., 2009; Tripathy and Murthy, 2012):

$$y = \beta_o + \sum_{i=1}^{k} \beta_i x_i + \sum_{i=1}^{k} \beta_{ii} x_i^2 + \sum_{i=1}^{k} \sum_{j=i+1}^{k} \beta_{ij} x_i x_j + \varepsilon \quad \text{(3.3)}$$

was fitted and solved using the method of least squares.

In **Equation 3.3**, y is the predicted response, β_o is the coefficient for intercept, β_i is the coefficient of linear effect, β_{ii} is the coefficient of quadratic effect, β_{ij} is the coefficient of interaction effect, ε is a term that represents other sources of variability not accounted for by the response function, k is the number of variables, x_i and x_j are coded predictor variables for the independent factors.

After determination of the coefficients of the regression model, the adequacies of the model were checked using the analysis of variance (ANOVA). To do the analysis, ANOVA uses the following methods:

- Fisher's variance ratio test (F-*test*), *to test evidence of lack of fit and significance of the regression model.*
- Standard errors of model coefficients (t-*test*), *to determine significance of regression coefficients of parameters; intercept term, linear terms, quadratic terms and interaction terms.*
- The coefficient of determination (R^2), *to check model accuracy; comparison between experimental results and predicted values obtained using the refitted model.*
- The absolute average deviation (AAD), *to check model plausibility; if found plausible, then the model can be used to predict response values at any regime in the interval of the experimental design.*

The coefficients of the regression model were estimated by fitting experimental results using Design Expert® 6 software. Design Expert® is a registered trademark of Stat-Ease, Incorporation, Minneapolis, USA (Design Expert® 6 manual, 2010).

3.2.5 Acid Leaching of CFA

The sulphuric acid leaching experiment consisted of a 500ml volumetric flask, a thermal reciprocal shaking bath and a filter funnel fitted with filter paper. The filter funnel was mounted on the 1000ml Erlenmeyer flask. Leaching experiments comprised of adding a weighted CFA sample, typically 50g, to the volumetric flask containing sulphuric acid then agitating the resulting slurry in a constant temperature reciprocal shaking bath shown in **Figure 3.3**. Separate samples were used for each allotted leaching condition. The leaching variables were acid concentration, time, temperature and solid to liquid ratio at a constant rate of 150 rpm. After leaching, the leached residual CFA was separated from the solution by filtration. Distilled water was used to remove all of the residual liquor that was absorbed by the leached ash. Subsequently, the leach liquor and wash solution were combined to produce the final leach liquor. The total volume of the final leach liquor was recorded. The dry residual CFA was analysed by X-ray fluorescence (XRF), X-ray diffraction (XRD) and the corresponding leach liquor by Inductively Coupled Plasma-Optical Emission Spectrometry (ICP-OES).

Figure 3.3 Agitation leaching test equipment (Reciprocal Shaking Bath, Model: 207, supplied by MERCK, South Africa)

To determine the possible influence of factors on the response (aluminium extraction) and to identify their appropriate upper and lower limits, preliminary leach tests were conducted. Leaching variables investigated included acid concentration, leaching time, temperature and solid to liquid ratio at a constant agitation rate of 150 rpm. The leaching conditions for the preliminary leach tests are given in **Table 3.3.**

TABLE 3.3 Sulphuric acid leaching conditions for the preliminary leach tests

Experiment run	Leaching Condition				
	Leaching Temperature (^{o}C)	Leaching Time (hrs)	Acid concentration (M)	Solid to Liquid ratio	Agitation Rate (rpm)
At different temperatures	30, 45, 60, 75, 80, 85	8	6	1:4	150
At different leaching times	60	4, 6, 8, 10,12	6	1:4	150
At different acid concentrations	60	8	2, 4, 6, 8, 10	1:4	150
At different solid to liquid ratios	60	8	6	1:2, 1:3, 1:4, 1:5, 1:6	150

To determine the effect of calcium sulphate formation on aluminium extraction, residue CFA was collected and analyzed for calcium sulphate content. Leaching variables investigated included acid concentration, temperature and solid to liquid ratio. The leaching conditions for the calcium sulphate experiment are given in **Table 3.4**.

TABLE 3.4 Sulphuric acid leaching conditions for effect of CaSO4 on the dissolution behaviour of CFA

Experiment run	Leaching condition				
	Leaching Temperature (^oC)	Leaching Time (hrs)	Acid concentration (M)	Solid to Liquid ratio	Agitation Rate (rpm)
At different temperatures	30,45, 60, 75, 85	8	6	1:4	150
At different acid concentrations	75	8	2, 4, 6, 8, 10	1:4	150
At different solid to liquid ratios	75	8	6	1:2, 1:3, 1:4, 1:5, 1:6	150

To determine the kinetics of dissolving alumina, the change in the rate of dissolution was observed, at three different temperatures, by monitoring the variation of aluminium sulphate [$Al_2(SO_4)_3$] concentration with time. The experimental procedure consisted of collecting 7mL aliquots at different times during the leaching reaction. The aliquot samples were filtered and the leach liquor was submitted for the analysis of Al concentration. The leaching conditions for the kinetics experiments are given in **Table 3.5**.

TABLE 3.5 Sulphuric acid leaching conditions for the kinetics experiments

Experiment Run	Leaching Condition				
	Leaching Temperature (^oC)	Aliquot Sampling Times (hrs)	Acid concentration (M)	Solid to Liquid ratio	Agitation Rate (rpm)
Run1	50	0.1, 0.3, 0.5, 1.5, 3, 8, 10	6	1:4	150
Run2	70	0.1, 0.3, 0.5, 1.5, 3, 8, 10	6	1:4	150
Run 3	82	0.1, 0.3, 0.5, 1.5, 3, 8, 10	6	1:4	150

3.2.6 Pelletization

The residue-CFA from the first leaching stage was pelletized with fine coal and calcium carbonate in the mass ratio of 5:4:1 to produce pellets that were strong enough to withstand sintering conditions in the muffle furnace. The residue-CFA, calcium carbonate and fine coal (100% passing 212 µm size fraction) was mixed with 10-20% water and pelletized to form 4-6mm spherical pellets for the sintering and leaching steps. The pellets were air-dried for 48 hrs for easy handling. In order to compare the two-step acid leach extraction results with the lime-sinter single-step acid leach, Raw-CFA was also pelletized and sintered using the same pelletization and sintering conditions as for residue-CFA.

3.2.7 Sintering of Pellets

Sintering was carried out under atmospheric conditions by using a muffle chamber furnace shown in **Figure 3.4**. Dry pellets were placed into an alumina crucible, mounted in a muffle furnace and heated to a temperature of 1150°C for 180 minutes to produce sintered pellets for stage two leaching.

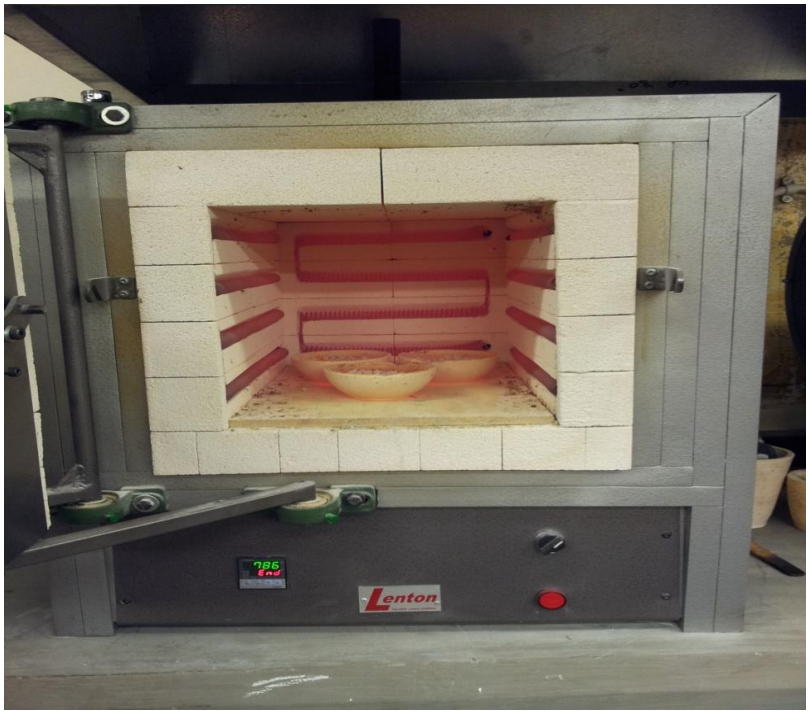

Figure 3.4 Sintering equipment; the 1300°C muffle chamber furnace (Model: LLC 13/42-PA, supplied by LENTON Furnaces, South Africa)

3.2.8 Post-sinter Leaching of the Sintered Pellets

Sintered pellets were crushed and ground to a course powder (100% passing 212µm) then leached with a 6M sulphuric acid solution as per the previously described acid leaching procedure. After leaching, the leached CFA and leach liquor mixture were filtered, residues were washed with distilled water and the final volume of the filtrate was recorded. The dry residue-CFA was analysed using X-ray fluorescence (XRF) and X-ray diffraction (XRD), and the corresponding leach liquor was analysed using Inductively Coupled Plasma- Optical Emission Spectrometry (ICP-OES).

3.2.9 Experimental Design

Table 3.6 shows the experimental design indicating test conditions, samples tested and the number of replicates in each experimental test.

Table 3.6 Experimental design

Test Type	Test Conditions	Materials/Samples Tested (Sulphuric acid was used in all leaching tests)	Replicates
Preliminary Acid Leaching Tests	• Acid concentration • Leaching time • Leaching temperature • Solid to liquid ratio	• Raw CFA	2
Identification of influential parameters	• Acid concentration • Leaching time • Leaching temperature • Solid to liquid ratio	• Raw CFA	2
Optimization of influential factors	• Leaching time • Leaching temperature	• Raw CFA	2
Post-sinter (second stage) leaching	• Acid concentration • Leaching time • Leaching temperature • Solid to liquid ratio	• Residue sintered CFA	2

All the tests were done at a constant agitation rate of 150 rpm

3.3 Data Analysis

The data was obtained as described in the foregoing sections of this chapter. The data obtained was used to determine relationships between aluminium extraction (the desired response) and the parameters tested. The experimental results and the relationships are discussed in the subsequent chapters of this dissertation. The aluminium extraction was calculated as a percentage of the aluminium in the liquid phase to that in CFA.

CHAPTER FOUR

PRELIMINARY ACID LEACHING

4.1 Introduction

The global demand for metal resources is increasing rapidly (Halada et al., 2008), and this increase in demand is closely linked to world economic growth. The development of major nations and advances in technologies are fuelling ever more demand. This has motivated more studies into resource recovery of valuable metals from primary as well as alternative secondary resources. Recently, much attention from the scientific community has been paid to research connected with the recovery of alumina from alternative alumina sources such as CFA using acidic routes. This is so because an economic process for recovering alumina from readily available CFA is needed.

The possibility of using an indirect acid leach method to process CFA has been discussed in section 2.4.3. The indirect leach process employs a pre-sinter and post-sinter (two-step acid leach) method to achieve optimum aluminium extraction from CFA.

In order to explore the possible influence of factors on the aluminium extraction and to identify their appropriate upper and lower limits, preliminary leach tests were initially conducted according to the procedure previously described in section 3.2.5. In addition, this study looks at alumina dissolution kinetics and the role of $CaSO_4$ in the dissolution behaviour of CFA by investigating the effect of parameters such as acid concentration, leaching temperature, leaching time and solid to liquid ratio at a constant agitation rate of 150 rpm. This understanding will be used as a basis for the subsequent screening, optimization and indirect acid leaching studies that follow from Chapter 5 to Chapter 7.

In order to describe the rate controlling mechanism for alumina dissolution, an attempt was made to fit the experimental kinetic data into the shrinking core model. Furthermore, the physical and chemical properties of CFA, such as the elemental composition of CFA by particle size, were investigated in order to understand the response of CFA to the beneficiation process.

4.2 Results and Discussion

4.2.1 Elemental Composition of CFA by Particle Size

The elemental composition of CFA in the size range of -38µm and +212µm is presented in **Table 4.1**. The results show a narrow CFA grade range. This indicates that the particle size of CFA may not have much influence on the extent of aluminium extraction as seen from the narrow grade range.

Table.4.1 Elemental composition of CFA by particle size

Size Fraction (µm)	< 38	+38	+45	+53	+63	+75	+106	+150	+212
Mass retained (wt)	174	39	72	7	386	148	186	71	34
Mass retained (%)	16	3	6	1	35	13	17	6	3
Al_2O_3 (wt %)	31.59	30.13	30.83	29.27	30.60	29.95	29.47	29.16	30.02

4.2.2 Effect of Temperature

The effect of temperature on aluminium extraction from CFA by sulphuric acid leaching to form $Al_2 (SO_4)_3$ is presented in **Figure 4.1**. The figure shows an increase in aluminium extraction with increase in temperature. An extraction of 10.0% was obtained at 30°C, 14.6% at 45°C, 16.5% at 60°C, 23.5% at 75°C, 22.9% at 80°C and 23.1% at 85°C. The figure illustrates that extraction increased with temperature up to 75°C with slight fluctuations in extractions between 75°C and 85°C. For this reason, 75°C was adopted as the appropriate leaching temperature. Higher aluminium extractions at higher temperatures were attributed to the fact that molecules at higher temperatures have more thermal energy required for effective reaction.

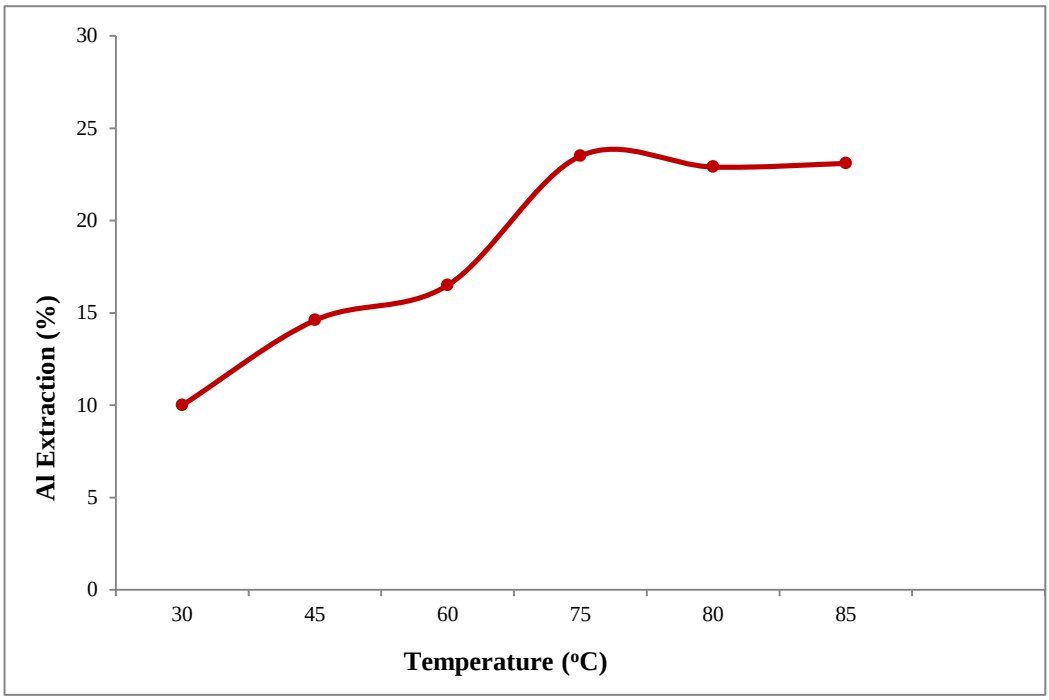

Figure 4.1 Effect of temperature on acid leaching of CFA

4.2.3 Effect of Time

The effect of time on aluminium extraction from CFA by sulphuric acid leaching is presented in **Figure 4.2.** The figure shows that extraction increased with increase in leaching time from 4hrs to 6hrs. An aluminium extraction of 13.9% was obtained after 4hrs of reaction, 16.8% after 6hrs, 16.5% after 8hrs, 17.7% after 10 hrs and 16.4% after 12hrs. The figure illustrates that extraction increased with increase in leaching time from 4hrs to 6 hrs with slight variations thereafter. Leaching beyond 6 hrs did not improve extraction to any great extent. This may have been due to the accumulation of calcium sulphate or any other product layer that covered the CFA and prevented the acid attack over time (Seidel et al., 1998) as the leaching temperature was kept constant at 60°C. Therefore, 6 hrs was adopted as the appropriate leaching time.

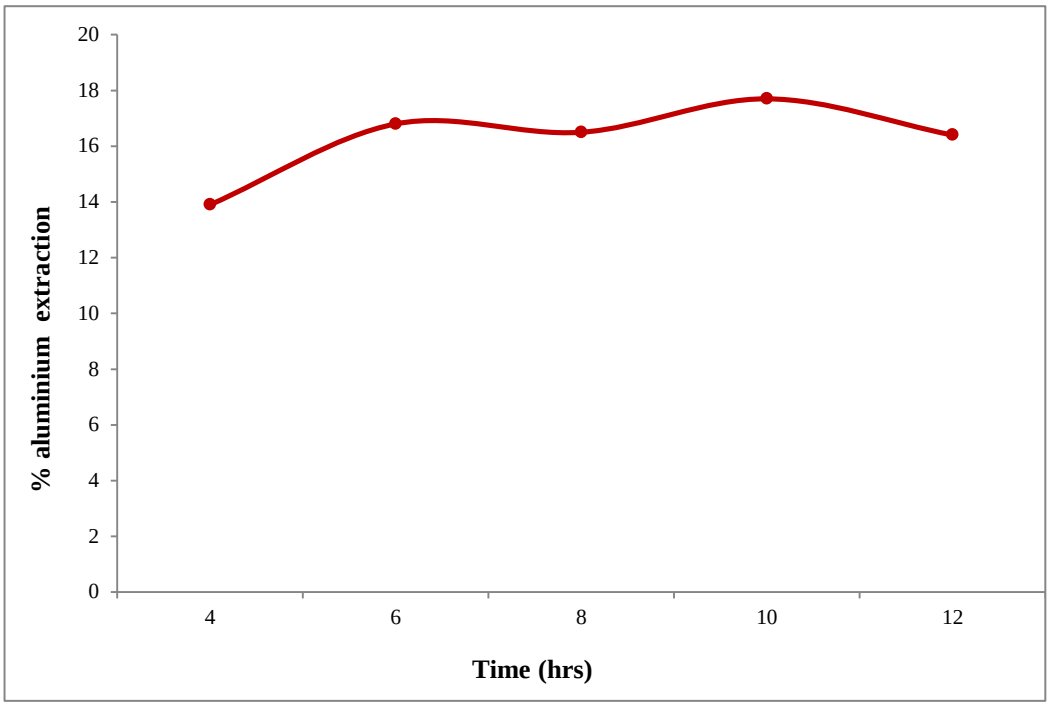

Figure 4.2 Effect of leaching time on acid leaching of CFA

4.2.4 Effect of Acid Concentration

The effect of sulphuric acid concentration on aluminium extraction is presented in **Figure 4.3.** The figure shows 15.7% aluminium extraction at 2M, 16.6% at 4M, 16.5% at 6M, 14.8% at 8M and 10.9% at 10M. Results show a decrease in aluminium extraction beyond 6M acid concentration. The decrease at higher acid concentration is probably due to low mass transfer rates of reactants and products caused by the increase in $CaSO_4$ formation in the slurry mixture. A similar phenomenon was also observed by Seidel and co-workers (1998). The authors postulated that increasing acid concentration produces two opposing effects simultaneously. An increase in the hydronium ion enhances the dissolution of alumina, whereas the increase in the concentration of the sulphate and dissolved calcium ions intensifies the formation of calcium sulphate precipitates. The precipitates hinder mass transfer across the ash particle thus inhibiting alumina dissolution. Based on this information, 6M was adopted as the appropriate acid concentration.

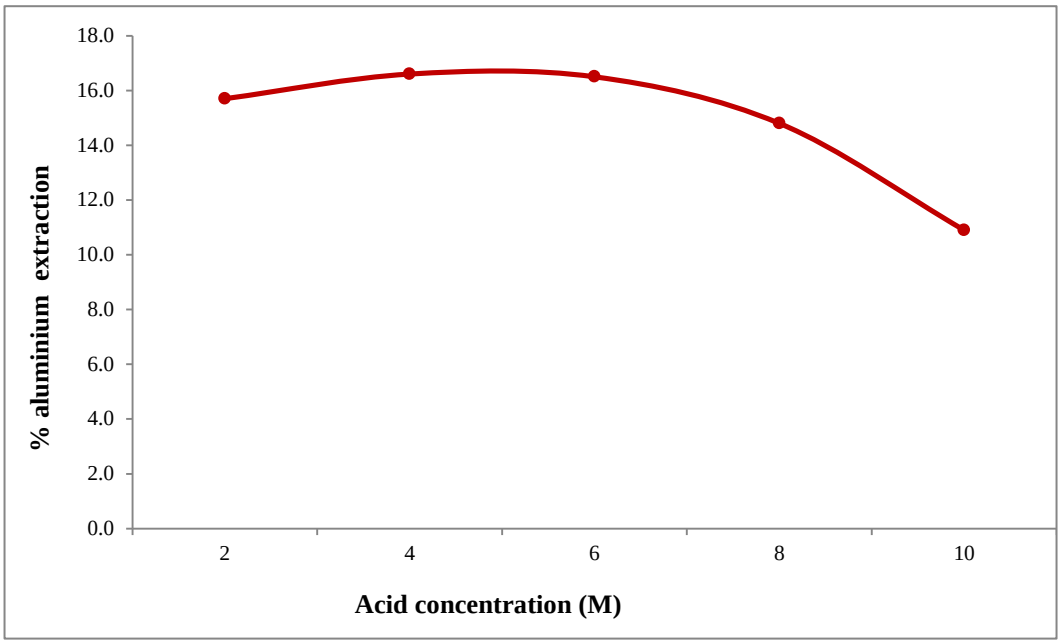

Figure 4.3 Effect of acid concentration on acid leaching of CFA

4.2.5 Effect of Solid to Liquid ratio

The effect of solid to liquid ratio is presented in **Figure 4.4.** The figure shows 15.0% aluminium extraction at 1:2 solid to liquid ratio, 15.4% at 1:3, 16.5% at 1:4, 16.2% at 1:5 and 14.8% at 1:6. Results show an optimum solid to liquid ratio of about 1:4 with much lower extractions on either side. The solid to liquid ratio is a representation of the ratio of weight of solids to volume of acid. A decrease in solid to liquid ratio therefore implies an increase in acid volume while the amount of solids remains constant. Increased acid volume creates a less dense slurry mixture, frees up ash particles creating additional surface area for contact between reactants. Larger surface areas for contact, in particular solid ones in heterogeneous systems, lead to higher reaction rates. An increase in both the ash particle surface contact and the hydronium ion enhances the dissolution of aluminium; whereas the increase in the ash particle surface contact and the sulphate ions and dissolved calcium ions intensifies the formation of calcium sulphate precipitates. The precipitates obstruct mass transfer across the CFA particle thus slowing down the reaction, inhibiting alumina dissolution and consequently causing lower aluminium extraction.

The decreased aluminium extraction for the solid to liquid ratio greater than 1:4 was probably due to low mass transfer rates of reactants and products caused by the increased density of the

CFA reaction mixture. This may have caused the particles not to be suspended efficiently in the solution as the stirring rate was kept constant. Based on this information, 1:4 was therefore adopted as the appropriate solid to liquid ratio.

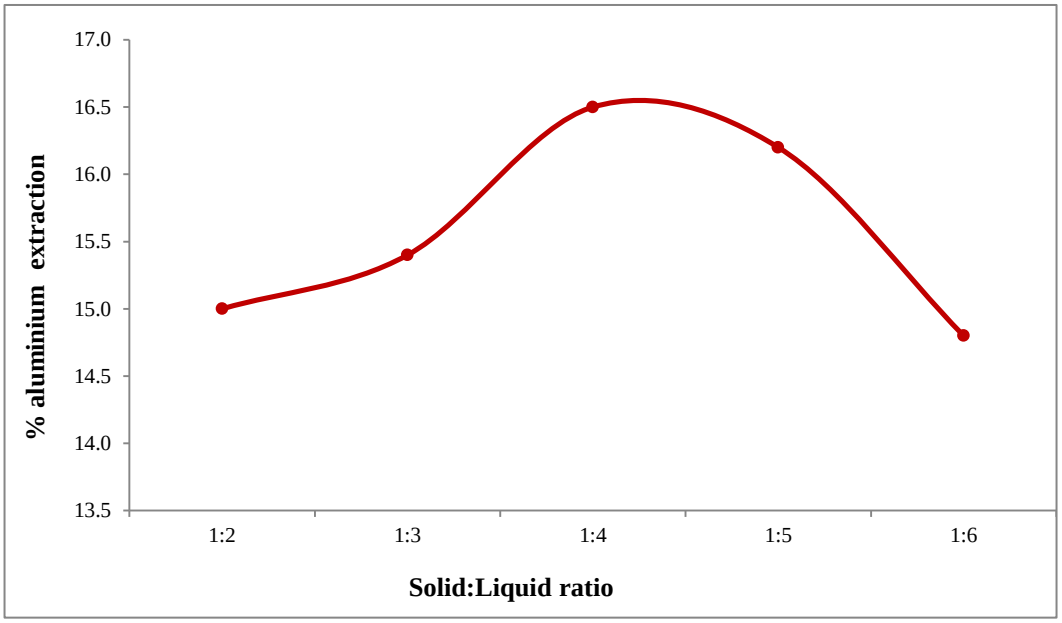

Figure 4.4 Effect of solid to liquid ratio on acid leaching of CFA

4.2.6 Role of Calcium Sulphate in the Dissolution Behaviour of CFA

CFA is formed under oxidizing conditions when coal is combusted at temperatures in excess of 1400°C to form metal oxides and other non-combustible ash residues. In these combustion reactions, vaporized compounds adsorb onto the outer surface layer of the CFA ash particle thus enriching it in carbon, potassium, sodium, calcium and magnesium (Landman, 2003). The ash particle outer layer is rich in calcium, the middle layer is predominantly rich in sodium and the inner layer is rich in sodium, silicon and aluminium (Sakamoto et al., 2003; Landman, 2003).

Calcium is present in these ashes, in form of CaO, as the third major constituent after silica and alumina. When reacted with sulphuric acid solution and by virtue of its outer layer position, calcium is predisposed to form a calcium sulphate precipitate layer which can encapsulate the CFA ash particle. The precipitate layer may hinder the mass transfer of reactants and products to and from the unreacted core of the ash particle thus adversely affecting alumina dissolution in CFA. When investigating the effect of parameters on calcium sulphate formation, 8 hrs leaching

time was chosen, instead of the 6 hrs preferred as appropriate in preliminary tests, in order to allow for as much calcium sulphate formation as possible.

Effect of acid concentration on calcium sulphate formation

The effect of acid concentration on calcium sulphate formation is presented in **Figure 4.5.** The figure shows a decrease in calcium sulphate formation between 2M and 6M acid concentration. The decrease in calcium sulphate formation may be attributed to other metal ions competing for sulphate ions in the acidic solution. The figure also shows that a decrease in calcium sulphate formation corresponds to an increase in aluminium extraction and vice versa thus indicating that calcium sulphate formation has an effect on alumina dissolution. The decrease in calcium sulphate formation may be attributed to other metal ions competing for sulphate ions in the acidic solution.

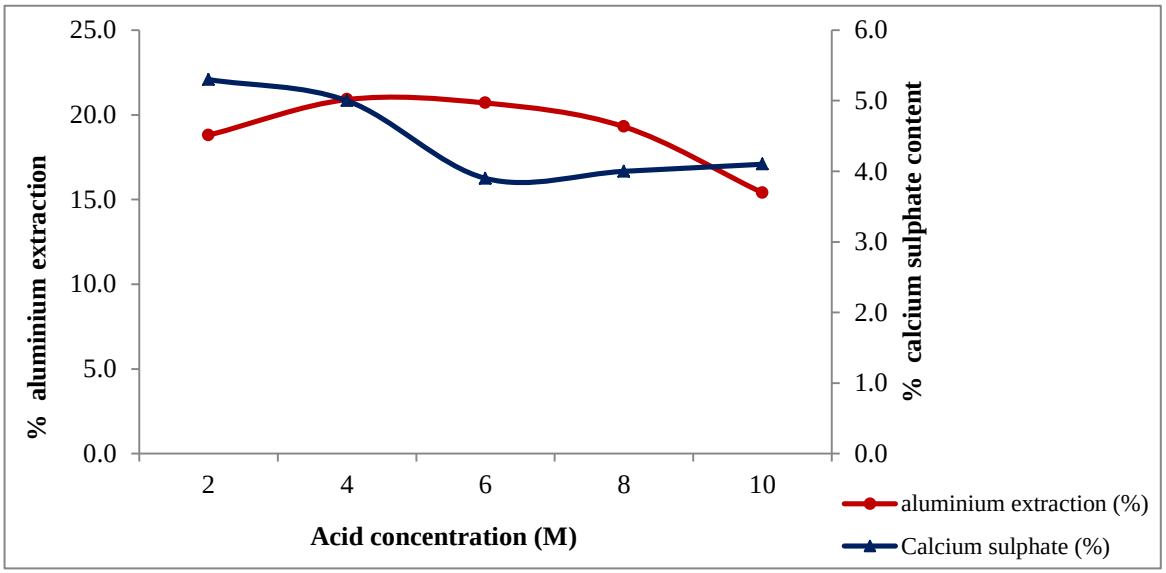

Figure 4.5 Effect of acid concentration on calcium sulphate formation at 75°C temperature; 8hrs, leaching time; 1:4, solid to liquid ratio

Effect of temperature on calcium sulphate formation

The effect of temperature on calcium sulphate formation is presented in **Figure 4.6.** The calcium sulphate formation was measured using XRD technique as mentioned in section 3.2.1. The figure shows an increase in calcium sulphate formation with increase in temperature. In contrast, to the

formation of precipitates, there is no decrease in aluminium extraction. This shows that much as the calcium sulphate precipitate formation was favoured at higher temperatures, the precipitate layer allowed the reactants to reach the unreacted core of the ash particle hence promoting alumina dissolution. This indicates that there could have been some permeability in the product layer. It, therefore, seems possible that high temperatures may have been helpful in breaking down the calcium sulphate precipitate layer obstruction hence causing the alumina dissolution reaction to proceed at a faster rate.

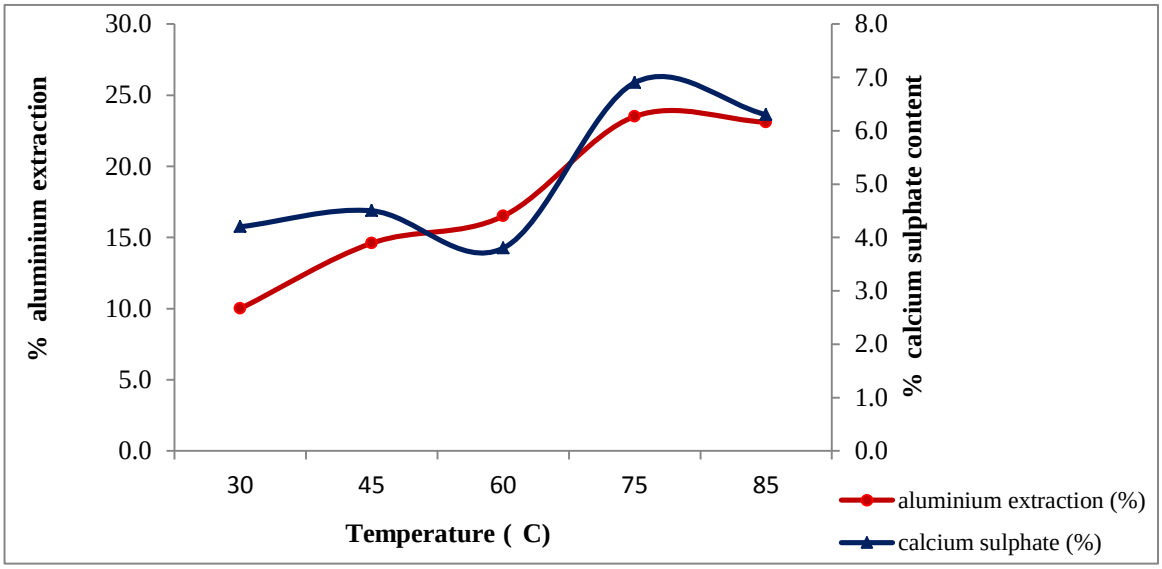

Figure 4.6 Effect of temperature on calcium sulphate formation at 6M, acid concentration; 8hrs, leaching time; 1:4, solid to liquid ratio

Effect of solid to liquid ratio on calcium sulphate formation

The effect of solid to liquid ratio on calcium sulphate formation is presented in **Figure 4.7.** The figure shows a decrease in calcium sulphate formation between the solid to liquid ratio of 1:2 and 1:4. The decrease in calcium sulphate formation may be attributed to other metal ions competing for sulphate ions in the acidic solution. However, further decrease in the solid to liquid ratio below 1:4 made more sulphate ions available resulting in increased calcium sulphate formation and a decrease in aluminium extraction.

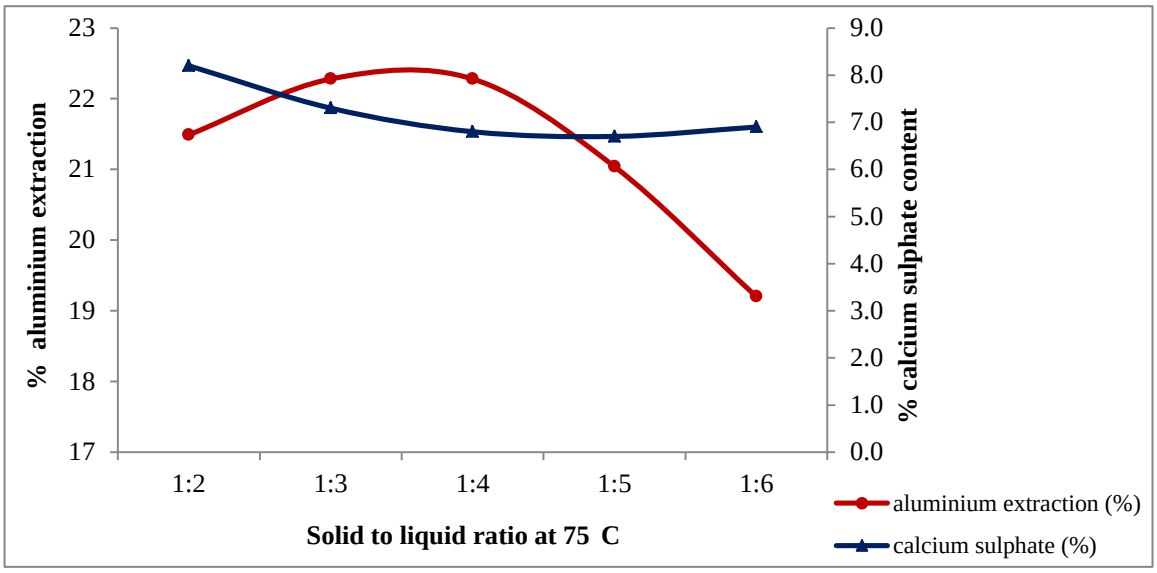

Figure 4.7 Effect of solid to liquid ratio on calcium sulphate formation at 75°C, temperature; 6M, acid concentration; 8hrs, leaching time

4.2.7 Kinetic Analysis

Rate controlling mechanisms

The dissolution rates of CFA were analyzed on the basis of the shrinking extraction type core model under the assumption that the material consists of homogeneous spherical solid particles that react isothermally with the fluid media (Gbor and Jia, 2004).

To determine the rate controlling regime, experimental results at different temperatures were plotted in terms of the standard equations of the shrinking core model. The reaction kinetic models are represented by linear kinetic equations, $x = kt$ for film diffusion control; $1- (1-x)^{1/3} = kt$, for chemical reaction control and $1-3(1-x)^{2/3} + 2(1-x) = kt$, for product layer (ash) diffusion control, where $\boldsymbol{x}$ is the conversion, $\boldsymbol{t}$ is the time in hours and $\boldsymbol{k}$ is the reaction rate constant (hr^{-1}). All the kinetics experiments were conducted with 6M acid concentration, 1:4 solid to liquid ratio and 10 hours leaching time. The leaching time in kinetics experiments was extended to 10 hours in order to allow for as much extraction as possible.

The kinetic equations as functions of time at a temperature of 50°C were plotted and are presented in **Figures 4.8** to **4.10**.

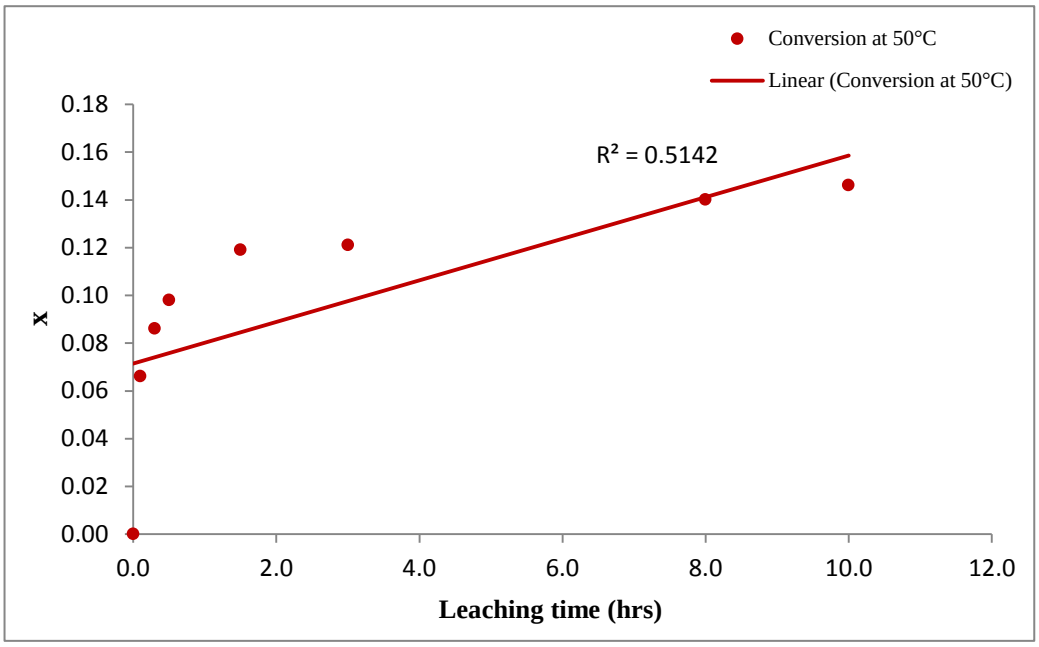

Figure 4.8 Plot of *x* versus *time* for the acid leaching of CFA at 50°C

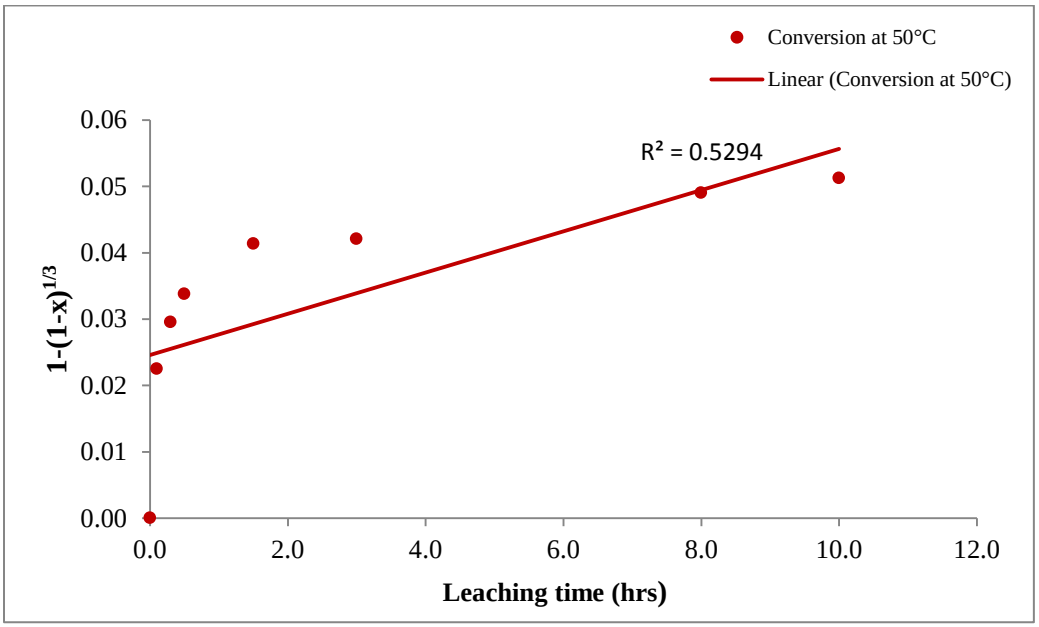

Figure 4.9 Plot of *1- (1-x)$^{1/3}$* versus *time* for the acid leaching of CFA at 50°C

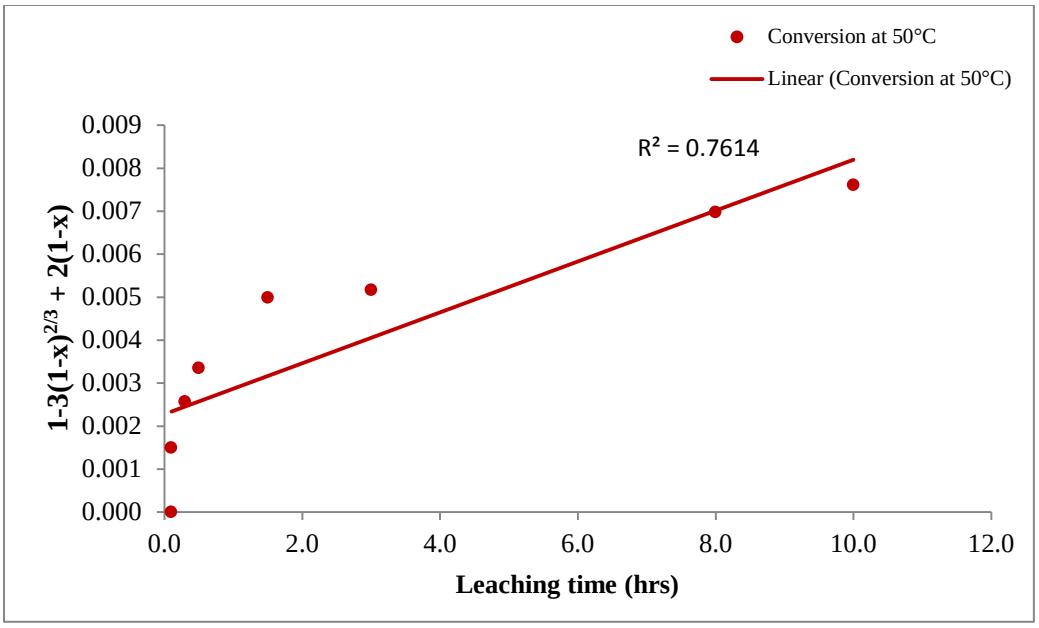

Figure 4.10 Plot of *1- 3(1-x)$^{2/3}$ + 2(1-x)* versus *time* for the acid leaching of CFA at 50°C

Examination of the kinetic equation plots as functions of time at 50°C did not give perfectly fitting straight lines. However, from the three kinetic equation plots, the plot with a linear correlation coefficient of 84.17% (**Figure 4.10**) shows a better fitting straight line. This indicates that the alumina dissolution rate at 50°C was better modelled by the reaction kinetic model represented by kinetic equation $1\text{-}3(1\text{-}x)^{2/3} + 2(1\text{-}x) = kt$ for product layer diffusion control.

The kinetic equations as functions of time at a temperature of 70°C were plotted and are presented in **Figures 4.11** to **4.13**.

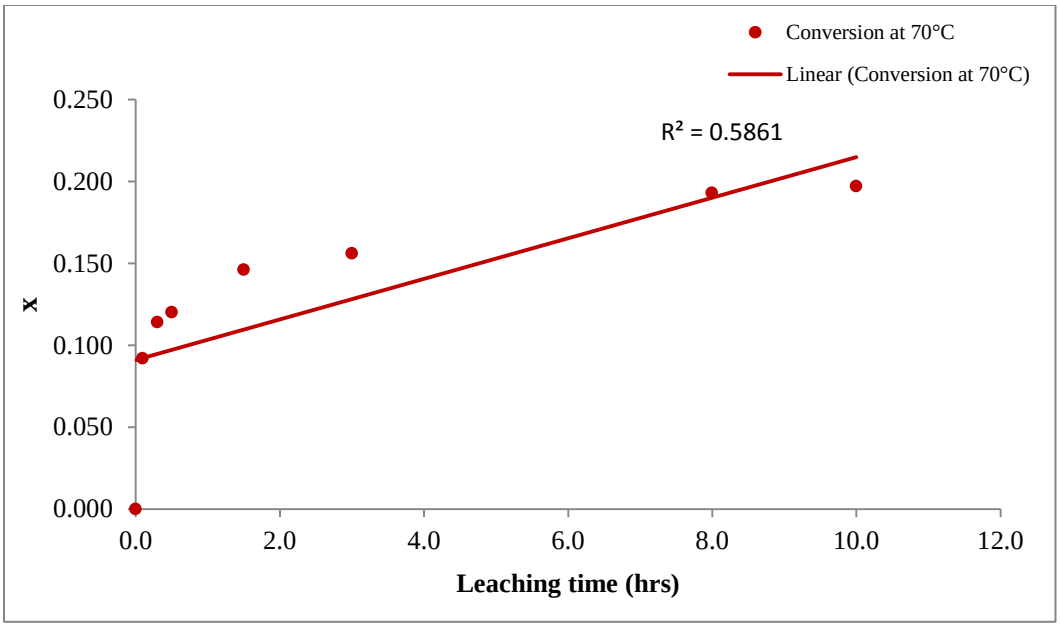

Figure 4.11 Plot of *x* versus *time* for the acid leaching of CFA at 70°C

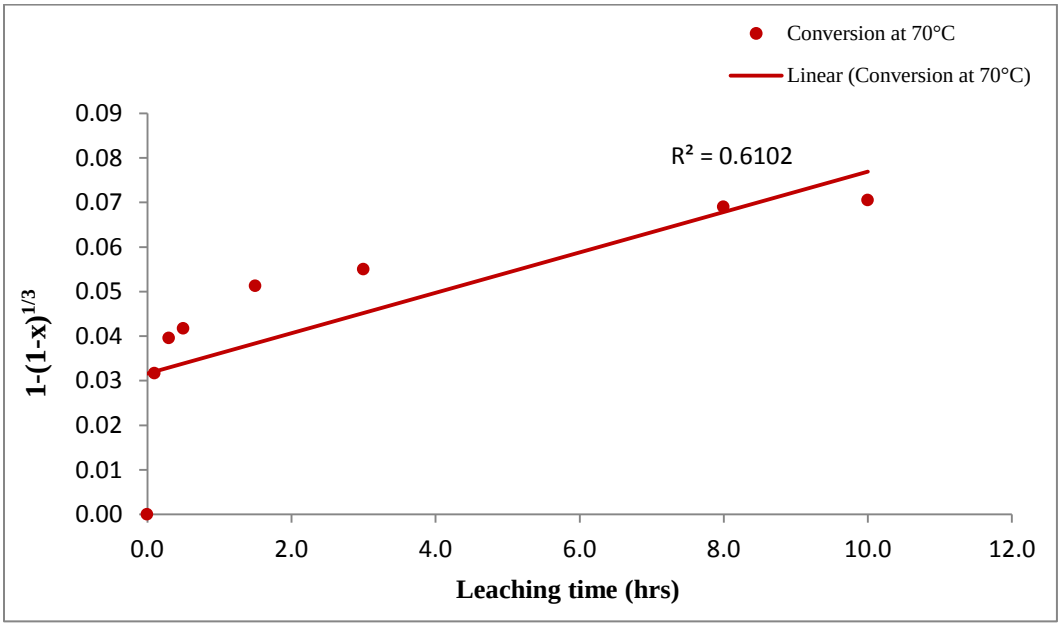

Figure 4.12 Plot of *1- (1-x)$^{1/3}$* versus *time* for the acid leaching of CFA at 70°C

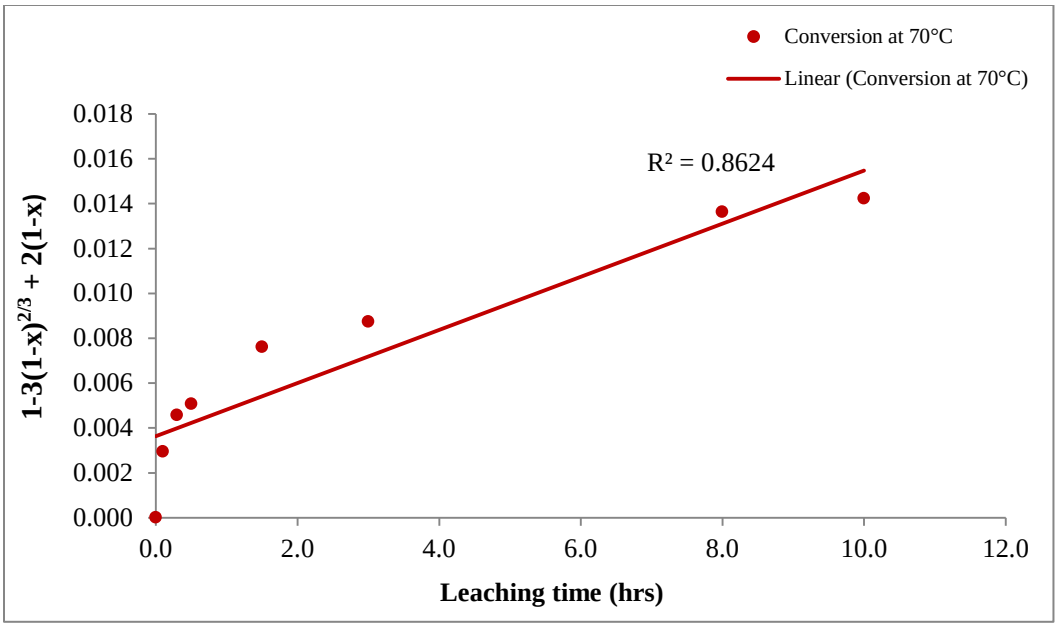

Figure 4.13 Plot of *1- 3(1-x)$^{2/3}$ + 2(1-x)* versus *time* for the acid leaching of CFA at 70°C

Analysis of the kinetic equation plots as functions of time at 70°C did not give perfectly fitting straight lines either. However, from the three kinetic equation plots, the plot with a linear correlation coefficient of 88.34% (**Figure 4.12**) shows a better fitting straight line. This indicates that the alumina dissolution rate at 70°C was better modelled by the reaction kinetic model represented by kinetic equation *1- (1-x)$^{1/3}$ = kt*, for chemical reaction control.

The kinetic equations as functions of time at a temperature of 82°C were plotted and are presented in **Figures 4.14** to **4.16**.

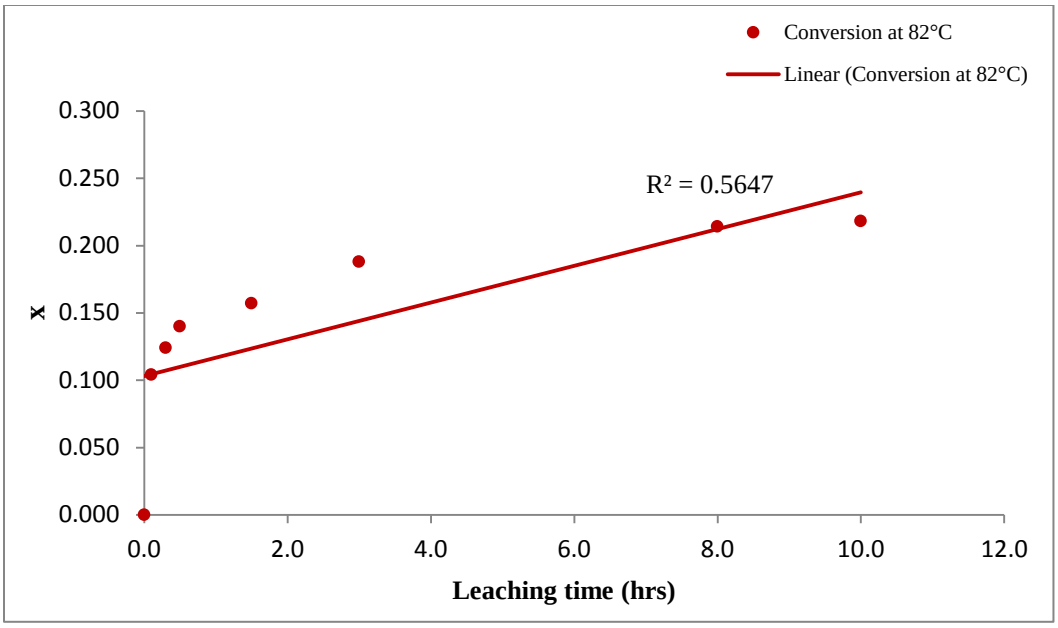

Figure 4.14 Plot of *x* versus *time* for the acid leaching of CFA at 82°C

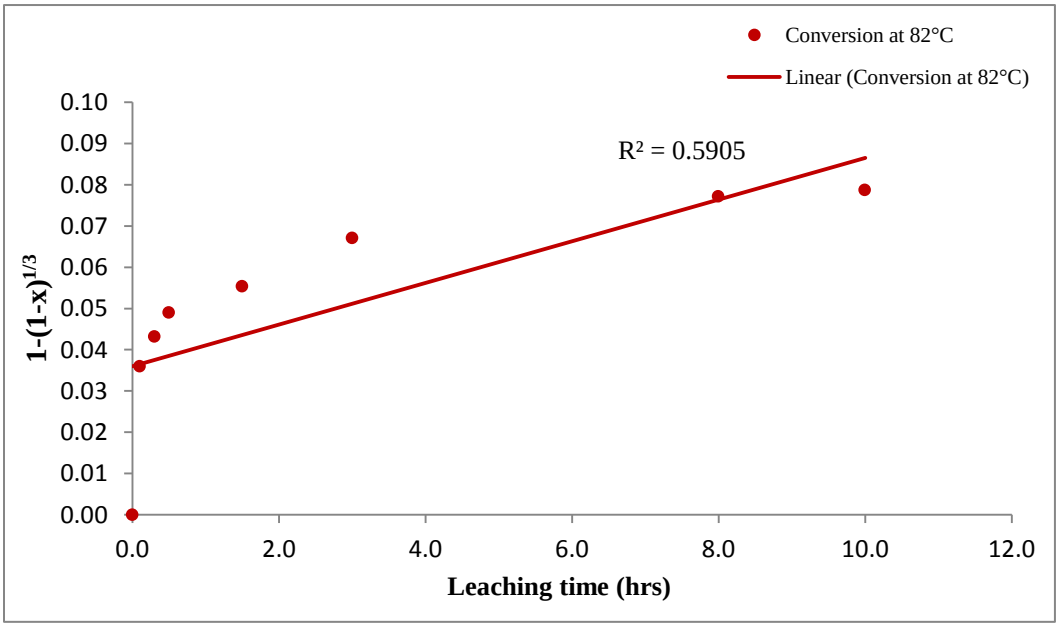

Figure 4.15 Plot of *1- (1-x)$^{1/3}$* versus *time* for the acid leaching of CFA at 82°C

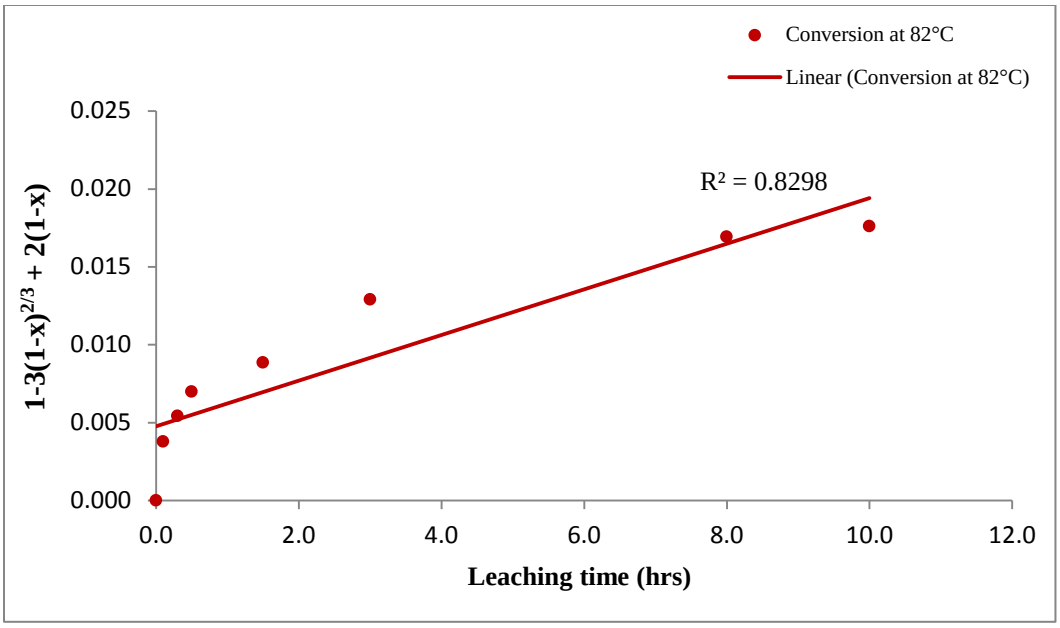

Figure 4.16 Plot of *1- 3(1-x)$^{2/3}$ + 2(1-x)* versus *time* for the acid leaching of CFA at 82°C

Analysis of the kinetic equation plots as functions of time at 82°C did not give perfectly fitting straight lines. However, from the three kinetic equation plots, the plot with a linear correlation coefficient of 82.98% (**Figure 4.16)** shows a better fitting straight line. This shows that the alumina dissolution rate at 82°C was better modelled by the reaction kinetic model represented by kinetic equation $1\text{-}3(1\text{-}x)^{2/3} + 2(1\text{-}x) = kt$ for product layer diffusion control.

From the analysis of the models, it was found that the dissolution rates at temperatures of 50°C, and 82°C were better expressed by the reaction kinetic model represented by kinetic equation $1\text{-}3(1\text{-}x)^{2/3} + 2(1\text{-}x) = kt$ for product layer diffusion control. However, the dissolution rate at 70°C was better expressed by the reaction kinetic model represented by kinetic equation $1\text{-}(1\text{-}x)^{1/3} = kt$, for chemical reaction control. This inconsistency may have been due to the effect of the non-coupling of the PSD to the shrinking core model as postulated by Gbor and Jia (2004). The coupling of PSD to the shrinking core model was not done in this study. Much as the CFA particle size may not have had much influence on the extent of aluminium extraction, not coupling the PSD with the shrinking core model may have caused erroneous shifts in the control regime. Therefore, in order to accurately predict the control regime in the leaching of CFA, the

use of a model that takes into account the coupling of PSD to the shrinking core model may be required.

In the following section, the activation energy was used as an alternative method for examining rate controlling mechanisms for the same aluminum extraction process.

Determination of Activation Energies

The Arrhenius equation gives a quantitative relation between the ***rate constant*** (***k)*** and ***temperature (T)*** according to **Equation 4.1**:

$$\boldsymbol{k = Ae^{\frac{-E_a}{RT}}} \qquad (4.1)$$

Where ***A*** is the ***frequency factor,*** $\boldsymbol{E_a}$ is the ***activation energy, R*** is the gas constant = 8.314 ($J \cdot mol^{-1} \cdot K^{-1}$) and ***T*** is the absolute temperature in Kelvin (*K*).

For a process run at two known temperatures and/or rate constants, **Equation 4.2** (Laidler, 1984; Logan, 1982; Chang, 2005; Segal, 1975), previously derived in section 2.4 may be used to determine activation energy ($\boldsymbol{E_a}$).

$$lnk_2 - lnk_1 = \frac{E_a}{R}\ \frac{1}{T_1} - \frac{1}{T_2} \qquad (4.2)$$

From the kinetics experiment, alumina dissolution in sulphuric acid solution was considered to proceed according to the following reaction:

$$CaO + Al_2O_3 + 4H_2SO_4 \rightarrow Al_2(SO_4)_3 + CaSO_4 + 4H_2O \qquad (4.3)$$

The changing rate in alumina dissolution was observed, at three different temperatures, by monitoring the concentration of aluminium sulphate [$Al_2(SO_4)_3$] with change in time as shown in **Figure 4.17**.

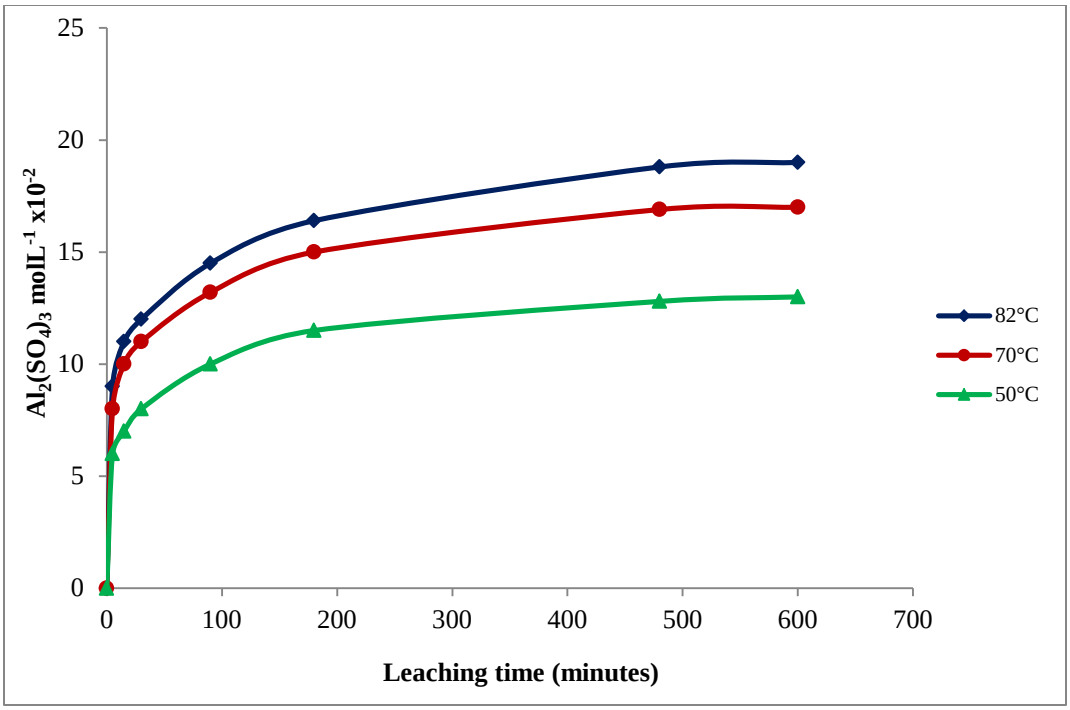

Figure 4.17 Variation of aluminium sulphate [$Al_2(SO_4)_3$] concentration with time

Using the graphs in **Figure 4.17**, the ***rate of reaction*** at any ***instant of time*** was determined by measuring the ***slopes of each curve*** at that ***time***. This also corresponds to the ***rate of reaction*** at an ***instant of concentration***. The ***rates of reaction*** were then plotted against ***concentration*** for each curve as shown in **Figures 4.18 to 4.20**.

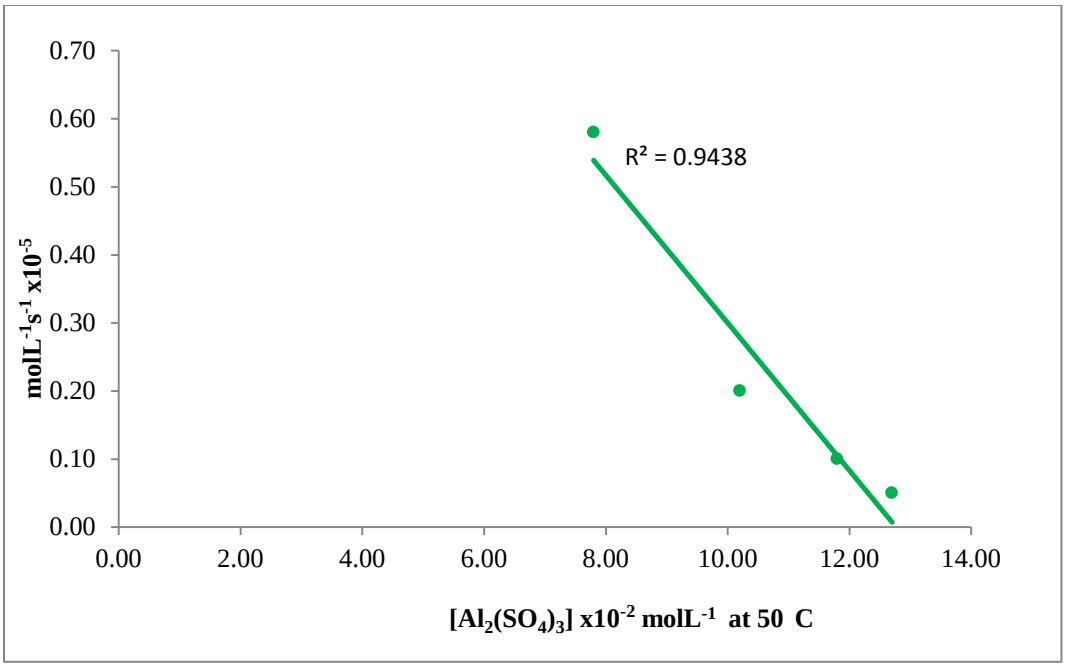

Figure 4.18 Variation of aluminium sulphate concentration with rate of reaction at 50°C

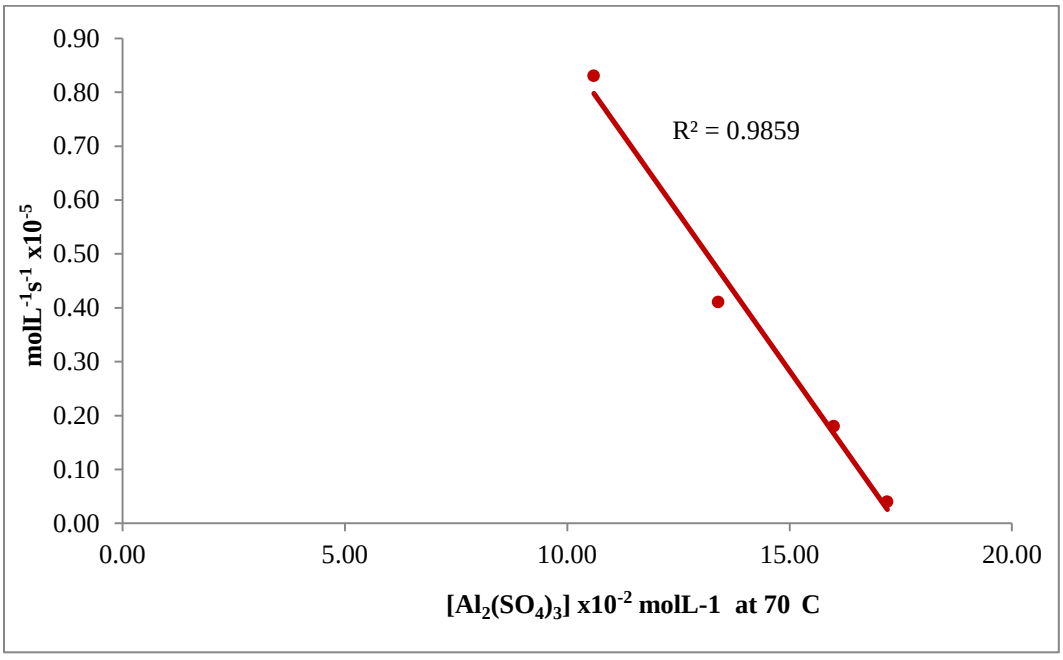

Figure 4.19 Variation of aluminium sulphate concentration with rate of reaction at 70°C

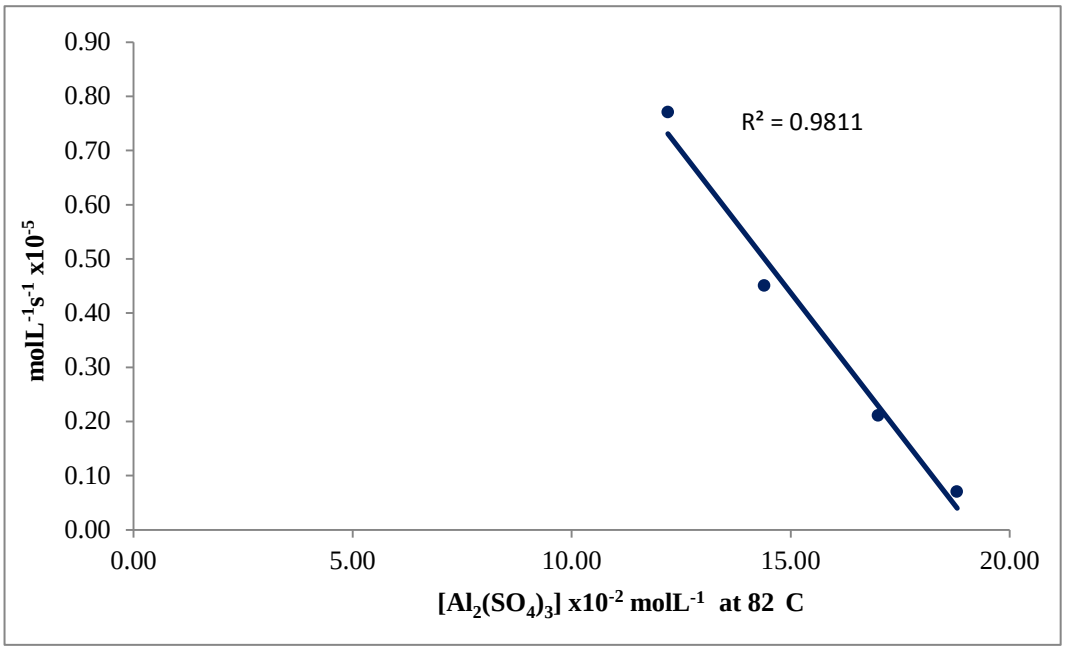

Figure 4.20 Variation of aluminium sulphate concentration with rate of reaction at 82°C

From the ***slopes*** of the ***rate of reaction versus concentration*** the values for the ***rate constants*** k_1 *at 50°C(323K),* k_2 *at 70°C(343K) and* k_3 *at 82°C(355K)* were determined as 6.3 x $10^{-5}s^{-1}$, 9.7 x$10^{-5}s^{-1}$ and 10.7 x10^{-5} s^{-1} respectively**.** Using the obtained ***k*** values and **Equation 4.2**, the calculated activation energies were 18.3kJmol^{-1} for the lower temperature range (50 – 70°C) and 7.7kJmol^{-1} for the higher temperature range (70°C – 82°C).

Based on activation energies for rate controlling mechanisms displayed in **Table 4.2** (Habashi, 1969; Potgieter et al., 2006), these low activation energies indicate that diffusion through the product layer was the rate controlling mechanism. The low activation energies are also indicative of the small potential energy barrier between reactant and product that must be overcome.

Table 4.2 Activation energies for rate controlling mechanisms (Habashi, 1969; Potgieter et al., 2006)

Regime	Activation Energy
Product (Ash) diffusion control	< 20 $kJmol^{-1}$
Film diffusion control	20 - 50 $kJmol^{-1}$
Chemical reaction control	> 50 $kJmol^{-1}$

4.3 Summary and Conclusions

In order to explore the possible influence of factors on the aluminium extraction and to identify their appropriate upper and lower limits, preliminary leach tests were conducted. In particular, this study looked at the effect of different parameters and calcium sulphate formation on the leaching characteristics of CFA. The study also looked at alumina dissolution kinetics. It has been deduced from this Chapter that alumina dissolution in CFA is influenced by acid concentration, leaching temperature, solid to liquid ratio and calcium sulphate formation.

Results from the elemental composition of CFA showed a narrow grade range indicating that the particle size of CFA may not have much influence on the extent of aluminium extraction.

Experimental results showed an increase in aluminium extraction with increase in leaching temperature. A maximum extraction of 23.5% was obtained at a temperature of 75°C. Therefore, 75°C was taken as the appropriate leaching temperature.

Aluminium extraction increased with increase in leaching time with slight variations beyond 6 hours of leaching. Based on this information, 6 hours was adopted as the appropriate leaching time.

Experimental results also showed that aluminium extraction decreased with increase in acid concentration beyond 6M. The decrease in extractions at higher acid concentration beyond 6M is attributed to low mass transfer rates of reactants and products caused by the increase in $CaSO_4$ formation in the slurry mixture. Therefore, 6M was adopted as the appropriate acid concentration.

Experimental results further showed 1:4 to be the optimum solid to liquid ratio with much lower extractions on either side. Decreased extractions at solid to liquid ratios higher than 1:4 were attributed to low mass transfer rates of reactants and products caused by the increased density of the CFA reaction mixture. Decreased extractions at solid to liquid ratios lower than 1:4 were attributed to low mass transfer of reactants and products caused by more calcium sulphate formation due to an increase in sulphate ions from increased acid volume. Based on this information, 1:4 was adopted as the appropriate solid to liquid ratio.

A decrease in calcium sulphate formation resulted in a corresponding increase in aluminium extraction and vice versa. This showed that other factors other than calcium sulphate formation influenced the extraction process.

The effect of temperature on leaching reactions was modeled by the Arrhenius equation. The calculated activation energies were found to be $18.3 kJmol^{-1}$ for the lower temperature range (50°C - 70°C) and $7.7 kJmol^{-1}$ for the higher temperature range (70°C - 82°C). Both activation energies were found to be characteristic of a product layer controlled mechanism. The shrinking core model predicted similar results for the leaching reactions at 50°C and 82°C. However, at 70°C, the model predicted differently, showing chemical reaction control as the rate controlling mechanism.

CHAPTER FIVE

IDENTIFICATION OF SIGNIFICANT FACTORS

5.1 Introduction

Engineers and scientists often perform one-factor-at-a-time (OFAT) experiments, which vary only one factor or variable at a time while keeping others constant. However, statistically designed experiments that vary several factors simultaneously are more efficient when studying two or more factors (Czitrom, 1999). A description of one-factor-at-a-time experiments and designed experiments is available in existing literature (Box et al., 1978; Montgomery, 1997; Mason et al., 1989). A comparison between the two shows a designed experiment to have a more effective way to determine the impact of two or more factors on a response than an OFAT experiment because a designed experiment makes use of a multivariate design. Some specific advantages that designed experiments have over OFAT experiments include the following (Czitrom, 1999):

- Designed experiments require fewer resources (experiments, time material, etc) for the amount of information obtained. This can be of major importance in industry, where experiments can be very expensive, time consuming and disruptive to operations.
- The estimates of the effects of each factor are more precise. Using more observations to estimate an effect results in higher precision or reduced variability. In designed experiments, all the observations are used to estimate the effect of each factor and each interaction, while typically two of the observations in an OFAT experiment are used to estimate the effect of each factor.
- The interaction between factors can be estimated systematically. An interaction of factors is a relationship where, the effect that a factor has on the product or process is altered due to the presence of one or more factors. Interactions are not estimable from OFAT experiments.
- There is experimental information in a larger region of the factor space. This improves the prediction of the response in the factor space. It also makes process optimization more efficient because the optimal solution is searched for over the entire factor space.

The purpose of this study was to investigate and identify factors that significantly influence the direct leaching of CFA. The study employed a statistical Design of Experiments (DOE) method

as a research tool to develop an experimentation plan for determining the significant factors affecting CFA leachability with sulphuric acid. The significance of each factor and associated interactive effects were evaluated using a two-level four-factor full factorial statistical design of experiments (2^4) and dissolved aluminium was taken as the measured response. Identification of influential factors is absolutely vital for process optimization and cost control.

The materials and reagents used in the experiment were as previously described in sections 3.2.1 and 3.2.2.

5.2 Experimental Plan for Statistical Design of Experiments (DOE)

Statistical Design of Experiments (DOE) was used in this work to study the leaching behaviour of CFA. This is the simultaneous study of several process variables which when combined results in better understanding of the process (Barrentine, 1999). An experimental design matrix was used in order to change several factors in a systematic way so as to ensure a reliable and independent study of main factors and their interactions. At this identification stage, the study looked at the influence of the main factors on the acid leaching of CFA. The main intention was to identify the key factors (independent variables) that affect the response (desired goal) and the interactions among themselves (two factor, three factor or four factor interactions). The major objective was to find the maximum and not necessarily the optimum solubilization of aluminium using sulphuric acid. The desired response was therefore aluminium extracted into solution. Leaching experiments were carried out at low and high factor levels represented by codified values of -1 and +1. For the quantitative variables (factors), -1 represents the low level and +1 the high level. The Factors investigated included: acid concentration, leaching time, leaching temperature and solid to liquid ratio.

Factors and Levels in Experimental Runs

Some factors that influence the dissolution of CFA have been studied and identified by previous researchers using various leaching methods (Seidel et al., 2001; Murtha and Burnet, 1983; Nayak and Chitta, 2009; Matjie et al., 2005, Kelmers et al., 1982; McDowell and Seeley, 1981a; McDowell and Seeley, 1981b). Therefore, the choice of factors and levels was based on past experience of CFA leaching. This study was designed to determine the influence of some of

these factors in the leaching of CFA using sulphuric acid and quantify them to make sure that the influence is both measurable and predictable. In this work, design factors were categorized as controlled factors and held constant factors. The controlled factors, presented in **Table 5.1**, were the factors selected for investigation. The held constant factor such as agitation rate is a factor that may have an influence on the response but is of no particular interest in the current study so it was held constant at 150 rpm.

Table 5.1 Experimental factors and levels for controlled factors

Controlled Factors	Level 1	Centre Point	Level 2
Acid concentration (M)	4	6	8
Leaching time (hrs)	6	8	10
Leaching temp (^{o}C)	45	60	75
Solid to Liquid ratio	1:3	1:4	1:5

At this diagnostic stage, the use of two levels for each factor allows for simplification of the analysis and provides substantial reduction in the number of runs required.

To simplify calculations and for uniform comparison, controlled factors were studied with their codified values of +1 or -1. The levels of controlled variables in coded units (Box et al., 1978) were obtained using the following formula:

$$\boldsymbol{coded\ value} = \frac{\boldsymbol{X - X_0}}{\boldsymbol{0.5(X_2 - X_1)}} \quad (5.1)$$

Where, $X = actual\ value, X_0 = mean\ value, X_1 = lowest\ value, X_2 = highest\ value$

5.2.1 Methodology for Data Analysis

Normal probability plot of effects

The normal probability plot of effects was carried out according to the procedure described in section 3.2.4. If the effects had occurred simply as the result of random variation about a fixed mean, and the changes in levels of the independent variables had had no real effect at all on the aluminium extraction, then all the 15 main effects and interactions would be distributed about zero (normal distribution). They would therefore plot on a normal probability plot as a straight line. To see whether they do, the 15 main effects are ordered in increasing order and plotted with an appropriate scale. The scale was obtained by employing the generalized equation (Box et al., 1978):

$$\boldsymbol{P = \ i - 0.5 \ * \frac{100}{m}} \qquad (5.2)$$

Where,

m = total number of effects, P = Probability points, i = Order number

An effect is the difference in response averages that are applicable to the levels of the factor. The effect of factor **A** on the response can be obtained by taking the difference between the average response when **A** is high and the average response when **A** is low (Barrentine, 1999; Box et al., 1978).

Effect of factor A = Average response at $\mathbf{A}_{high}$ – Average response at $\mathbf{A}_{low}$

For example,

Table C2 Replicate 1(Appendix C)

Average response at A_{high}, is given by averaging the results obtained by running experiments 2, 4, 6, 8, 10, 12, 14 and 16, and average response at A_{low} by averaging the results obtained from running experiments 1, 3, 5, 7, 9, 11, 13 and 15.

Average extractions at $A_{high} = (10.3 + 14.0 + 16.2 + 20.3 + 12.0 + 11.7 + 13.0 + 18.1)/8 = 14.45$

Average extractions at $A_{low} = (11.7 + 13.5 + 16.4 + 18.0 + 11.4 + 13.4 + 17.8 + 17.3)/8 = 14.94$

Difference = $14.45 - 14.94 = -0.49$

∴ Effect of factor A = -0.49

Effect of factor A is also referred to as a main effect. The negative effect implies that increasing the factor level from low to high lowers the response.

Pareto chart

The Pareto chart (Tague, 2004; Wilkinson, 2006) was plotted according to the procedure described in section 3.2.4.

Graphical residual analysis

Normal plotting of residuals provides a diagnostic check for any tentatively entertained model (Box et al., 1978). The normal probability plots of the residuals for the data tests the theory that the residuals have a normal distribution. This should be a straight line if the residuals have a normal distribution.

A plot of residuals versus the predicted values (fitted model values) is a test of the theory that the variations are the same in each group. Studentized 'deleted' residuals were calculated for each run in order to remove undue influence from outliers. A Studentized residual, therefore, is evaluated based on the predicted value when the value itself is excluded from the analysis. The residuals were calculated using **Equation 5.3** (Simate and Ndlovu, 2008):

$$Residual = \frac{R_{i,observed} - R_{i,predicted}}{\sigma_{i,residual}} \quad (5.3)$$

Where, $R_{i,observed}$ is the *i*th observation (extraction) in the experimental data, $R_{i,predicted}$ is the predicted value of the response from the fitted model, $\sigma_{i,residual}$ is the standard deviation of all residuals from the regression analysis that deleted the *i*th observation.

Test for curvature check using centre points

The check for local planarity is supplied by comparing Y_f, the average of the factorial points, with Y_c, the average at the centre of the design. By thinking of the design as sitting on a saucer like surface, it is seen that $Y_f - Y_c$ is a measure of overall curvature of the surface (Box et al., 1978). If Y_c is the average aluminium extraction of total runs at the centre and Y_f the average aluminium extraction of the total runs at the factorial points under study, then, if the two averages are very similar (for example, difference of 0.1%) then the centre points lie on or near the plane passing through the factorial points and hence there's no quadratic curve and no curvature. However, if $Y_f - Y_c$ is large, then quadratic curvature is present (Montgomery, 2005).

All experiments were randomly run in order to "average out" the effects of extraneous factors that may have been present (Montgomery, D. C., 1976).

The experimental procedure was as previously described in section 3.2.5.

5.3 Results and Discussion

5.3.1 Significant factors

Aluminium extraction results from experimental runs for the 2^4 full factorial design with codified and actual values are given in **Table 5.2**.

The aluminium extraction in the sulphuric acid leaching of CFA presented in **Table 5.2** was calculated as a percentage of aluminium in leach liquor to that in the unprocessed CFA (a sample calculation is given in **Appendix A**).

Table 5.2 Aluminium extraction results for the 2^4 full factorial design

Standard Run Order	Random Run Order	Control Factors				% Al Extraction (average)
		A	B	C	D	
1	1	-1	-1	-1	-1	11.7
2	4	+1	-1	-1	-1	10.3
3	14	-1	+1	-1	-1	13.5
4	18	+1	+1	-1	-1	14.0
5	6	-1	-1	+1	-1	16.4
6	19	+1	-1	+1	-1	16.2
7	25	-1	+1	+1	-1	18.0
8	15	+1	+1	+1	-1	20.3
9	24	-1	-1	-1	+1	11.4
10	5	+1	-1	-1	+1	12.0
11	7	-1	+1	-1	+1	13.4
12	27	+1	+1	-1	+1	11.7
13	10	-1	-1	+1	+1	17.8
14	26	+1	-1	+1	+1	13.0
15	17	-1	+1	+1	+1	17.3
16	9	+1	+1	+1	+1	18.1

The actual factor levels coded as values of (-1) and (+1) in the table are as follows:

A (Acid concentration): 4M (-1) and 8M (+1); B (Leaching time): 6hrs (-1) and 10hrs (+1);

C (Leaching temp): 45^{o}C (-1) and 75^{o}C (+1); D (Solid: Liquid ratio): 1:3(-1) and 1:5(+1)

The experimental data given in **Table 5.2** was used to estimate the main and interaction effects presented in **Figure 5.1**.

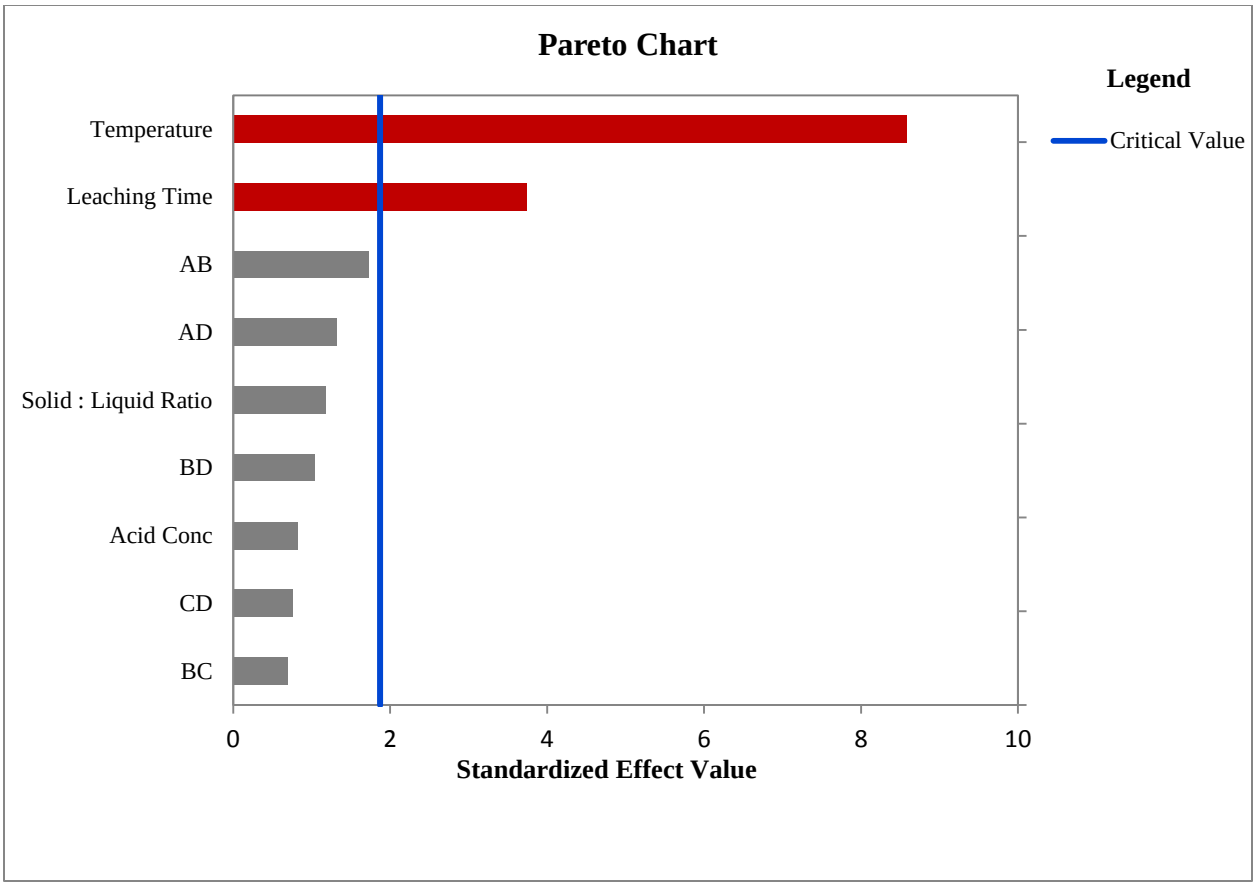

Figure 5.1 Pareto chart showing significance of main and interactive effects of acid concentration, leaching time, temperature and solid to liquid ratio

- *A – acid concentration*
- *B – leaching time*
- *C – temperature*
- *D – solid : liquid ratio*
- *AB, AD, BD, CD and BC: interactive effects*
- *Vertical line across the bar graphs = Critical Value*
- *Bar graph to the left of the Critical Value line = Non-significant Value*
- *Bar graph beyond the Critical Value line = Significant Value*

Analysis of the individual factors on the Pareto chart showed that leaching time and leaching temperature were statistically significant since they overshot the critical value line. Acid concentration and solid to liquid ratio were not statistically significant because they fell short of the critical value line. There was no significant interaction among the factors because all the interactions fell short of the critical value line. The experimental data given in **Table 5.2** was also used to estimate the main and interaction effects presented in **Figure 5.2**.

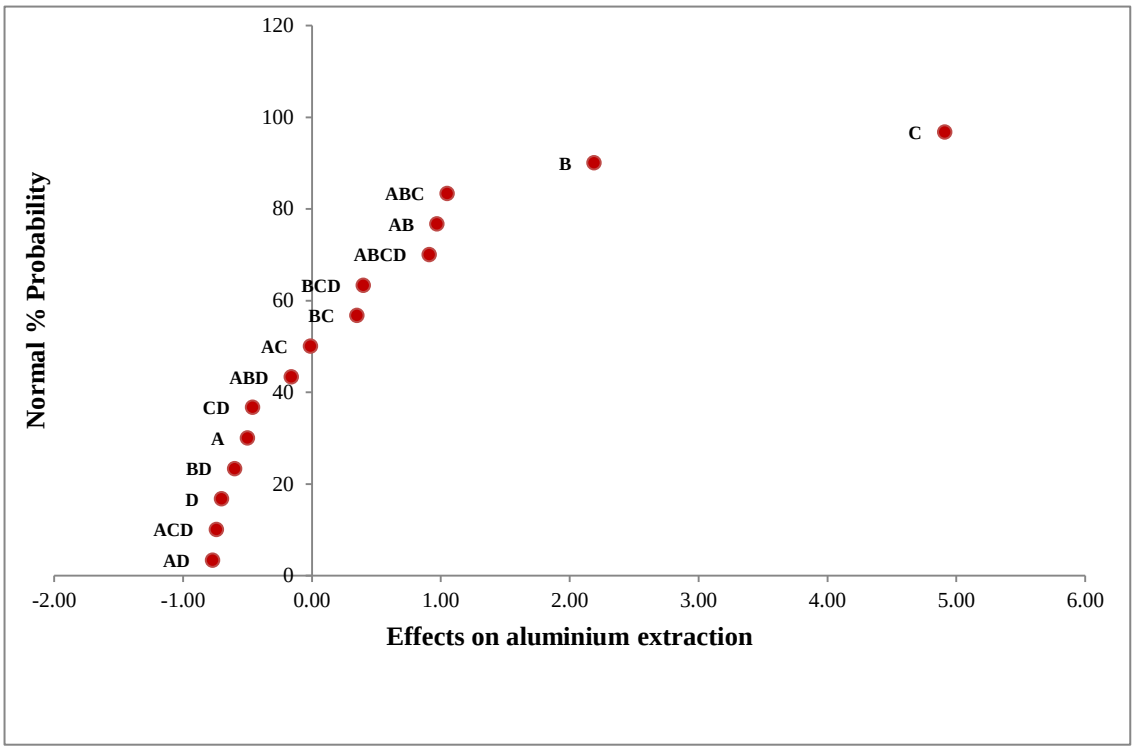

Figure 5.2 Normal plot of effects of main factors and factor interactions from the 2^4 full factorial design A, B, C and **D** are main factors: **A**-acid concentration, **B**-time, **C**-temperature, **D**-solid:liquid ratioAB, AC, BC, AD, BD, CD, ABC, ABD, ACD, BCD and ABCD are factor interactions.

The normal probability plot of effects presented in **Figure 5.2** was used to determine the significant effects. Analysis of the individual factors on the probability plots showed that leaching time (B) and leaching temperature (C) were statistically significant since they were not distributed about a fixed zero mean. They are far from the zero mean (normal distribution). Acid concentration (A) and solid to liquid ratio (D) are not statistically significant because they do not differ much from normal distribution. They are very close to zero mean. There was no significant

interaction among the factors because all the interactions do not differ much from normal distribution.

The significance of leaching time and temperature compared factors refers to the plausibility of the effect in light of the statistical data. In other words, there is reason to believe that the effect of the two factors is relevant to the extraction process. This also means that the other factors may be statistically insignificant but they are scientifically important (Simate et al., 2009).

A first order polynomial model (fitted model) between significant factors and the response was developed to illustrate the dependence of the response on the significant factors. The model is expressed below as:

$$R = 14.68 + 1.09X_B + 2.45X_C \quad (5.4)$$

Where ***R*** is the aluminium extraction, X_B and X_C are predictor variables which take the value of -1 or +1 (low or high) according to the columns of signs in the design matrix in **Table 5.2** for factors **B** (time) and **C** (temperature) respectively.

In **equation 5.4**, the positive signs in the prediction model indicate that in order to maximize the acid leaching of CFA, these factors must be kept at high levels.

The aluminium extraction results for centre points for the full factorial design (24) are presented in **Table 5.3.**

Table 5.3 Aluminium extraction results for center point replicates for the 2^4 full factorial design

Run	Control Factors				% Al Extraction (average)
	A	B	C	D	
1	0	0	0	0	14.0
2	0	0	0	0	15.3
3	0	0	0	0	14.3
4	0	0	0	0	15.1
5	0	0	0	0	13.8
6	0	0	0	0	14.9

The actual factor levels coded as values of (0) in the table are centre point values and are as follows:
A (Acid concentration): 6M (0); B (Leaching time): 8hrs (0); C (Leaching temp): 60^{o}C (0);
D (Solid: Liquid ratio): 1:4(0)

The observed aluminium extractions at the six centre points were: 14.0%, 15.3%, 14.3%, 15.1%, 13.8% and 14.9%. The average of these points is 14.6%. The average of the 16 factorial points of the 2^4 factorial design in **Table 5.2** is 14.7%. Since the two averages are very similar (difference of 0.1%), it is clear that the planar model is adequate. In other words, curvature is absent. The absence of cross products (significant interaction effects) in the fitted model, in **Equation 5.4**, further suggests the absence of curvature.

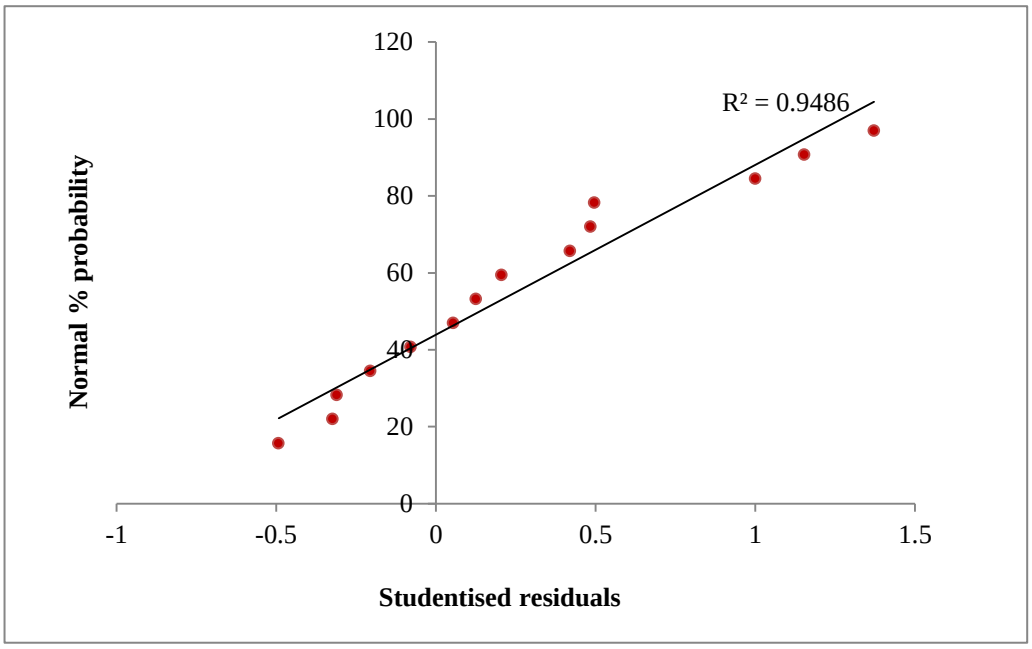

Figure 5.3 Normal plot of residuals

Figure 5.3 is a normal plot of residuals. As illustrated in the figure, all residues lie close to the straight line with a linear correlation coefficient of 94.86%, which shows that the residuals were distributed normally.

A plot of residuals versus predicted extraction (fitted model values) is a test of the assumption that the variations are the same in each group (**Figure 5.4**). This implies that the random errors are distributed with mean zero and constant variance (Simate and Ndlovu, 2008). All residuals were distributed between -2 and +1.5 without any systematic structure. Since the residuals were distributed normally with constant variance, mean zero and independently as illustrated in **Figure 5.3** and **Figure 5.4**, it can be concluded that **Equation 5.4** fitted the experimental data well.

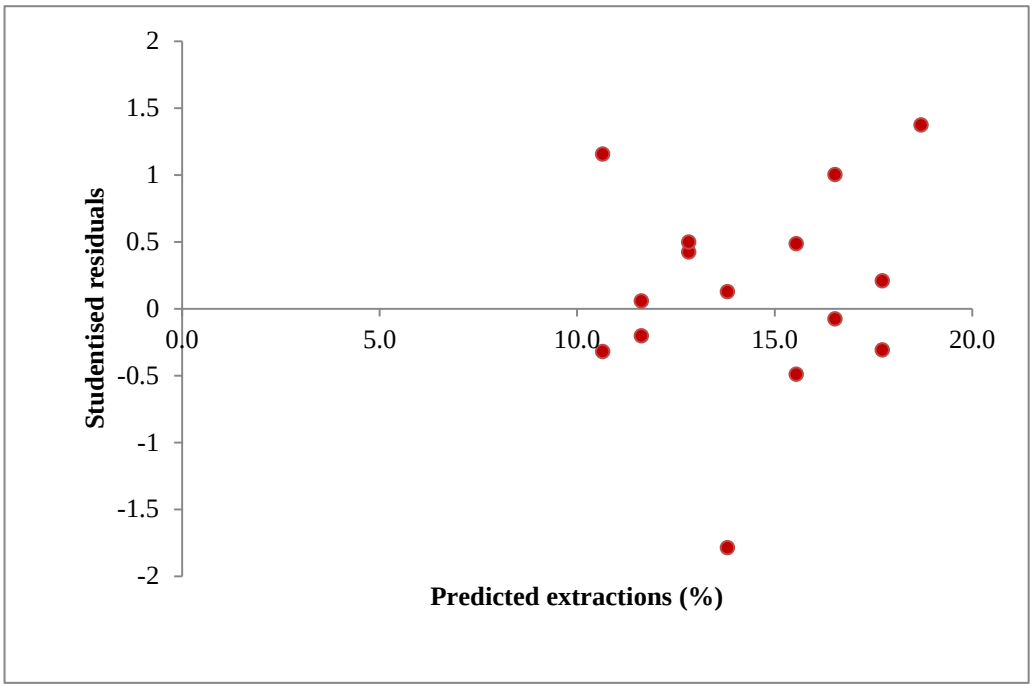

Figure 5.4 Plot of residuals versus predicted extractions

5.3.2 Influence of factors on extraction

It is standard procedure that the main effect of a variable should be individually interpreted only if there's no evidence that the variable interacts with other variables. When there's evidence of one or more such interaction effects, the interacting variables should be considered jointly (Box et al., 1978). In this study the interaction amongst variables was found to be insignificant. The variables were therefore interpreted individually.

Effect of acid concentration

The effect of acid concentration on aluminium extraction is presented in **Figure 5.5**. The figure shows aluminium extraction from CFA at 4M and 8M which are low and high acid concentration levels respectively. Higher aluminium extraction was obtained at lower acid concentration whereas higher acid concentration gave low extraction. As previously mentioned in Chapter 4, this may be attributed to more calcium sulphate precipitate formation at higher acid concentrations due to increased sulphate ions. The precipitate forms around and in the pores of the ash particle thus causing resistance to mass transfer of reactants and products (Seidel et al., 1998) hence inhibiting aluminium extraction.

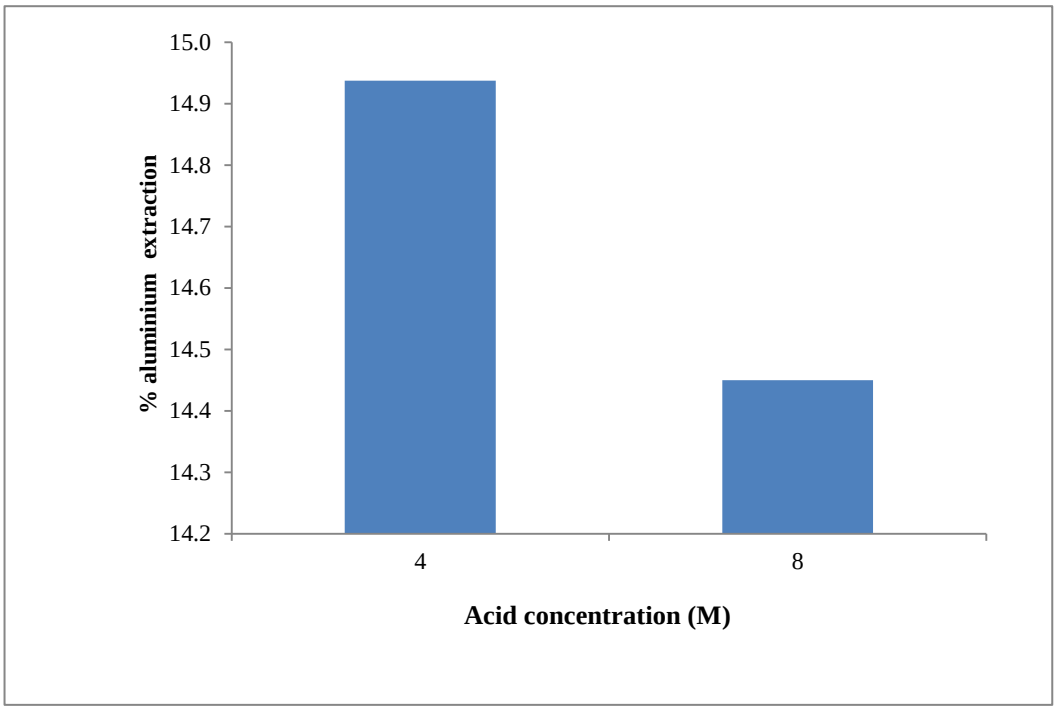

Figure 5.5 Effect of acid concentration on acid leaching of CFA

Effect of leaching time

The effect of leaching time on aluminium extraction is shown in **Figure 5.6.** The figure illustrates extractions from CFA for 6hrs and 10hrs of leaching time. Higher aluminium extraction was achieved with longer leaching time. The increased extraction with longer leaching time signifies the fact that adequate leaching time is necessary to overcome resistance to mass transfer of reactants and products caused by precipitate formations such as calcium sulphate. A similar phenomenon was also observed by Seidel and co-workers (1998) when they compared the leachability of conditioned and unconditioned CFA. The conditioned CFA was leached with hydrochloric acid to remove calcium sulphate prior to leaching with sulphuric acid. Their results showed that, for the same maximum aluminium extraction, the conditioned CFA leached within a shorter period of time compared to the unconditioned one. This led them to conclude that calcium sulphate precipitates slow down the aluminium leaching rate in CFA and hence the reason why longer leaching times yield higher extractions.

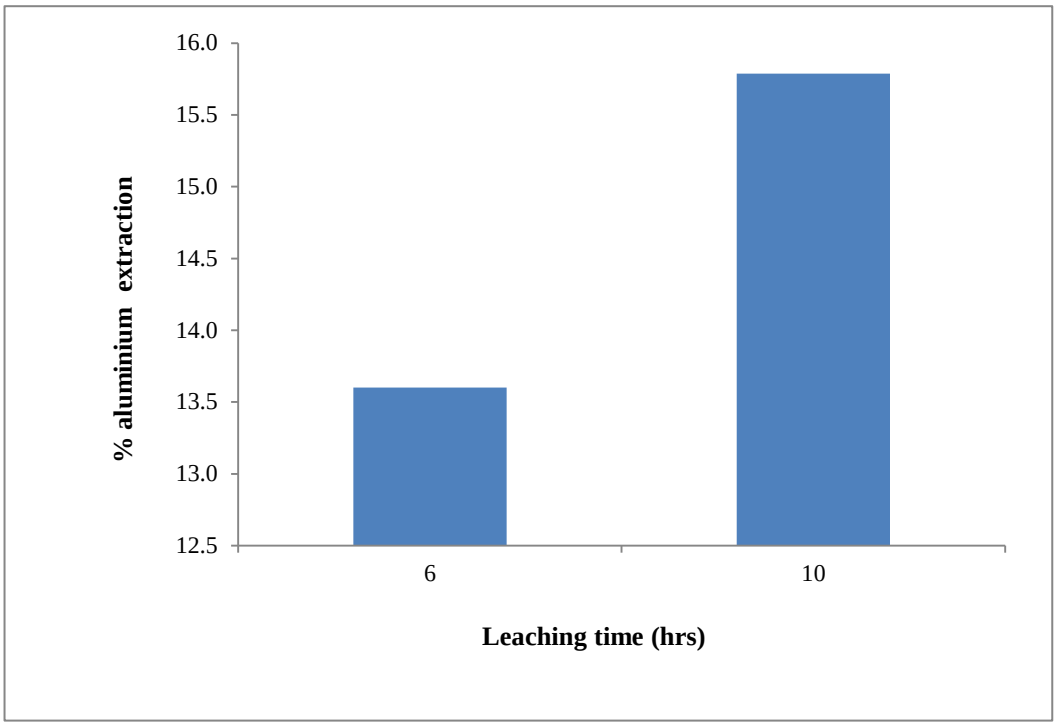

Figure 5.6 Effect of leaching time on acid leaching of CFA

Effect of temperature

The effect of leaching temperature on aluminium extraction is presented in **Figure 5.7**. The figure shows aluminium extraction from CFA at leaching temperatures of 45^{o}C and 75^{o}C. Higher aluminium extraction was obtained at higher temperature. This is because molecules at higher temperature have more thermal energy required for effective reaction. Although collision frequency is greater at higher temperatures, this alone contributes only a very small proportion to the increase in the rate of reaction. Much more important is the fact that, at higher temperature, the proportion of reactant molecules with sufficient energy to react is significantly higher. In this case, however, higher extractions at higher temperature could be explained with reference to activation energy experimental results obtained in section 4.2.7. The calculated activation energies were found to be 18.3kJmol^{-1} for the lower temperature range (50°C - 70°C) and 7.7kJmol^{-1} for the higher temperature range (70°C - 82°C). The lower activation energy at higher temperatures is an indication of increase in reaction rate with increase in temperature.

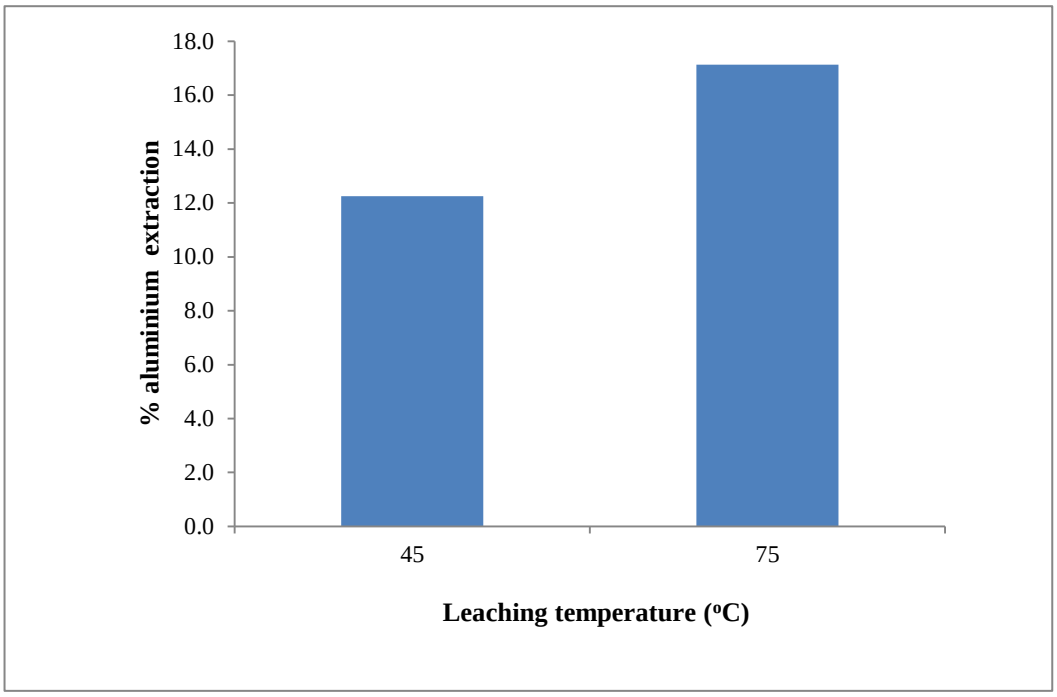

Figure 5.7 Effect of temperature on acid leaching of CFA

Effect of solid to liquid ratio

The effect of solid to liquid ratio on aluminium extraction is presented in **Figure 5.8**. The figure shows aluminium extraction from CFA at solid to liquid ratios of 1:3 and 1:5 which are high and low solid levels respectively. Higher aluminium extraction was attained at the higher solid to liquid ratio of 1:3 than at the lower solid to liquid ratio of 1:5. The higher aluminium extraction at the higher solid to liquid ratio may be ascribed to a possible attrition effect among ash particles at the higher slurry mixture density, preventing calcium sulphate precipitate layer build up, hence allowing high mass transfer rates of reactants and products. It must be noted, however, that further increase in solid to liquid ratio beyond 1:3 may result in lower aluminium extraction due to increased density of the mixture, poor suspension of solids and low mass transfer of reactants and products.

Lower aluminium extraction at the lower solid to liquid ratio may be attributed to increased sulphate ions due to increased acid volume hence promoting more formation of calcium sulphate precipitates. The precipitates obstruct mass transfer across the fly ash particle thus obstructing alumina dissolution and consequently causing lower aluminium extraction.

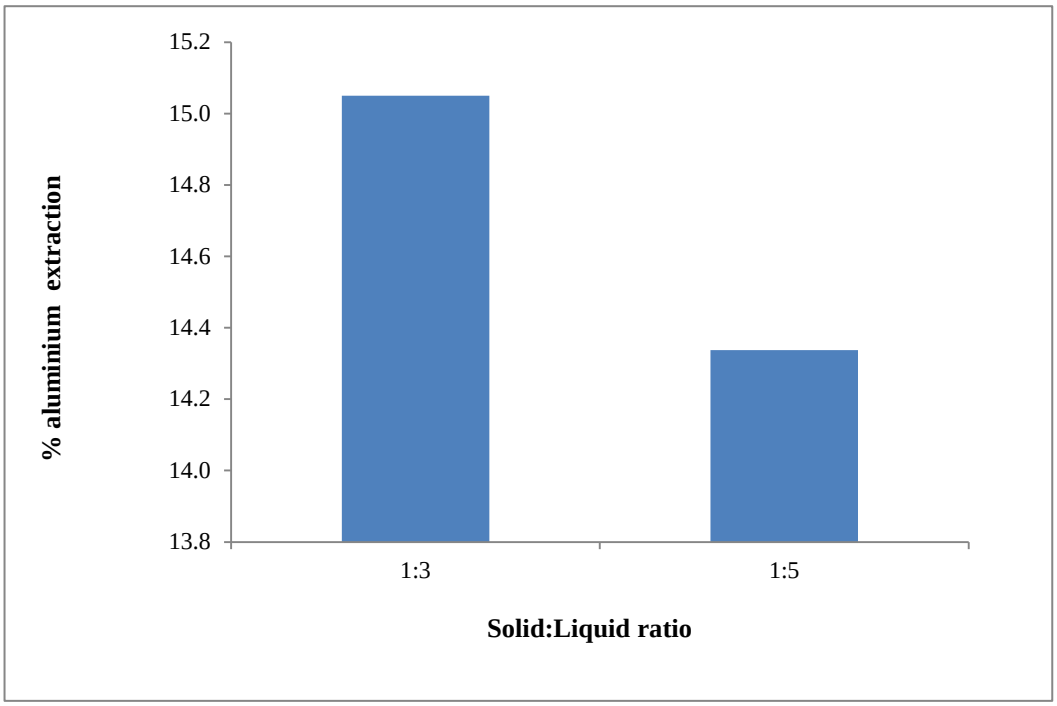

Figure 5.8 Effect of solid to liquid ratio on acid leaching of CFA

Factor interaction

Factor interaction among the various variables, in the ranges studied, was found to be insignificant. All the interaction effects were normally distributed about the zero mean and fitted reasonably well on a straight line as illustrated in **Figure 5.2**.

5.4 Summary and Conclusions

In this chapter, the main objective was to identify significant factors that influence the aluminium extraction process. To achieve this, screening experiments were used to obtain experimental data using a two-level full factorial design. In order to determine the significance of each factor, the experimental data was statistically analysed using the normal probability plots and the Pareto chart. The factors investigated included acid concentration, leaching time, solid to liquid ratio and temperature. All experiments were run at a constant agitation rate of 150 rpm. The experimental results obtained in this chapter served as an input to the optimization study presented in the next chapter (Chapter 6).

From the analysis of the experimental data, temperature and leaching time were found to be statistically significant factors while acid concentration and solid to liquid ratio were statistically insignificant. This means that temperature and leaching time have a significant influence on alumina dissolution in CFA.

A comparison of the two significant factors, temperature and leaching time, shows that temperature was more significant than leaching time in influencing aluminium extraction. This indicates that aluminium dissolution in CFA is a temperature driven process.

A further analysis of the experimental data also showed that interaction among factors was statistically insignificant. This implies that the effect that each factor has on the aluminium extraction process is not significantly altered due to the presence of the other factors.

The next chapter focuses on the optimization of the two variables that have been identified, in this chapter, as significant factors, namely, temperature and leaching time.

CHAPTER SIX

OPTIMIZATION OF SIGNIFICANT FACTORS

6.1 Introduction

While designing systems and products requires a deep understanding of influences that achieve a desirable performance, the need for an efficient and systematic decision-making approach drives the need for optimization strategies (Biegler, 2010).

Optimization may be defined as finding an alternative with the most cost effective or highest achievable performance under the given constraints, by maximizing desired factors and minimizing undesired ones. The main objective in process optimization is maximization of yield, minimization of variability and overall process improvement.

Fundamentally, there are three aspects of optimization; the first termed operating-procedure-optimization, is concerned with instructions detailing relevant steps to accomplishing tasks or activities of a process in the best way possible. Cited by Simate and co-workers (2009), Edgar and Himmelblau (1988) term the second type of optimization as topological and the third type as parametric or control optimization. Topological optimization is concerned with using equipment to its fullest advantage whereas parametric optimization is concerned with operating variables such as temperature, pressure, pH, solid to liquid ratio and agitation rate for a given process.

For any given scope of optimization problem for a system or process such as a metallurgical or chemical process, the task is to find the best solution for this process within constraints. This task requires the following elements (Biegler, 2010):

- An objective function that provides a scalar quantitative performance measure that needs to be minimized or maximized. This can be a system's cost, yield or profit.
- A predictive model that describes the behaviour of the system. For the optimization problem this translates into a set of equations and inequalities termed constraints. These constraints comprise a feasible region that defines limits of performance for the system.

- Variables that appear in the predictive model. These variables must be adjusted to satisfy the constraints. This can usually be accomplished with multiple instances of variable values leading to a feasible region that is determined by a subspace of these variables.

In this study, parametric optimization was deemed fit using a statistically-based optimization approach called response surface methodology (RSM) to determine the optimum conditions of temperature and time for the acid leaching of CFA. RSM is a famous technique used to find optimal conditions by using a quadratic polynomial regression model and is applied after diagnostic or screening experiments (Box et al., 1978).

The data for fitting the second order response was collected by using the central composite rotatable design (CCRD). A CCRD consists of 2^k factorial points, coded±1, augmented by 2k axial points, coded ±α (**Table 6.1**) and n_c replicate points at the centre {(0,0,0…..,0)}, where k is the number of factors studied, α is the distance of an axial point from the centre (Khuri and Cornell, 1987). This augmentation of the full factorial design with axial points and centre runs makes the CCRD complete with five factor levels (-α, -1, 0, +1, +α).

Table 6.1 Axial points (Khuri and Cornell, 1987)

1	2	…k
-α	0	0
+α	0	0
0	-α	0
0	+α	0
0	0	-α
0	0	+α

To ensure a constant variance of the predicted response at all points equidistant from the design centre, the number of centre point replications, n_c, for the two factors studied was calculated using the following equation (Khuri and Cornell, 1987).

$$\mathbf{n_c} \sim 0.8385\,(2^{k/2} + 2)^2 - 2^k\text{-}2k \qquad (6.1)$$

Where $\mathbf{n_c}$ is the number of centre point replications and **k** is the number of factors studied.
For $\mathbf{k = 2}$, $\mathbf{n_c = 5}$

The experimental results were analyzed statistically by using the analysis of variance (ANOVA).

6.2 Experimental Design for the Response Surface Methodology and CCRD

In previous experiments (Chapter 5) it was identified that temperature and leaching time were statistically significant operating parameters, while acid concentration and solid to liquid ratio were not statistically significant in the aluminium extraction process. Interaction parameters were also found to be statistically insignificant. Results from follow up experiments using the steepest ascent method further showed an aluminium extraction of 23.5% at 6M acid concentration, 1:4 solid to liquid ratio, at 75°C temperature after 8.75hrs of leaching time.

Response surface methodology and central composite rotatable design (CCRD) have been used in this study in an attempt to determine the optimal conditions of temperature and leaching time for the acid leaching of CFA. Factors were studied with their codified values ($-\alpha$, -1, 0, +1, $+\alpha$). **Table 6.2** shows a relationship between the coded values and actual values for the five levels of each factor.

Table 6.2 Relationship between coded and actual values of the variable (Napier-Munn, 2000)

Code	Actual value of a factor
$-\lambda$	ξmin
-1	$(\xi max + \xi min)/2 - (\xi max - \xi min)/2\lambda$
0	$(\xi max + \xi min)/2$
+1	$(\xi max + \xi min)/2 + (\xi max - \xi min)/2\lambda$
$+\lambda$	ξmax

ξmin and ξmax are the minimum and maximum values of the natural variables respectively,
$\lambda = 2^{(k-q)1/4}$

Where,

λ is the distance of an axial point from the centre

k is the number of factors studied, for this study k = 2 (temperature and time)

q is a fraction of number of factors. For a full factorial design, q = 0

∴ $\lambda = 1.414$

The five levels of each factor shown in actual and coded values calculated using the relationships in **Table 6.2** are shown in **Table 6.3**.

Table 6.3 Experimental layout and runs for the two factor central composite rotatable design

Factor Levels				Standard Run
Coded		Actual		
A (Temp)	B (Time)	A Temp(^{o}C)	B Time(hrs)	
-1	-1	70	7.75	1
+1	-1	80	7.75	2
-1	+1	70	9.75	3
+1	+1	80	9.75	4
-1.414	0	68	8.75	5
+1.414	0	82	8.75	6
0	-1.414	75	7.34	7
0	+1.414	75	10.16	8
0	0	75	8.75	9
0	0	75	8.75	10
0	0	75	8.75	11
0	0	75	8.75	12
0	0	75	8.75	13

In **Table 6.3**, the experimental lay out and standard runs for the central composite rotatable design is outlined. Five centre points were worked out from **Equation 6.1**.

For the two variables under consideration, a second order polynomial regression model was proposed as follows (Simate et al., 2009; Tripathy and Murthy, 2012):

$$y = \beta_o + \sum_{i=1}^{2} \beta_i x_i + \sum_{i=1}^{2} \beta_{ii} x_i^2 + \sum_{i=1}^{2} \sum_{j=i+1}^{2} \beta_{ij} x_i x_j + \varepsilon \quad \text{.....(6.2)}$$

Where,

y is the predicted response, β_o is the coefficient for intercept, β_i is the coefficient of linear effect, β_{ii} is the coefficient of quadratic effect, β_{ij} is the coefficient of interaction effect, **ε** is a term that represents other sources of variability not accounted for by the response function, x_i and x_j are predictor variables for independent factors.

The experimental procedure was as previously described in section 3.2.5.

6.3 Results and Discussion

6.3.1 Derivation of the model

The experimental results for the aluminium extraction are presented in **Table 6.4.** The coefficients of the regression model were estimated by fitting the experimental (observed) values using Design Expert® 6 software.

Table 6.4 Observed values for the aluminium extraction

Factor Levels				%Al Extraction [Observed]	Standard Run
Coded		Actual			
A (Temp)	B (Time)	A Temp(^oC)	B Time(hrs)		
-1	-1	70	7.75	20.2	1
+1	-1	80	7.75	22.7	2
-1	+1	70	9.75	20.8	3
+1	+1	80	9.75	23.4	4
-1.414	0	68	8.75	20.3	5
+1.414	0	82	8.75	23.3	6
0	-1.414	75	7.34	21.4	7
0	+1.414	75	10.16	22.1	8
0	0	75	8.75	21.8	9
0	0	75	8.75	21.8	10
0	0	75	8.75	22.1	11
0	0	75	8.75	21.6	12
0	0	75	8.75	21.7	13

The fitted second order model was obtained as:

$$\hat{y} = 21.80 + 1.17x_1 + 0.29x_2 + 0.025x_1x_2 - 0.025x_2^2 \quad (6.3)$$

Where, x_1 = temperature, and x_2 = time, within predictor variable limits:

$$-\lambda \leq x_i \leq +\lambda; i = 1,2$$

Where x_i are coded predictor variables and $\lambda = 2^{(k-q)1/4} = 1.414$ (for k = 2, -q = 0) is the distance of the axial points from the centre of the CCRD that ***gives the limits of the valid region*** under experimentation.

6.3.2 Checking the Adequacy of the Developed Model

The adequacy of the fitted model was carried out using the analysis of variance (ANOVA) given in **Table 6.5.**

Table 6.5 ANOVA for the fitted model

Source	Terms	Sum of Squares	Degrees of Freedom	Mean Square	F-Value	Prob>F
Model		11.570	5	2.31	66.43	<0.0001
	x_1	10.910	1	10.91	313.14	<0.0001
	x_2	0.660	1	0.66	18.81	0.0034
	x_1^2	0.000	1	0.000	0.000	1.000
	x_2^2	0.0004	1	0.0004	0.12	0.7343
	x_1x_2	0.0003	1	0.0003	0.072	0.7965
Residual		0.24	7	0.035		
Lack of fit		0.10	3	0.035	0.99	0.4826
Pure error		0.14	4	0.035		
Total		11.82	12	-		

For each source of terms, the probability (Prob>F) is examined to see if it falls below the chosen statistical significance level. For a statistical significance with a confidence level limit of 95%,

the probability (Prob>F) is examined against a factor of 0.05 (5%). A probability (Prob>F) value which is less than 0.05 shows significance.

A close examination of the ANOVA table shows that the regression model has a value of <0.0001. Since this value is less than 0.05, the model is therefore significant. Both the quadratic terms (x_1^2 and x_2^2), and the interactive term (x_1x_2) are insignificant since they have values greater than 0.05. Furthermore, the model does not show significant lack of fit. To obtain a simple and yet realistic model, the fitted model was re-fitted using only the variable terms that are significant at greater or equal to 95% confidence level and eliminating all insignificant terms. The re-fitted model is:

$$\hat{y} = 21.80 + 1.17x_1 + 0.29x_2 \quad (6.4)$$

The lack of fit for the re-fitted model was examined using the probability (Prob>F) value for lack of fit given as 0.7693. This is greater than 0.05, implying that the model does not present any evidence of lack of fit. The significance of the re-fitted regression model was examined using the probability (Prob>F) value for regression model significance. The obtained value of <0.0001 is less than 0.05, implying that the regression model is significant at a confidence level limit of 95%. The ANOVA for the re-fitted model is given in **Table 6.6**.

Table 6.6 ANOVA for the re-fitted model

Source	Terms	Sum of Squares	Degrees of Freedom	Mean Square	F-Value	Prob>F
Model		11.570	2	5.78	230.56	<0.0001
	x_1	10.910	1	10.91	434.99	<0.0001
	x_2	0.660	1	0.66	26.13	0.0005
Residual		0.24	10	0.025		
Lack of fit		0.11	6	0.018	0.53	0.7693
Pure error		0.14	4	0.035		
Total		11.82	12	-		

The mean summary statistics are presented in **Table 6.7.** The standard deviation value of 0.16 was flagged as low by the Design Expert® 6 program and the R-squared value of 97.9% as high. An exhibition of low standard deviation and high R-squared values is an indicator of a well-fitting model. Based on this, the model was found to be statistically plausible to define the true behaviour of the experimental system. This means that the aluminium extraction values at any regime in the interval of the experiment design can be calculated from **Equation 6.4**.

Table 6.7 Mean Summary Statistics

Source	Std. Dev.	R-Squared	Adjusted R-Squared	Predicted R-Squared
Linear	0.16	0.9788	0.9745	0.9655

Experimental results and predicted values obtained using the re-fitted models are given in **Table 6.8**. The relationship between experimental and predicted aluminium extraction is presented in **Figure 6.1**. The figure shows that the predicted values are reasonably comparable to the experimental values with the linear correlation coefficient (R^2) of 0.978. Statistically, this means that 97.8 % of the sample variation can be explained by the independent variables.

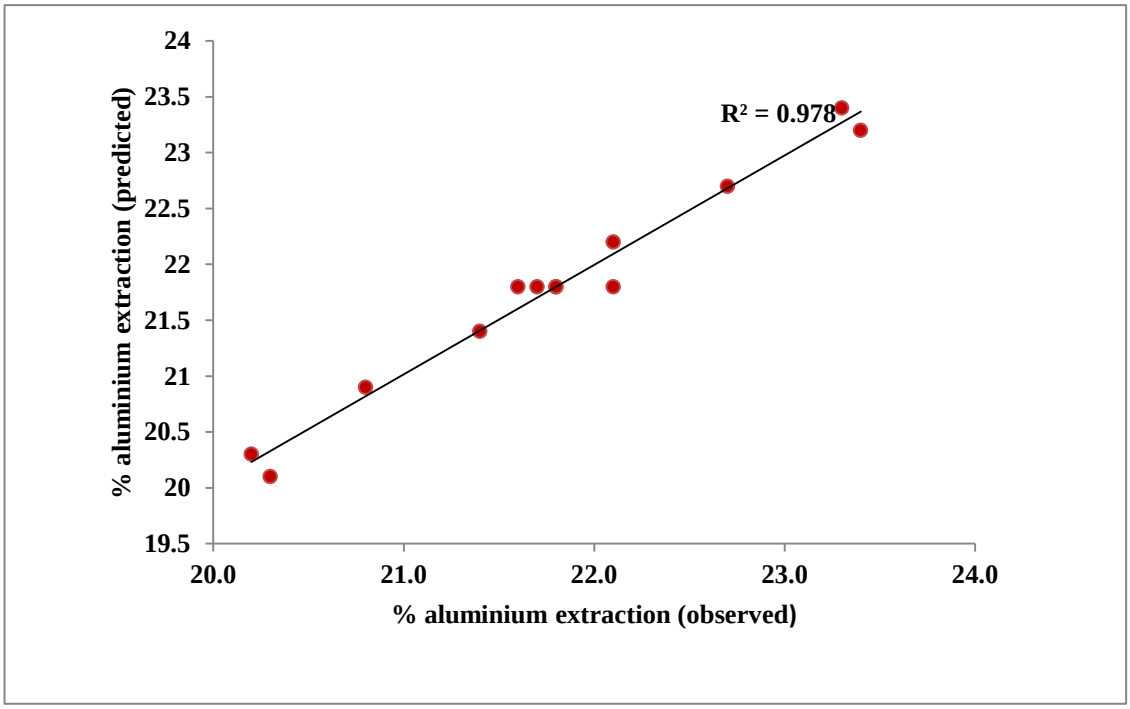

Figure 6.1 Relationship between experimental and predicted aluminium extraction

Table 6.8 Observed and predicted values for the aluminium extraction

Factor Levels				Aluminium Extraction (%)		Standard Run
Coded		Actual		Observed	Predicted	
A (Temp)	B (Time)	A Temp(^{o}C)	B Time(hrs)			
-1	-1	70	7.75	20.2	20.3	1
+1	-1	80	7.75	22.7	22.7	2
-1	+1	70	9.75	20.8	20.9	3
+1	+1	80	9.75	23.4	23.2	4
-1.414	0	68	8.75	20.3	20.1	5
+1.414	0	82	8.75	23.3	23.4	6
0	-1.414	75	7.34	21.4	21.4	7
0	+1.414	75	10.16	22.1	22.2	8
0	0	75	8.75	21.8	21.8	9
0	0	75	8.75	21.8	21.8	10
0	0	75	8.75	22.1	21.8	11
0	0	75	8.75	21.6	21.8	12
0	0	75	8.75	21.7	21.8	13

6.3.3 Determination of Optimum Conditions

As earlier stated, the major objective of the study described in this chapter is to determine the conditions that maximize aluminium extraction from CFA. Consequently, after the model was checked for adequacy of fit in the region defined by the coordinates of the design and was found to be adequate, the model can be used to locate the point of maximum response.

For quadratic regression models, the point for which the *response* is *optimized* is the point at which the partial derivatives $\frac{\partial \hat{y}}{\partial x_1}, \frac{\partial \hat{y}}{\partial x_2}, \ldots \frac{\partial \hat{y}}{\partial x_k}$, are all *equal to zero*. This point is called the *stationary point*. The stationary point may be a point of *maximum response*, *minimum response* or a *saddle point*. These conditions are easy to identify in the case of *two factor experiments*, by the *inspection of contour plots*. When more than two factors exist in an experiment, then the

general mathematical solution for the *location of the stationary* point has to be used. However, since the re-fitted model in **Equation 6.4** is linear, the maximum response coincides with the distance of the axial points from the centre of the CCRD that gives the limits of the valid region under experimentation. This means that the optimum aluminium extraction values can be calculated using **Equation 6.4.**

Using coded values of $x_1 = 1.414$ for optimum temperature and $x_2 = 1.414$ for optimum time in **Equation 6.4**,

Predicted aluminium extraction, $\hat{y}$ = **23.9%.**

The re-fitted model with actual values is expressed as:

$$\hat{y} = 21.80 + 0.236(Temp - 75) + 0.29(Time - 8.75) \quad \text{.....} \quad (6.5)$$

Using actual values, of Temp = 82°C for optimum temperature and Time = 10.16hrs for optimum time, in **Equation 6.5,**

Predicted aluminium extraction, $\hat{y}$ = **23.9%.**

6.3.4 Confirmatory Experiments

In order to test the validity of the optimized conditions given by the model, replicated experiments were carried out with parameters suggested by the model. The conditions used in the confirmatory experiments were as follows: temperature (82°C) and time (10.2hrs).

The aluminium extraction after leaching at 6M and solid to liquid ratio of 1:4 was found to be 24.8% (**Table 6.9**), which is consistent with the model. With an error margin of 3.4% between the predicted value and the confirmatory test value, the model fits the experimental data very well, and can therefore be considered to be acceptably valid.

Table 6.9 Aluminium extraction at optimum conditions

Parameter	Temperature (°C)	Time (hrs)	% Aluminium extraction
Model	**82**	**10.16**	**23.9**
Confirmatory tests	**82**	**10.16**	**24.8**

6.4 Summary and Conclusions

The necessity to develop and propose an efficient and economically viable process for recovering alumina from large quantities of unexploited CFA drives the need for optimization strategies. This entails finding an alternative with the most cost effective or highest achievable performance under the given constraints, by maximizing desired factors and minimizing undesired ones.

In this chapter the objective was to optimize the two variables that were identified as significant factors in Chapter 5, namely, temperature and leaching time. To achieve this, optimization experiments were designed using the central composite rotatable design (CCRD) and response surface methodology (RSM) in order to determine the optimal set of the two significant factors.

A second order quadratic regression model for factor optimization was derived using computer simulation software (Design Expert® 6) by applying least squares method based on the experimental design. The data for fitting the model was collected by using the central composite rotatable design (CCRD) and a fitted predictive model was developed as a mathematical expression of aluminium extraction from CFA. To study the effects of the individual variables as well as their joint interactive effects on aluminium extraction, a statistical analysis of variance (ANOVA) tool was used to analyse the experimental data.

From the prediction model, an optimal aluminium extraction efficiency of 23.95% was obtained at optimal values of 82°C temperature and 10.2 hrs leaching time.

A confirmatory test showed an extraction efficiency of 24.8%, giving an error margin of 3.4%, with a linear correlation coefficient of 97.8%, hence verifying the good fitting of experimental data and the fitness of the model.

The work undertaken in this chapter is a culmination of the first stage leaching process as well as a precursor to the second leaching stage. This means that, the residue-CFA produced from the optimized first leaching stage, becomes the feed material to the second leaching stage.

The next chapter (Chapter 7) looks at the second and final leaching stage for the extraction of aluminium from residue-CFA.

CHAPTER SEVEN

POST-SINTER (SECOND STAGE) LEACHING

7.1 Introduction

The possibility of using an indirect acid leach process based on a post-sinter (two-step acid leach) method has been discussed in section 2.4.3. The process makes use of the difference in the response characteristics of the two alumina phases found in CFA. The two alumina phases, amorphous and mullite play a major role in alumina dissolution kinetics. The amorphous phase is amenable to inorganic acids such as sulphuric acid whereas the mullite phase is insoluble due to its refractory nature. For this reason, the mullite phase is unable to participate in the pre-sinter (first stage) direct acid leaching process. The mullite phase requires phase transformation to make it leachable.

In the pre-sinter (first stage) leaching, CFA is directly contacted with sulphuric acid. Direct acid leaching of CFA using an inorganic acid such as sulphuric acid is achieved by proton attack. The hydronium ion displaces the metal cation from the ash particle matrix, thus inducing the dissolution of metals according to the following reaction:

$$CaO + Al_2O_{3(s)} + 8H^+_{(aq)} + SO_4^{2-}{}_{(aq)} \rightarrow 2Al^{3+}_{(aq)} + CaSO_{4(s)} + 4H_2O_{(l)} \qquad (7.1)$$

The resultant aluminium sulphate leach liquor is separated and the non-acid soluble phases of the ash, such as mullite, and calcium sulphate precipitate are retained as residue-CFA. The residue is used as feed for further alumina extraction in the post-sinter (second stage) leaching.

The residue-CFA is first sintered before post-sinter (second stage) leaching in order to transform the mullite in the residue into a phase that is acid-leachable. The leaching of sintered residue-CFA using sulphuric acid is also achieved by proton attack. The following is the possible reaction (based on the mineralogical phase transformations after post sinter-leaching, **Table 7.2**):

$$CaO{\cdot}Al_2O_3{\cdot}2SiO_{2(s)} + 8H^+_{(aq)} + SO_4^{2-}{}_{(aq)} \rightarrow 2Al^{3+}_{(aq)} + CaSO_{4(s)} + 2SiO_{2(s)} + 4H_2O_{(l)} \qquad (7.2)$$

The non-acid soluble phases from the post-sinter leaching are retained as post-sinter leaching residue and could be considered as a co-product in this process and could possibly be suitable for use as a lightweight aggregate in masonry concrete applications or cement production (Matjie et al., 2005). The resultant aluminium sulphate leach liquor is combined with the pre-sinter (first stage) leach liquor and separated for purification and recovery of alumina by processes such as solvent extraction, precipitation, crystallization and calcination.

The aim of the work contained in this chapter was to:

- Extract aluminium contained in residue-CFA from the pre-sinter (first stage) leaching.
- Investigate the response of the mullite phase to the sintering process.
- Investigate the response of pre-sinter phases to post-sinter (second stage) leaching.
- Determine the extent of aluminium extraction from the sinter product.

In order to achieve the above objectives, experiments were conducted according to the procedure previously described in sections 3.2.6 to 3.2.8.

In addition, the study investigated the leachability of sintered residue-CFA and sintered raw-CFA under the same leaching conditions in order to compare the aluminium extraction results of the two-step acid leach method to the current lime-sinter process.

The study also investigated the effect of recycling leach liquor from the pre-sinter (first stage) leaching process on the post-sinter leaching of sintered residue-CFA. This was done in order to establish whether it would be possible to use the recycled leach liquor (filtered leach solution) from the first leaching stage during the second leaching step. Recycling the leach liquor has the advantage of using less fresh sulphuric acid thus minimizing reagent consumption.

Optimized leaching conditions were used in all experiments.

7.2 Results and Discussion

7.2.1 Effect of Sintering

The effect of the sintering process on residue-CFA is presented in **Table7.1.** The table illustrates changes in the phase mineralogy of residue-CFA before and after sintering.

Table 7.1 Phase mineralogy of residue-CFA before and after sintering

CFA Phase	**Raw-CFA (Unprocessed)** (wt %)	**Residue-CFA After 1st Stage Leaching (Before Sintering)** (wt %)	**Residue-CFA (After Sintering)** (wt %)
Amorphous	52.9	45.79	23.03
Hematite (Fe_2O_3)	0.8	-	-
Magnetite (Fe_3O_4)	1.65	-	-
Mullite ($3Al_2O_3{\cdot}2SiO_2$)	30.68	32.53	8.02
Quartz (SiO_2)	13.97	14.31	6.60
Cristobalite (SiO_2)	-	-	8.07
Anhydrite ($CaSO_4$)	-	2.21	0.22
Gypsum ($CaSO_4{\cdot}2H_2O$)	-	5.17	-
Plagioclase ($CaO{\cdot}Al_2O_3{\cdot}2SiO_2$)	-	-	54.07

The presence of plagioclase, a calcium aluminosilicate solid solution, after the sintering process, indicates a possible reaction that may have occurred between mullite and calcium oxide. This may have effected mullite phase transformation according to the following possible reactions:

$$CaCO_3 \rightarrow CaO + CO_2 \quad (7.3)$$

$$3Al_2O_3{\cdot}2SiO_2 + 3CaO + 4SiO_2 \rightarrow 3(CaO{\cdot}Al_2O_3{\cdot}2SiO_2) \quad (7.4)$$

The transformation of the mullite phase to the plagioclase phase is not only vital to the subsequent post-sinter (second stage) leaching process but also an indication of the positive mullite response to the sintering process.

The results in **Table 7.1** show the presence of cristobalite after the sintering process. This indicates that the high sintering temperatures, typically, 1150°C, may have favoured the formation of the cristobalite, a high temperature polymorph of silica, which has a different crystal structure but the same chemical formula, SiO_2.

Table 7.1 also shows the absence of hydrous calcium sulphate (gypsum) after sintering. The absence of this substance indicates that it may have decomposed to the anhydrous form at high sintering temperatures. Following the decomposition, the anhydrous calcium sulphate may have undergone thermal decomposition under furnace oxidizing conditions to form calcium oxide according to the following possible reactions (Kuusik, 1985):

$$C + {}^1/_2O_2 \rightarrow CO \quad (7.5)$$

$$CaSO_4 + CO \rightarrow CaO + SO_2 + CO_2 \quad (7.6)$$

The calcium oxide formed in **Equation 7.6** may have reacted with mullite ($3Al_2O_3{\cdot}2SiO_2$) to form plagioclase ($CaO{\cdot}Al_2O_3{\cdot}2SiO_2$) according to **Equation 7.4**.

7.2.2 Effect of Post-sinter (Second Stage) Leaching

The effect of leaching on post-sinter CFA material was analysed by examining the mineralogy changes and extraction profile.

Post-sinter leaching mineralogy changes

The effect of the post-sinter (second stage) leaching process on sintered residue-CFA is presented in **Table 7.2.** The table shows changes in the phase mineralogy of sintered residue-CFA before and after the leaching process.

The mullite and quartz contents after the second leaching stage remained unchanged because of their high insolubility in inorganic acids under these leaching conditions (Matjie et al., 2005; Nayak and Chitta, 2009; Shcherban et al., 1995; Phillips and Wills, 1982).

Table 7.2 Phase mineralogy of sintered residue-CFA before and after post-sinter leaching

CFA Phase	**Raw CFA (Unprocessed)** (wt %)	**Sintered Residue-CFA Before Post-sinter Leaching** (wt %)	**Sintered Residue-CFA After Post-sinter Leaching** (wt %)
Amorphous	52.9	23.03	52.9
Hematite (Fe_2O_3)	0.8	-	-
Magnetite (Fe_3O_4)	1.65	-	-
Mullite ($3Al_2O_3{\cdot}2SiO_2$)	30.68	8.02	8.98
Quartz (SiO_2)	13.97	6.60	7.09
Cristobalite (SiO_2)	-	8.07	4.68
Anhydrite ($CaSO_4$)	-	0.22	23.18
Gypsum ($CaSO_4{\cdot}2H_2O$)	-	-	2.89
Plagioclase ($CaO{\cdot}Al_2O_3{\cdot}2SiO_2$)	-	54.07	-
Calcite ($CaCO_3$)	-	-	0.26

The re-appearance of the hydrated calcium sulphate (gypsum) after post-sinter (second stage) leaching may have resulted from the formation and hydration of calcium sulphate arising from the dissolution of the calcium aluminosulphate phase.

The complete dissolution and disappearance of the plagioclase phase ($CaO{\cdot}Al_2O_3{\cdot}2SiO_2$) after post-sinter (second stage) leaching, may be attributed to the good solubilization of this phase in sulphuric acid solution. This clearly demonstrates that the formation and presence of plagioclase is a key driving factor in the post-sinter aluminium extraction process.

The increase in amorphous phase after post-sinter leaching may have come from the reactions of the amorphous and plagioclase phases with sulphuric acid.

The presence of small amounts of calcite may have arisen from traces of unreacted calcium carbonate from the pelletization step.

Extraction profile

The post-sinter (second stage) aluminium extraction profile is presented in **Figure 7.1.** The figure shows an increase in aluminium extraction with increase in leaching time. An extraction of 71.0% was obtained after 5 minutes; 82.0% after 15 minutes; 84.3% after 30 minutes and 84.1% after 45 minutes. Leaching beyond 30 minutes did not result in any increment in aluminium extraction. Analysis of the graph shows that alumina dissolution in sintered residue-CFA is a relatively rapid process. The rapid alumina dissolution is indicative of a high rate of reaction possibly due to the low activation energy that must be overcome between reactants and products as well as low energy bonds in the calcium aluminosilicate structure ($CaO{\cdot}Al_2O_3{\cdot}2SiO_2$).

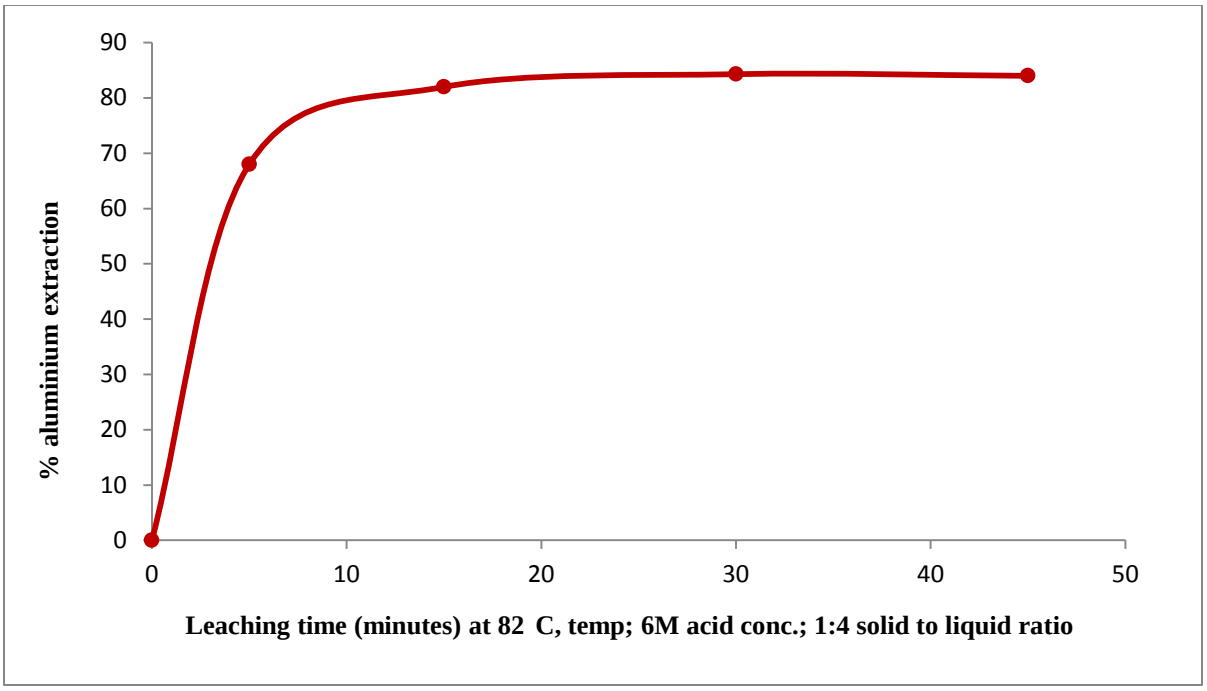

Figure 7.1 Aluminium extraction from sintered residue-CFA in post-sinter leaching

Table 7.3 shows experimental results from the leaching of sintered residue-CFA and sintered raw-CFA with fresh H_2SO_4 and leaching of sintered residue-CFA with recycled leach liquor from pre-sinter leaching. The table shows 84.3% and 85.2% aluminium extraction efficiencies obtained from the leaching of sintered residue-CFA and sintered raw-CFA respectively. The leaching of sintered residue-CFA with recycled leach liquor yielded an aluminium extraction efficiency of 3.5%.

Table 7.3 Aluminium extraction results from clinker-leaching experiments

	Lixiviant	Material	Leaching Process	Al extraction (%)
A	**Fresh H_2SO_4 (6M)**	**Residue-CFA (Clinker) Sintered at 1150°C**	Post-sinter leaching using fresh H_2SO_4	84.3
B	**Fresh H_2SO_4 (6M)**	**Raw-CFA (Clinker) Sintered at 1150°C**	Post-sinter leaching using fresh H_2SO_4	85.2
C	**Recycled leach liquor**	**Residue-CFA (Clinker) Sintered at 1150°C**	Post-sinter leaching using **recycled leach liquor** from pre-sinter leaching	3.5

The 85.2% extraction obtained from the leaching of sintered raw-CFA is in agreement with extractions obtained in previous works such as the lime-sinter process conducted by Matjie and co-workers (2005) in which they achieved an aluminium extraction efficiency of 85.0%.

The 84.3% extraction achieved from the leaching of sintered residue-CFA compared well with that of the sintered raw-CFA despite the sintered residue-CFA being less alumina-loaded compared to the sintered raw-CFA. This indicates possibility of higher aluminium extractions from sintered residue-CFA if sintering reaction conditions are probably varied in favour of more mullite to plagioclase transformation.

The 3.5% aluminium extraction obtained from the leaching of sintered residue-CFA with recycled leach liquor shows that the leach liquor was not effective in leaching. It can be seen that leaching with fresh sulphuric acid compared with the recycled leach liquor from the first leach stage has a distinct advantage. This shows that recycled leach liquor has no advantage over fresh sulphuric acid solution.

7.2.3 The Pre-sinter and Post-sinter Combined Aluminium Extraction

The combined aluminium extraction from the pre-sinter and post-sinter leaching processes was found to be 88.2% (calculations are shown in **Appendix A**). **Table 7.4** illustrates a metallurgical accounting for the aluminium extraction process. Calculations are based on a CFA sample weight of 100g.

Table 7.4 Overall aluminium extraction from 100g of CFA containing 30.52% Al_2O_3

CFA Phase	Al_2O_3 (wt %)	Al (g)	Extraction		
			Pre-sinter (g)	Post-sinter (g)	Total (%)
Amorphous	27.8	4.49	4.01	-	88.2
Hematite(Fe_2O_3)	-	-	-	-	
Magnetite(Fe_3O_4)	-	-	-	-	
Mullite($3Al_2O_3 \cdot 2SiO_2$)	72.2	11.67	-	10.24	
Quartz(SiO_2)	-	-	-	-	
Unextracted		16.16	12.15	1.91	

Table 7.4 shows a total aluminium input of 16.16g from 100g of CFA, a pre-sinter extraction of 4.01g, a post-sinter extraction of 10.24g and a discard of 1.91g in post-sinter residue.

The 4.01g pre-sinter extraction is equivalent to 24.8% pre-sinter aluminium extraction from 16.16g of aluminium in CFA. The 24.8% extraction represents 89.3% aluminium extraction from the amorphous phase.

The 10.24g post-sinter extraction is equivalent to 84.3% post-sinter aluminium extraction from 12.15g of aluminium in sintered residue-CFA. The combined extraction of 4.01g from the pre-sinter and 10.24g from the post-sinter leaching processes gave a total of 14.25g of aluminium representing an overall aluminium extraction of 88.2%.

The 88.2% aluminium extraction achieved from the two-step acid leach process was higher than the 85.2% extraction obtained from the conventional lime-sinter method. The high extraction was attributed to the two-step acid leach design. Pre-sinter leaching alters the CFA surface morphology, phase mineralogy and chemical composition. The leaching eliminates most of the amorphous phase that surrounds the insoluble crystals of mullite. Hence by dissolution of the

amorphous phase, high surface area crystalline phases are exposed (Nayak and Panda, 2010) leading to optimized reaction and transformation of the mullite phase during sintering.

Sinter performance

The performance of a sintering process can be seen through the results obtained from post-sinter leaching. This is because sintering conditions have an effect on the leachability of the sinter product. It follows, therefore, that post-sinter extraction is an indicator of sinter performance which may be used to compare two sintering processes such as the two-step acid leach method and the lime-sinter process. However, it must be stated here that in the two-step acid leach process, feedstock to the sinter process is pre-leached CFA after 89.3% extraction of aluminium from the amorphous phase (section 7.2.3) whereas in the lime-sinter process, the sinter feed is raw 'unprocessed' CFA. Further, it must also be mentioned that the main objective of sintering is to transform mullite. Therefore, for uniform comparison, sinter performance calculations were based on the mullite phase.

Using **Tables 7.3** and **7.4**, post-sinter extractions from sintered residue-CFA and sintered raw-CFA were calculated and compared (calculations are shown in **Appendix A**). The post-sinter aluminium extraction was calculated as a percentage of the aluminium in the liquid phase to the aluminium in the sintered CFA material. The sintered residue-CFA representing the two-step acid leach method yielded a sinter performance of 83.6% whereas the sintered raw-CFA representing the lime-sinter process was 79.5%.

The higher sinter performance by the two-step acid leach method could be attributed to more mullite transformation to plagioclase compared to the lime-sinter process. The higher mullite transformation may have been due to the better mullite crystalline surface exposure after the dissolution of the amorphous phase during pre-sinter leaching.

7.3 Summary and Conclusions

The overall purpose of employing the post-sinter (second stage) leaching step was to extract the alumina from the residue-CFA mullite phase. The results obtained revealed the following:

- Sintering of residue-CFA successfully transformed most of the mullite phase into a leachable plagioclase phase all of which underwent dissolution during second stage leaching. This shows that the sintering of residue-CFA is vital to mullite transformation and subsequent alumina extraction.

- An aluminium extraction of 3.5% was obtained from the leaching of sintered residue-CFA with recycled leach liquor. The low extraction was attributed to acid weakness.

- Pre-sinter leaching alters the CFA surface morphology, phase mineralogy and chemical composition. The leaching eliminates most of the amorphous phase that surrounds the insoluble crystals of mullite. Hence, by dissolution of the amorphous phase, high surface area crystalline mullite phases are exposed.

- Pre-sinter leaching reactions produce calcium sulphate ($CaSO_4$) as a by-product which can be utilized as part of the pellet mixture for sintering. Calcium sulphate acts as a sinter temperature modifier and also forms easily leachable alumina phases such as calcium aluminosulphate ($4CaO{\cdot}3Al_2O_3{\cdot}SO_4$) hence saving on energy as well as optimizing alumina extraction in post-sinter leaching. Alternatively, under furnace oxidizing conditions, $CaSO_4$ may undergo thermal decomposition to form calcium oxide which then reacts with the mullite phase to form plagioclase.

- In the pre-sinter and post-sinter (two-step acid leach) method, feedstock to the sinter process is pre-leached CFA whereas in the lime-sinter process, the sinter feed is raw CFA. These two types of sinter feed respond differently to the sinter process and post-sinter leaching. The sinter performance from the two-step acid leaching method was 83.6% compared to 79.5% for the lime-sinter process. The higher sinter performance by the two-step acid leach method is an indication of better mullite response to the sinter process.

- Due to the co-leaching of several metal oxide species such as Fe, Ti, K, Na and Mg, pre-sinter leaching has the potential to reduce CFA residue weight resulting in reduced load on downstream processes such as the sinter process thus saving on energy.

- The pre-sinter and post-sinter (two-step acid leach) method is able to extract up to a total of 88.2% aluminium at 82°C, 6M acid concentration and 1:4 solid to liquid ratio whereas the lime-sinter process can extract up to 85.2% under the same leaching conditions. The overall extraction of the two-step process is therefore higher than that of a one-step process where the CFA is pre-treated by sintering. This illustrates that not only will it be possible to save energy using a two-step leach process, but the extraction can also be improved upon.

- The post-sinter leaching for the two-step acid leach method was found to be relatively rapid, lasting about 30 minutes to completion compared to 4-12hrs required for the lime–sinter process. The rapid alumina dissolution was indicative of a high rate of reaction possibly due to the low activation energy required and little resistance to the mass transfer of reactants and products.

- Despite the high silica content in CFA, typically 46-60 wt%, filtration was conducted under atmospheric conditions with no requirement for a suction pump or dilution of the slurry. Leachate viscosity was normal and caused no filtration problems in all experiments.

- The sintered residue-CFA pellets required little crushing effort. The pellets were crushed to course powder (100% passing 212µm).

The next chapter (Chapter 8) draws conclusions and recommendations from the overall work in previous chapters.

CHAPTER EIGHT

CONCLUSIONS AND RECOMMENDATIONS

8.1 Conclusions

8.1.1 Introduction

Based on its amphoteric properties, alumina is capable of dissolution in either acidic or alkaline media and therefore amenable to hydrometallurgical methods of extraction. Minerals acids are able to leach metallic species from CFA which is predominantly made up of metallic oxides. The main objective of this work was to extend this concept in order to investigate the possibility of using sulphuric acid in the acid leaching of CFA. CFA contains significant amounts of alumina (Al_2O_3), but it is incapable of fully responding to mineral (inorganic) acids because the alumina in the ash is in two dissimilar phases which have different response characteristics. The amorphous phase is reactive and is acid soluble whereas the mullite phase is refractory and insoluble in inorganic acids. A review of literature suggested a possibility that the alumina can be extracted by first leaching one phase directly then transforming the other to make it leachable in sulphuric acid.

In order to investigate this possibility, the aims of the study were defined as to:

- Investigate the extent of aluminium extraction from CFA using sulphuric acid.
- Investigate parameters that promote alumina dissolution in CFA using pre-sinter and post-sinter leaching processes.
- Investigate the physical and chemical properties of CFA during leaching so as to understand the response of the ash to the beneficiation process.

8.1.2 Preliminary Acid Leaching

The direct leaching of CFA with sulphuric acid at different parameter levels of acid concentration, leaching time, temperature and solid to liquid ratio provided a better

understanding of the CFA acid leaching process and reaction conditions. The results presented in this study have shown that alumina dissolution in CFA is influenced by various parameters.

The elemental composition of CFA by particle size showed a narrow grade range. The highest CFA alumina grade was found to be 31.59 % and the lowest was 29.16% showing a variance of 2.43% within a size range of -38 µm and +212 µm. Therefore, particle size of CFA was found not to have much influence on the extent of aluminium extraction.

Preliminary leaching results showed a maximum aluminium extraction at 6M acid concentration. Aluminium extraction efficiencies of 14.8% and 10.9% obtained above 6M acid concentration were attributed to low mass transfer of reactants and products due to more calcium sulphate formation on CFA particles due to an increase in sulphate ions from sulphuric acid in the presence of calcium ions from CFA. Therefore, 6M was considered as the appropriate acid concentration.

Experimental results showed that aluminium extraction increased with increase in leaching time. An aluminium extraction efficiency of 16.8% was achieved after 6 hours of leaching. Leaching beyond 6 hours showed slight increase in extraction. However, increased extraction with longer leaching times signifies that adequate leaching time is necessary to overcome resistance to the mass transfer of reactants and products caused by precipitate formation such as calcium sulphate. Based on this information, 6 hours was adopted as the appropriate leaching time.

An aluminium extraction of 23.5% showed an increase with increase in temperature up to 75°C with slight fluctuations in extractions between 75°C and 85°C. Aluminium extractions at higher temperatures were attributed to the fact that molecules at higher temperatures have more thermal energy required for effective reaction. In addition, higher temperatures may have been helpful in breaking down the calcium sulphate precipitate layer in and around the CFA particles thus increasing the rate of reaction. Based on this information, 75°C was adopted as the appropriate leaching temperature.

An aluminium extraction of 16.5% was obtained at a solid to liquid ratio of 1:4. A 14.8% extraction obtained at a solid to liquid ratio of 1:6 was attributed to low mass transfer rates of

reactants and products caused by increased calcium sulphate precipitate formation on CFA particles due to increased acid volume. However, a 15.4% extraction obtained at a solid to liquid ratio of 1:3 may have been caused by increased slurry mixture density causing inefficient suspension of CFA particles. The ratio of 1:4 was therefore adopted as the appropriate solid to liquid ratio.

Calcium sulphate precipitates were found to have an adverse effect on aluminium extractions. Increase in calcium sulphate formation resulted in decreased extractions and vice versa. An inverse relationship was observed and established between calcium sulphate formation and aluminium extraction.

8.1.3 Identification of Significant Factors

A statistical Design of Experiments (DOE) method was employed as a research tool to develop an experimentation strategy for influential factor determination. Factors investigated included: acid concentration, leaching time, temperature and solid to liquid ratio. The significance of each factor and associated interactive effects were evaluated using a two-level, four-factor full factorial statistical design (2^4) and dissolved aluminium was taken as the measured response.

The design of experiments (DOE) and statistical method approach were able to convincingly determine statistically significant and insignificant factors.

Acid concentration and solid to liquid ratio were found to be statistically insignificant while leaching time and temperature were statistically significant. This means that acid concentration and solid to liquid ratio did not significantly influence aluminium extraction while leaching time and temperature had significant influence on the alumina extraction process. The results also indicated that aluminium extraction was maximized at higher temperature and longer leaching time values. This means that in order to achieve optimal aluminium extraction, temperature and leaching time need to be kept at high factor levels. The interaction of parameters among the variables was found to be statistically insignificant.

8.1.4 Optimization of Significant Factors

Optimization using a statistically-based approach called response surface methodology (RSM) was employed to determine optimum conditions for the significant factors. This was a follow up to diagnostic (screening) experiments (Box et al., 1978).

A second order quadratic polynomial regression model for factor optimization was derived using computer simulation software by applying least squares method based on the experimental design. The data for fitting the model was collected by using the central composite rotatable design (CCRD) and a fitted predictive model was developed as a mathematical expression of aluminium extraction from CFA. The experimental conditions for optimizing the significant factors, temperature and leaching time were 6M acid concentration and 1:4 solid to liquid ratio. These factor levels were chosen because they were adopted as appropriate levels in the preliminary acid leach experiments.

From the prediction model, an optimal aluminium extraction efficiency of 23.95% was obtained at optimal values of 82°C temperature and 10.2 hrs leaching time. A confirmatory test showed an extraction efficiency of 24.8%, an error margin of 3.4%, and a linear correlation coefficiency of 97.8%, hence verifying the fitting of experimental data and the fitness of the model. The 24.8% aluminium extraction represents 89.3% extraction of aluminium from the CFA amorphous phase. Therefore, it can be concluded from the experimental results that CFA can be optimally leached to achieve alumina dissolution from the amorphous phase by using sulphuric acid.

8.1.5 Kinetic Analysis

Mathematical modeling of fluid-solid systems is usually used to interpret experimental results and to gain insight into these reaction mechanisms. The shrinking core model and activation energy models were employed in the modeling of the CFA leaching system.

The experimental kinetic data for determining reaction mechanisms was collected by running kinetic experiments at 50°C, 70°C and 82°C with intermittent aliquot sampling. The leaching condition for the experiments were 6M acid concentration, 1:4 solid to liquid ratio and 10hrs

leaching time. The acid concentration and solid to liquid ratio factor levels were chosen because they were adopted as appropriate levels in preliminary experiments. The 10hrs leaching time was chosen in order to allow for as much aluminium extraction as possible.

From the activation energies governing rate controlling mechanisms, the calculated activation energies were found to be 18.3kJmol^{-1} for the lower temperature range (50°C - 70°C) and 7.7kJmol^{-1} for the higher temperature range (70°C - 82°C). Both activation energies were found to be characteristic of a product layer controlled mechanism. The shrinking core model predicted similar results for the leaching reactions at 50°C and 82°C. However, at 70°C, the model predicted differently, showing chemical reaction control as the rate controlling mechanism. This inconsistency in prediction by the shrinking core model may have been due to the lack of coupling the PSD with the shrinking model which can lead to an erroneous prediction of the rate controlling mechanism.

8.1.6 Post-sinter Leaching

The CFA pre-treatment approach using pelletization and sintering was able to transform the mullite phase into another leachable phase which was amenable to inorganic acid leaching.

A post-sinter (second stage) aluminium extraction efficiency of 84.3% was achieved from the leaching of sintered residue-CFA whereas 85.2% was obtained from the leaching of sintered raw-CFA showing that residue-CFA pre-conditioning is vital to alumina extraction. The post-sinter aluminium extraction efficiency of sintered residue-CFA was found to be comparable to that of sintered raw-CFA. This indicates possibility of higher aluminium extractions from sintered residue-CFA if reaction conditions are varied in favour of more mullite transformation to the easily leachable plagioclase phase.

Analysis of the sinter performance results showed that 83.6% post-sinter aluminium extraction from the mullite phase using the pre-sinter and post-sinter (two-step acid leach) method were achieved. However, a post-sinter aluminium extraction of 79.5% from the mullite phase using the lime-sinter process was obtained under the same sintering and leaching conditions.

An extraction efficiency of 3.5% was obtained from the leaching of sintered residue-CFA using recycled leach liquor. This showed that leaching with fresh sulphuric acid compared with the recycled leach liquor from the first leach stage has a distinct advantage. This also showed that recycled leach liquor was not effective in leaching and therefore has no advantage over fresh sulphuric acid solution.

.

The transformation of the mullite phase to the plagioclase phase and subsequent successful leaching of the formed phase showed that mullite phase transformation is a key factor in the post-sinter (second stage) aluminium extraction process. This study, therefore, has demonstrated that residue-CFA can be pre-treated and leached to optimally extract aluminium from CFA using sulphuric acid.

A pre-sinter aluminium extraction efficiency of 89.3% from the amorphous phase and a post-sinter extraction efficiency of 83.6% from the mullite phase yielded a total aluminium extraction efficiency of 88.2% whereas an aluminium extraction efficiency of 85.2% was obtained from the conventional (single-step acid leach) lime-sinter method.

8.1.7 Specific Outcomes

This study has added a new dimension to the potential of developing an alternative process technology for the production of smelter grade alumina from CFA. The possible extraction of smelter grade alumina from CFA will result in the achievement of specific outcomes such as:

- Alumina import substitution
- Promotion of self-sufficiency for the aluminium industry in the country
- Savings on disposal and containment costs
- Environmental protection
- Employment creation and economic empowerment

8.2 Recommendations

With the knowledge gained from this work, the following recommendations for further studies are proposed:

The role of calcium sulphate formation in alumina dissolution

This work had shown that when CFA is directly leached with sulphuric acid, aluminium extraction decreased with increase in acid concentration due to calcium sulphate formation at acid concentrations higher than 6M. In contrast, aluminium extraction increased with increase in acid concentration between 1M and 6M due to decrease in calcium sulphate formation within this acid range. This phenomenon may need to be investigated against the background of the aqueous-sulphate system characteristics. In aqueous-sulphate systems, sulphate ions (SO_4^{-2}) are known to decrease with increase in pH to form bisulphate (HSO_4^{-1}) ions. This leads to a depletion of sulphate ions and an increase in bisulphate ions. A speciation study can be done to investigate the influence of the various species in the acid solution as leaching progresses. The study could look at how these species in solution impact on calcium sulphate formation and aluminium extraction. In addition, the study could look at the possibility of some mineralogical phase transformations or precipitates formed that also contributed to the significant drop in aluminium extraction in the presence of acid concentrations. This study could also investigate the nature of calcium sulphate encapsulation which is assumed to be in and around the pores of the CFA particle and how it can be eliminated to enhance alumina dissolution. Further, this work can be extended to find an explanation for the drop in calcium sulphate content from 45-60°C and a sharp increase from 60-70°C.

Recycle of pre-sinter leach liquor

In acid leaching processes acid recovery is a mitigating factor to operational costs. This work had shown that leach liquor from pre-sinter (first stage) leaching could not be effectively used in the subsequent post-sinter (second stage) leaching. This work can be extended to experimentally see why the recycled leach liquor was not effective as well as study measures required to improve its effectiveness.

Economic Analysis

This work had shown that by employing a two-step acid leach method based on a leach-sinter-leach method, CFA can be optimally leached. This can be extended to a comparative study of economic aspects associated with the pre-sinter and post-sinter (two-step acid leach) process, the conventional lime-sinter process and the Bayer process. In particular, the study can look at economic aspects such as reagent consumption, processing time and energy usage by doing a cost benefit analysis. Further economic assessment is required to see if the 3% increase in aluminium extraction efficiency from 85.2 – 88.2% is economically justifiable.

Optimization of post-sinter leaching

In this study, parameters used in the second leaching stage were based on literature and optimized parameters from the pre-sinter leaching. This work can be extended to study the optimization of sintering and post-sinter leaching conditions. In particular, the study can look at optimizing parameters such as: sinter feed mixing ratio (residue-CFA: Coal: CaO), sintering temperature, sintering time, leaching time, leaching temperature, solid to liquid ratio and acid concentration.

Kinetics of leaching processes

In this work, controlling reaction mechanisms were modelled using the shrinking core models and activation energy rate controlling mechanisms. The shrinking core model showed an inconsistency in predicting the controlling reaction mechanism when compared to the activation energy model prediction. Extant literature (Gbor and Jia, 2004) suggests that coupling the PSD to the shrinking core model yields better prediction of reaction mechanisms. This work can be extended to investigate the use of a model that takes into account CFA particle size distribution to see its effect on the accuracy of reaction mechanism prediction.

REFERENCES

Aluminium., 2013. Encyclopedia Britannica, *Internet Version <http://www.britannica.com>*. Retrieved 16 February 2013.

ASTM® Manual., 2012. Form and Style for American Society for Testing and Materials International. ASTM® International, Pennsylvania.

Authier-Martin, M., Forte, G., Ostap, S., See, J., 2001. The Mineralogy of Bauxite for Producing Smelter Grade Alumina. *Journal of the Minerals, Metals and Materials Society*, Vol. 53, No. 12, pp. 36-40.

Babcock and Wilcox Company., 2007. Steam, Its Generation and Use. Internet Version <*http://www.Gutenberg.org*>. Retrieved 16 February 2013.

Barrentine, L.B., 1999. An Introduction to Design of Experiments: A Simplified Approach. ASQ Quality Press, Wisconsin.

Biegler, L.T., 2010. Nonlinear programming. Concepts, Algorithms, and Applications to Chemical Processes. MOS-SIAM, Philadelphia.

Box, G.E.P., Hunter, W.G., Hunter, J.S., 1978. Statistics for Experimenters: An Introduction to Design, Data Analysis and Model Building. John Wiley and Sons, New York.

Burnet, G., Murtha, M.J., Dunker, J.W., 1984. Recovery of metals from coal ash. Ames Laboratory, US DOE Iowa State University Ames, Iowa 50011.

Chang, R., 2005. Physical Chemistry for the Biosciences. University Science Books, Sausalito (CA), pp. 311-347.

Czitrom, V., 1999. One-Factor-At-a-Time Versus Designed Experiments. *The American Statistician,* Vol. 53, No. 2, pp. 126 – 131.

Daniel, C., 1959. Use of Half Normal plots in Interpreting Factorial Two Level Experiments. *Technometrics*, 1 (4), 311-341.

Dean, J.A., 1992. Lange's Handbook of Chemistry. McGraw Hill, New York.

Design Expert® 6 Manual., 2010. Internet Version <*http://www.statease.com*>. Stat-Ease, Incorporation, Minneapolis. Retrieved 5 February 2013.

Duval, D.J., Risbud, S.H., Shackelford, J.F., 2008. Ceramic and Glass Materials Structure, Properties and Processing. Springer, New York.

Earnshaw, A., Greenwood, N.N., 1997. Chemistry of the Elements (2nd Edition). Butterworth-Heinemann, Oxford.

Edgar, T.F., Himmelblau, D. M., 1988. Optimisation of Chemical Processes. McGraw-Hill, New York.

ELGA LabWater, 2009. Pure Lab Water Guide – An Essential Overview of Lab water Purification, Applications, Monitoring and Standards. <http://www.elgawater.com>. Retrieved 18 February 2013.

Gbor, P.K., Jia, C.Q., 2004. Critical Evaluation of Coupling Particle Size Distribution with the Shrinking Core Model. *Chemical Engineering Science*, Vol. 59, pp. 1979-1987.

Gilliam, T.M., Canon, R.M., Egan, B.Z., Kelmers, A.D., Seeley, F.G., and Watson, J.S., 1982. Economic Metal Recovery from Fly Ash. *Resources and Conservation*, pp. 155-168.

Grades of chemicals., 2008. Internet Version <*http://www.reagents.com*>. Retrieved 18 February 2013.

Gupta, C, K., 2003. Chemical Metallurgy: Principles and Practice. Wiley-VCH Verlag GmbH & Co. KGaA, Weinheim.

Habashi, F., 1969. Principles of Extractive Metallurgy: General principles. Gordon and Breach, New York.

Habashi, F., 2005. A Short History of Hydrometallurgy. *Hydrometallurgy,* Vol. 79, pp. 15-22.

Halada, K., Shimada, M., Ijima, K., 2008. Forecasting of the Consumption of metals up to 2050. *Materials Transactions*, Vol. 49, No. 3, pp. 402 – 410.

Hansen, K.R.N., von Rahden, H.V.R., Regester, W.V., McCulloch, H.W., 1966. The Extraction of Alumina from Sasol Coal Ash. *National Institute for Metallurgy*, Research report No. 30.

Housecroft, C.E., Sharpe, A.G., 2008. Inorganic Chemistry (3rd Edition). Pearson, England.

Jackson, E., 1986. Hydrometallurgical Extraction and Reclamation. John Wiley and Sons, New York.

Jinping, L.I., Haobo, H., Jinhua, G., Shujing Z., Yongjie, X., 2007. Extraction of Aluminium and Iron from Boiler Slag by sulphuric acid. *Wuhan University Journal of Natural Sciences*, Vol. 12, No. 3, pp. 541-547.

Kelmers, A.D., Canon, R.M., Egan, B.Z., Felker, L.K., Gilliam, T.M., Jones, G., Owen, G.D., Seeley, F.G., Watson, J.S., 1982. Chemistry of the direct leach, Calsinter, and Pressure Digested Acid leach methods for the recovery of Alumina from Fly Ash. *Resources and Conservation*, pp. 271-279.

Khuri, A. I., Cornell, J. A., 1987. Response Surfaces: Designs and Analyses. Marcel Dekker, Inc., New York.

Kutchko, B.G., Kim, A.G., 2006. Fly Ash Characterization by SEM-EDS, *Fuel*, pp. 2537-2544.

Kuusik, R., Saikkonen, P., Niinisto, L., 1985. Thermal Decomposition of Calcium Sulphate in Carbon Monoxide. *Journal of Thermal Analysis*, Vol. 30, pp. 187-193.

Laidler, K., 1984. Development of the Arrhenius Equation. *Journal of Chemical Education*, Vol. 61, No. 6, pp. 494.

Landman, A.A., 2003. Aspects of Solid-state Chemistry of Fly Ash and Ultramarine Pigments: Literature review of Fly Ash. University of Pretoria ETD. Retrieved 28 March 2010.

Levenspiel, O., 1972. Chemical Reaction Engineering. John Willey and Sons, New York.

Lide, D, R, ed., CRC Handbook of Chemistry and Physics, Internet Version 2007 (87th Edition), <*http://www.hbcpnetbase.com*>. Retrieved 18 August 2012.

Logan, S.R., 1982. The Origin and Status of the Arrhenius Equation. *Journal of Chemical Education*, Vol. 59, No. 4, pp. 279.

Loubser, M., Verryn, S., 2008. Combining XRF and XRD analyses and sample preparation to solve mineralogical problems. *South African Journal of Geology*, Vol. 111, pp. 229-238.

Maleka, E.M., Mashimbye, L., Goyns, P., 2010. South African Energy Synopsis 2010, Internet Version 2010, <http://www.energy.gov.za>, Department of Energy, Pretoria. Retrieved 8 February 2013.

Mason, R.L., Gunst, R.F., Hess, J.L., 1989. Statistical Design and Analysis of Experiments. John Wiley and Sons, New York.

Matjie, R.H., Bunt, J.R., Van Heerden J.H.P., 2005. Extraction of Alumina from Coal Fly Ash generated from a selected low rank bituminous South African coal. *Minerals Engineering*, Vol. 18, pp. 299-310.

McCabe, W.L., Smith, J.C., Harriott, P., 1993. Unit Operations of Chemical Engineering (5th Edition). McGraw-Hill, New York.

McDowell, W.J., Seeley, F.G., 1981a. Recovery of Aluminum and other Metal Values from Fly Ash. Oak Ridge, patent US4252777.

McDowell, W.J., Seeley, F.G., 1981b. Salt-Soda sinter process for recovering Aluminum from Fly Ash. Oak Ridge, patent US4254088.

Montgomery, D.C., 1976. Design and Analysis of Experiments. John Wiley and Sons, New York.

Montgomery, D.C., 1997. Design and Analysis of Experiments. John Wiley and Sons, New York.

Montgomery, D.C., 2005. Design and Analysis of Experiments. John Wiley and Sons, New Jersey.

Murtha, M.J., 1983. Process for the Recovery of Alumina from Fly Ash. Patent US4397822.

Murtha, M.J., Burnet, G., 1983. Power Plant Fly Ash – Disposal and Utilization. *Environmental Progress*, Vol. 2, No.3

Napier-Munn, T. J., 2000. The Central Composite Rotatable Design. JKMRC, The University of Queensland, Brisbane, Australia, pp. 1-9.

Nayak, N., Chitta, R. P., 2009. Aluminium extraction and leaching characteristics of Talcher Thermal Power Station Fly Ash with Sulphuric Acid. *Fuel*, pp. 53-58.

Nehari, S., Hasharon R., Gorin, C., Haim, K., Israel, L. J., 1999. Process for recovery of Alumina and Silica. Patent US5993758.

NIST/SEMATECH e-Handbook of Statistical Methods., 2012. Internet Version <http://www.itl.nist.gov/div898/handbook>. Retrieved 19 February 2013.

Padilla, R., Sohn, H. Y., 1985. Sintering Kinetics and Alumina Yield in Lime-Soda-Sinter Process for Alumina from Coal Waste. *Metallurgical Transactions*, Vol. 16, pp. 385.

Perry, R.; Green D., Maloney, J., 1984. Perry's Chemical Engineers' Handbook (6th Edition). McGraw-Hill, New York.

Phillips, C.V., Wills, K.J., 1982. A Laboratory study of the extraction of Alumina of Smelter grade from China Clay Micaceous residues by a Nitric Acid Route. *Hydrometallurgy*, pp. 15-28.

Potgieter, J.H., Kabemba, M.A., Teodorovic, A., Potgieter-Vermaak, S.S., Augustyn, W.G., 2006. An investigation into the feasibility of recovering valuable metals from solid oxide compounds by gas phase extraction in a fluidized bed. *Minerals Engineering*, Vol. 19, pp. 140-146.

Quality Guide., 2012. Pareto Analysis. <http://erc.msh.org/quality/pstools/pspareto.cfm.> Retrieved 25 March 2013.

Richardson, J.F., Harker, J.H., Backhurst, J.R., 2002. Particle Technology and Separation Processes, Chemical Engineering (5th Edition). Butterworth-Heinmann, Oxford.

Saeed, M.T., Ahmad, J., Shaheen, M.Y., 2009. Commercial Application of Extracting Reagents for Metal Recovery. *Journal of Pakistani Institute of Chemical Engineers*, Vol. 13, No. 59, pp. 1- 4.

Sakamoto, T., Shibata, K., Takanashi, L., Owari, M., Nihei, Y., 2003. Analysis of surface composition and internal structure of fly ash particles using an iron and electron multibeam micro analyzer. *Applied Surface Science*, pp. 762-766.

SD Fine-Chemicals Price List., 2012. Internet Version <*http://www.sdfine.com*>, Retrieved 28 January 2013.

Segal, I.H., 1975. Enzyme Kinetics: Behaviour and Analysis of Rapid Equilibrium and Steady State Enzyme Systems. John Wiley and Sons, New York. pp. 931-933.

Seidel, A., Sluszny, A., Shelef, G., Zimmels, Y., 1998. Self inhibition of Aluminum leaching from Coal Fly Ash by Sulphuric acid, *Chemical Engineering Journal*, pp. 195-207.

Seidel, A., Zimmels, Y., 1998. Mechanism and Kinetics of Aluminium and Iron leaching from coal fly ash by Sulphuric acid. *Chemical Engineering Science*, Vol. 53, No. 22, pp. 3835-3852.

Seidel, A., Zimmels, Y., and Armon, R., 2001. Mechanism of bioleaching of coal fly ash by Thiobacillus thiooxidans. *Chemical Engineering Journal*, pp. 123-130.

Shcherban, S., Raizman V., Pevzner, I., 1995. Technology of Coal Fly Ash Processing into Metallurgical and Silicate Chemical Products. Kazakh Politechnical University, Alma-Ata.

Simate, G.S., Ndlovu, S., 2008. Bacterial leaching of nickel laterites using chemolithotropic microorganisms: Identifying influential factors using statistical design of experiments. *International Journal of Mineral Process*, Vol. 88, pp. 31-36.

Simate, G.S., Ndlovu, S., Gericke, M., 2009. Bacterial leaching of nickel laterites using chemolithotropic microorganisms: Process optimization using response surface methodology and central composite rotatable design. *Hydrometallurgy*, Vol. 98, pp. 241-246.

Tague, N.R., 2004. The Quality Toolbox, Second Edition, ASQ Quality Press, Wisconsin.

Thiemann, M., Scheibler, E., Wiegand, K.W., 2005. Nitric acid, Nitrous acid and Nitrogen Oxides – Ullmann Encyclopedia of Industrial Chemistry, Wiley-VCH, Weinheim.

Thompson, J.V., 1995. Alumina: Simple Chemistry - Complex plants. *Engineering and Mining Journal 42*.

Tripathy, S.K., Murthy, Y.R., 2012. Modeling and optimization of spiral concentrator for separation of ultrafine chromite. *Powder Technology,* Vol.221, pp. 387-394.

Van, H., Kent, R, (ed)., 1967. Aluminium, Design and Application (Volume 2). *American Society for Metals*, Ohio.

Wen, C.Y., 1968. Non-catalytic Heterogeneous Solid-fluid Reaction Models. *Industrial and Engineering Chemistry*, Vol. 60, pp. 34-54

Wilkinson, L., 2006. Revising the Pareto chart. *American Statistician,* Vol. 60, No.4, pp. 332-334.

APPENDICES

APPENDIX A

SAMPLE CALCULATIONS

%Aluminium Extraction

The % aluminium extraction during the leaching of CFA was calculated as a percentage of the aluminium in the liquid phase to that in the CFA.

Example

Pre-sinter (first stage) Aluminium Extraction

Basis of calculation:

CFA weight (actual) before leaching = 100g

% Al_2O_3 content in CFA (XRF analysis) = 30.5 wt%

Al_2O_3 molecular weight = $102 gmol^{-1}$

Al molecular weight = $27 gmol^{-1}$

Al moles in Al_2O_3 = 2

Calculations

Al content in CFA = $\frac{30.52*2*27}{102} = \mathbf{16.16g}$

After Leaching:

Leach liquor volume = 500 mL ($500*10^{-3}$ Litres)

Al in leach liquor (ICP analysis) = 8020 ppm ($8020*10^{-3}$ gpl)

Al content in 500mL = $\frac{500*8020}{1000*1000} = 4.01g$

$\therefore$ **% Aluminium extraction** = $\frac{\mathbf{4.0*100}}{\mathbf{16.2}} = \mathbf{24.8}\%$

Actual residue-CFA weight after leaching = **92.47g**

Al content in residue-CFA = $16.16 - 4.01 = \mathbf{12.15g}$

Sinter Feed Mixture

Pelletization

Residue CFA weight	=	$\mathbf{50g}$
Mixing ratio (**CFA: Coal: $CaCO_3$)**	=	$\mathbf{5:4:1}$
CFA	=	$\frac{100*50}{100} = \mathbf{50g}$
Coal	=	$\frac{100*40}{100} = \mathbf{40g}$
$CaCO_3$	=	$\frac{100*10}{100} = \mathbf{10g}$
Total weight of sinter feed mixture	=	$\mathbf{100g}$

Aluminium from Coal material

% Al in coal material	=	**1.05%** (Chapter 3 section 3.2.3)
Aluminium in mixture **from coal**	=	$\frac{1.05*40}{100} = \mathbf{0.42g}$

Sintering

Pellet mixture before sintering	=	100g (actual weight)
Pellets mixture after sintering	=	68g (actual weight)
% weight loss due to sintering	=	$\mathbf{32.0}\%$

Actual weight loss	=	$\frac{100*32.0}{100} = \mathbf{32g}$
∴ % Al in clinker from coal addition	=	$\frac{0.42*100}{68} = \mathbf{0.62}\%$

Post-sinter (second stage) aluminium Extraction

Basis of calculation:

Sintered residue-CFA weight (actual)	=	50g
% Al_2O_3 in sintered residue-CFA (XRF analysis)	=	25.89 wt%
Aluminium from coal material in residue-CFA	=	0.62%
Al_2O_3 molecular weight	=	$102gmol^{-1}$
Al molecular weight	=	$27gmol^{-1}$
Al moles in Al_2O_3	=	2

Calculations

Al content in residue-CFA	=	$\frac{25.89*50*2*27}{102*100} = \mathbf{6.85g}$
Aluminium from coal in residue-CFA	=	$\frac{0.62*50}{100} = 0.31g$
Al in residue-CFA **less aluminium from coal***	=	$6.85 - 0.31 = \mathbf{6.54g}$

After Leaching:

Leach liquor volume	=	500 mL ($500*10^{-3}$ Litres) = 0.5L
Al in leach liquor (ICP analysis)	=	11640 ppm =11.64 gpl
Al content in 0.5L	=	$0.5 * 11.64 = 5.82g$
Al in leach liquor **less aluminium from coal***	=	$5.82 - 0.31 = \mathbf{5.51g}$
∴ % Post-sinter aluminium extraction	=	$\frac{\mathbf{5.51*100}}{\mathbf{6.54}} = \mathbf{84.3}\%$

* The leachability of aluminium in coal was not investigated and therefore not known. However, it was assumed that the aluminium was leachable. Therefore, in order to get a true reflection of the actual aluminium extraction from residue-CFA, the aluminium in coal was deducted from both the residue-CFA feed and leach liquor.

Pre-sinter and Post-sinter Combined Aluminium Extraction

Pre-sinter aluminium extraction

Basis of calculation

CFA weight (actual) before leaching	=	100g
% Al_2O_3 content in CFA (XRF analysis)	=	30.52 wt%
Al_2O_3 molecular weight	=	$102gmol^{-1}$
Al molecular weight	=	$27gmol^{-1}$
Al moles in Al_2O_3	=	2
Al content in CFA	=	$\frac{100*30.52*27*2}{100*102} = 16.16g$
Pre-sinter (first stage) extraction efficiency	=	24.8%
∴ Extracted aluminium	=	4.01g
Al remaining in residue-CFA	=	$16.16 - 4.01 = \mathbf{12.15g}$
Residue-CFA weight (actual)	=	$\mathbf{92.47g}$

Pelletization

Residue-CFA weight (actual)	=	92.47g
Mixing ratio (**CFA: Coal: $CaCO_3$)**	=	$\mathbf{5:4:1}$
CFA	=	$\frac{184.94*50}{100} = 92.47g$
Coal	=	$\frac{184.94*40}{100} = 73.98g$
$CaCO_3$	=	$\frac{184.94*10}{100} = 18.49g$
Total weight of mixture	=	184.94g

Sintering

Residue-CFA pellets before sintering (actual) = 184.94g

Sintered residue-CFA pellets after sintering (actual) = $\mathbf{125.76g}$

Post-sinter aluminium extraction

Basis of calculation

Al from CFA in residue-CFA= Al content in pelletized residue-CFA= Al in sintered residue-CFA= $12.15g$(**equation 7.6**)

Post-sinter Al extraction efficiency = **84.3%**

∴ Extracted aluminium $= \frac{84.3*12.15}{100} = \mathbf{10.24g}$

Combined extraction

Extracted aluminium from first stage leaching = $4.01g$

Extracted aluminium from second stage leaching = 10.24g

Total extracted aluminium = 14.25g

∴ **Combined aluminium extraction efficiency** = $\frac{\mathbf{14.25*100}}{\mathbf{16.16}} = \mathbf{88.2}\%$

Sinter Performance

Sinter performance was calculated as a percentage of the total aluminium extracted in the pre-sinter and post-sinter leaching less the aluminium from the amorphous phase to that in the mullite phase.

Pre-sinter and post sinter technique

Total aluminium extracted in pre-sinter leaching	=	4.01g
Total alumina in amorphous phase	=	4.49g
Unextracted alumina from amorphous phase	=	0.48g
Mullite phase alumina in residue		$12.15 - 0.48 = 11.67$g
Alumina extracted from mullite phase	=	$10.24 - 0.48 = 9.76$g
% Sinter performance	=	$\frac{9.76*100}{11.67} = 83.6\%$

Conventional lime-sinter technique

Extraction efficiency from raw-CFA	=	85.2%
Total aluminium in CFA	=	16.16g
Total aluminium extracted	=	$\frac{85.2*100}{16.1} = 13.77$g
Total alumina in amorphous phase	=	4.49g
Aluminium extracted from mullite phase	=	$13.77 - 4.49 = 9.28$g
Total aluminium in mullite phase	=	$16.16 - 4.49 = 11.67$g
% Sinter performance	=	$\frac{9.28*100}{11.67} = 79.5\%$

A Phase Quantification of Alumina in CFA

A phase quantification of alumina in CFA was determined based on the difference between the total alumina in CFA as per the XRF analysis and the mullite phase alumina as per the XRD analysis.

Example

Basis of calculation:

Sample weight	=	100g
% **Al_2O_3** in raw CFA (XRF analysis)	=	30.52%wt
Aluminium molecular weight	=	$27gmol^{-1}$
Silicon molecular weight	=	$28gmol^{-1}$
Oxygen molecular weight	=	$16gmol^{-1}$
Al_2O_3 molecular weight	=	$102gmol^{-1}$
Mullite ($3Al_2O_3 \cdot 2SiO_2$) molecular weight	=	$426gmol^{-1}$

In a 100g sample,

Total **Al_2O_3** in CFA = 30.52g ……①

Total **Al** in CFA = $\frac{30.52*2*27}{102} = 16.16g$ ……②

% Amorphous in raw CFA (XRD analysis) = **52.9%wt**

% Mullite ($3Al_2O_3 \cdot 2SiO_2$ or $Al_6Si_2O_{13}$) in raw CFA (XRD analysis) = **30.68%wt**

In a 100g sample,

Total mullite = 30.68g ……..③

Al_2O_3 in mullite phase = $\frac{30.68*3*102}{426} = 22.04g$ ……④

Al in mullite phase = $\frac{22.04*2*27}{102} = 11.67g$ ……⑤

From equations ① and ④

% **Al_2O_3** in mullite phase = $\frac{22.04*100}{30.52} = 72.2\%$ ……⑥

From equations ② and ⑤

% **Al** in mullite phase = $\frac{11.67*100}{16.16} = 72.2\%$ ……⑦

From equations ① and ④

Al_2O_3 in amorphous phase = $30.52 - 22.04 = 8.48g$

% **Al_2O_3** in amorphous phase = $\frac{30.52-22.04}{30.52} * 100 = \frac{8.48}{30.52} * 100 = 27.8\%$ …..⑧

From equations ② and ⑤

% **Al** in amorphous phase = $\frac{16.16-11.67}{16.16} * 100 = \frac{4.49}{16.16} * 100 = 27.8\%$ ……⑨

	Raw CFA		
Phase	Amorphous (52.9%)	Mullite (30.68%wt)	Other (16.42%)
Al_2O_3	27.8%	72.2%	-
Al	27.8%	72.2%	-

% Calcium sulphate content in CFA

Calcium sulphate content in CFA was calculated as a percentage of the total calcium sulphate in the anhydrous and hydrous phase to the CFA sample weight.

Example

Basis of calculation

CFA sample weight = 100 g

Gypsum ($CaSO_4 \cdot 2H_2O$) content in CFA (XRD analysis) = 1.56 wt%

Gypsum ($CaSO_4 \cdot 2H_2O$) molecular weight = 172 $gmol^{-1}$

$CaSO_4 \cdot 2H_2O$ molecular weight	=	136 $gmol^{-1}$
Calcium sulphate moles in $CaSO_4 \cdot 2H_2O$	=	1
Calcium sulphate content in CFA from gypsum	=	$\frac{100*1*136*1.56}{100*172} = \mathbf{1.23g}$
Anhydrite ($CaSO_4$) content in CFA (XRD analysis)	=	6.93 wt%
$CaSO_4$ content in CFA from anhydrite	=	6.93 g
% Total $CaSO_4$ content in CFA	=	$\frac{(6.93+1.23)*100}{100} = \mathbf{8.2\%}$

Determination of Activation Energies

Example

From the kinetics experiment, alumina dissolution in sulphuric acid was considered to proceed according to the following reaction:

$$CaO + Al_2O_3 + 4H_2SO_4 \rightarrow Al_2(SO_4)_3 + CaSO_4 + 4H_2O$$

The changing rate in alumina dissolution was observed, at different temperatures, by monitoring the concentration of aluminium sulphate [$Al_2(SO_4)_3$].

- The ***rate of reaction*** at any instant of time was determined by measuring the slope of the curve at that time. This also corresponds to the rate of reaction at an ***instant of concentration***.
- From the ***rate of reaction*** at an ***instant of concentration***, the ***rates of reaction versus concentrations*** were determined and plotted.
- The slopes from the plots of ***rates of reaction versus concentrations*** gave the values for the ***rate constants k_1, k_2 and k_3*** as 6.3 x 10^{-5}, 9.7 x$10^{-5}$and 10.7 x10^{-5} respectively at corresponding temperatures of T_1 = 50°C= 323K, T_2=70°C=343K and T_3= 82°C=355K.

Using the Arrhenius equation previously derived in Chapter 2 section 2.4 (Chang, 2005; Segal, 1975; Laidler, 1984; Logan, 1982),

$$logk_2 - logk_1 = \frac{\boldsymbol{E_a}}{2.303R}\ \frac{1}{T_1} - \frac{1}{T_2}$$

And,

$logk_1 = log6.3x10^{-5} = -4.2,$

$Logk_2 = log9.7x10^{-5} = -4.01,$

$logk_3 = log10.7^{-5} = -3.97.$

At,

$T_1 = 50°C = 323K,$

$T_2 = 70°C = 343k,$

$T_3 = 82°C = 355K.$

Activation energy between T_1 and T_2 is calculated as follows:

$-4.01 - \ -4.20 \ = \frac{E_a}{2.303x8.314}\ \frac{1}{323} - \frac{1}{343}$,

$0.19 = 0.052 * E_a * 0.0002,$

$\therefore \boldsymbol{E_A = 18.3kJmol^{-1}}$

Similarly using above Arrhenius equation for T_2 and T_3 we have,

$logk_3 - logk_2 = \ \frac{\boldsymbol{E_a}}{2.303R}\ \frac{1}{T_2} - \frac{1}{T_3}$,

And activation energy between T_2 and T_3 is calculated as follows:

$-3.97 - \ -4.01 \ = \frac{E_a}{2.303x8.314}\ \frac{1}{343} - \frac{1}{355}$,

$0.04 = 0.052 * E_a * 0.0001,$

$\therefore\ \boldsymbol{E_a = 7.7kJmol^{-1}}.$

Design of Experiments

Main Effect

An effect is the difference in response averages that are applicable to the levels of the factor. The effect of factor **A** on the response can be obtained by taking the difference between the average response when **A** is high and the average response when **A** is low.

Effect of factor A = Average response at $\mathbf{A}_{high}$ – Average response at $\mathbf{A}_{low}$

Example

Replicate 1 Table C2

Average response at A_{high}, is given by averaging the results obtained by running experiments 2, 4, 6, 8, 10, 12, 14 and 16, and average response at A_{low} by averaging the results obtained from running experiments 1, 3, 5, 7, 9, 11, 13 and 15.

Average extractions at $A_{high} = (10.3 + 14.0 + 16.2 + 20.3 + 12.0 + 11.7 + 13.0 + 18.1)/8 = 14.45$

Average extractions at $A_{low} = (11.7 + 13.5 + 16.4 + 18.0 + 11.4 + 13.4 + 17.8 + 17.3)/8 = 14.94$

Difference = $14.45 - 14.94 = -0.49$

∴ Effect of factor A = -0.49

Effect of factor A is also referred to as a main effect.

Interaction Effect

An interaction is a cross product of two or more factors. The net sign of the interaction is also a cross product of the individual signs of the factors. The identity of an interaction comes from the identity of the individual factors involved in the cross product. A cross product of factor **A** and factor **B** yields a two factor interaction **AB**.

An interactive effect is the difference in response averages that are applicable to the levels of the interaction. The interactive effect of interaction **AB** on the response can be obtained by taking the difference between the average response when **AB** is high and the average response when **AB** is low.

Effect of interaction AB = Average response at AB_{high} – Average response at AB_{low}

Example

Replicate 1 Table C2

Average response at AB_{high}, is given by averaging the results obtained by running experiments 2, 4, 6, 8, 10, 12, 14 and 16, and average response at AB_{low} by averaging the results obtained from running experiments 1, 3, 5, 7, 9, 11, 13 and 15.

Average response at $AB_{high} = (11.7 + 14.0 + 16.4 + 20.3 + 11.4 + 11.7 + 17.8 + 18.1)/8 = 15.18$

Average response at $AB_{low} = (10.3 + 13.5 + 16.2 + 18.0 + 12.0 + 13.4 + 13.0 + 17.3)/8 = 14.21$

Difference = $15.18 - 14.21 = 0.97$

∴ Effect of interaction AB = 0.97

Applying the same approach as above to the rest of the factorial design in replicate 1 Table C2 the main and interactive effects are calculated and arranged in ascending order of magnitude as shown in Table A1.

Table A1 Main and interactive effects

Order Number *i*	1	2	3	4	5	6	7	8	9	10	11	12	13	14	15
Effect	-0.77	-0.74	-0.70	-0.60	-0.49	-0.46	-0.16	-0.01	0.35	0.40	0.91	0.97	1.05	2.19	4.91
Identity of effect	AD	ACD	D	BD	A	CD	ABD	AC	BCD	BC	ABCD	AB	ABC	B	C

Normal probability plots

Normal probability plots are a plot of probability $\boldsymbol{P = 100(i - \frac{1}{2})/15}$ for $\boldsymbol{i = 1, 2, 3, 4, \ldots m}$ where $\boldsymbol{m}$ = the number of effects under consideration, excluding the average, on the y-axis against effects in **Table A1** on the x-axis.

Computing $\boldsymbol{P = 100(i - \frac{1}{2}))/15}$ for $\boldsymbol{i = 1, 2, 3, 4, \ldots 15}$ and adding the obtained values to **Table A1** gives the effects for normal probability plots as shown in **Table A2**.

Table A2 Normal probability plots

Order Number *i*	1	2	3	4	5	6	7	8	9	10	11	12	13	14	15
Effect	-0.77	-0.74	-0.70	-0.60	-0.49	-0.46	-0.16	-0.01	0.35	0.40	0.91	0.97	1.05	**2.19**	**4.91**
Identity of effect	AD	ACD	D	BD	A	CD	ABD	AC	BCD	BC	ABCD	AB	ABC	B	C
P=100(i-1/2)/15	3.3	10	16.7	23.3	30.0	36.7	43.3	50.0	56.7	63.3	70.0	76.7	83.3	90.0	96.7

Modeling the significant effects for extraction prediction

Beginning with effects with magnitudes close to zero, 13 of the estimates fit reasonably well on a straight line. Those corresponding to **B** and **C** do not fit on the straight line. It can therefore be concluded that the effects B and C are not easily explained as chance occurrences. This suggests that all effects with the exception of the average extraction 14.68, B= 2.19 and C = 4.91 can be explained by noise.

Therefore, $Extraction, Y = \bar{Y} + \frac{B}{2} X_B + \frac{C}{2} X_C$

Where, $\bar{Y}$ represents the average of all the data for the runs (i.e. average of all extractions) and X_B and X_C are the predictor variables (i.e. +1 or -1), B and C are effects.

The coefficients that appear in the equations are half the calculated effects because a change from x = -1 to x = +1 is a change of two units along the x-axis.

Therefore,

Predicted extraction,

Y = $14.68 + \frac{2.19}{2}X_B + \frac{4.91}{2}X_C$

= $14.68 + 1.09X_B + 2.45X_C$

The predicted extraction is calculated by substituting an appropriate predictor variable in a particular run.

Example

Replicate 1 Table C2

In run1, the predictor variables are X_B = -1, X_C = -1

Predicted extraction = $14.68 - 1.09 - 2.45 = 11.14\%$

The positive signs of the variables of the prediction model equation indicate that in order to maximize the acid leaching of CFA, these factors must be kept in high levels.

Residual

This is the difference between the actual extraction and the predicted extraction for each run.

Example

Replicate 1 Table C2

Actual extraction = 11.7, predicted extraction = 11.14

Residual = $11.7 - 11.14 = 0.56$

APPENDIX B

PRELIMINARY ACID LEACHING

Table B1 Aluminium concentration (ppm)

Conditions for acid leaching of CFA at different acid concentrations:

Leaching time 8hrs, temperature 60°C, solid to liquid ratio 1:4

Acid concentration (M)	ppm	ppm
2	2446	2212
4	2592	2724
6	2662	2468
8	2313	2224
10	1698	1902

Table B2 Aluminium extraction (%)

Conditions for acid leaching of CFA at different acid concentrations:

Leaching time 8hrs, temperature 60°C, solid to liquid ratio 1:4

Acid concentration (M)	%	%
2	15.1	13.7
4	16.0	16.9
6	16.5	15.3
8	14.3	13.8
10	10.5	11.8

Table B3 Aluminium concentration (ppm)

Conditions for acid leaching of CFA at different leaching times:

acid concentration 6M, temperature 60°C, solid to liquid ratio 1:4

Leaching time (hrs)	ppm	ppm
4	2172	2392
6	2618	2840
8	2662	2468
10	2755	2534
12	2556	2335

Table B4 Aluminium extraction (%)

Conditions for acid leaching of CFA at different leaching times:

acid concentration 6M, temperature 60°C, solid to liquid ratio 1:4

Leaching time (hrs)	%	%
4	13.4	14.8
6	16.2	17.6
8	16.5	15.3
10	17.1	15.7
12	15.8	14.5

Table B5 Aluminium concentration (ppm)

Conditions for acid leaching of CFA at different leaching temperatures:

acid concentration 6M, time 8hrs, solid to liquid ratio 1:4

Leaching temperature (°C)	ppm	ppm
30	1610	1859
45	2361	2210
60	2662	2468
75	3804	3479
80	3694	3626
85	3740	3526

Table B6 Aluminium extraction (%)

Conditions for acid leaching of CFA at different leaching temperatures:

acid concentration 6M, time 8hrs, solid to liquid ratio 1:4

Leaching temperature (°C)	%	%
30	10.0	11.5
45	14.6	13.7
60	16.5	15.3
75	23.5	21.5
80	22.9	22.4
85	23.1	21.8

Table B7 Aluminium concentration (ppm)

Conditions for acid leaching of CFA at different solid to liquid ratios:

acid concentration 6M, time 8hrs, temperature 60°C

Solid to liquid ratio	ppm	ppm
1:2	2430	2339
1:3	2484	2713
1:4	2662	2468
1:5	2617	2388
1:6	2399	2307

Table B8 Aluminium extraction (%)

Conditions for acid leaching of CFA at different solid to liquid ratios:

acid concentration 6M, time 8hrs, temperature 60°C

Solid to liquid ratio	%	%
1:2	15.0	14.5
1:3	15.4	16.8
1:4	16.5	15.3
1:5	16.2	14.8
1:6	14.8	14.3

APPENDIX C

IDENTIFICATION OF SIGNIFICANT FACTORS

Table C1 Aluminium concentration (ppm) for 2^4 full factorial design

Acid leaching conditions: agitation rate 150 rpm. The actual factor levels coded as values of (-1) and (+) in the table are as follows: A (Acid concentration): 4M (-1) and 8M (+1); B (Leaching time): 6hrs (-1) and 10hrs (+1); C (Leaching temp): 45^{o}C (-1) and 75^{o}C (+1); D (Solid: Liquid ratio): 1:3(-1) and 1:5(+1)

Std Runs	Control Factors				Replicate 1	Replicate 2
	A	B	C	D		
1	-1	-1	-1	-1	1893	1807
2	+1	-1	-1	-1	1658	1575
3	-1	+1	-1	-1	2176	2198
4	+1	+1	-1	-1	2260	1855
5	-1	-1	+1	-1	2658	2460
6	+1	-1	+1	-1	2614	2276
7	-1	+1	+1	-1	2910	3089
8	+1	+1	+1	-1	3277	3467
9	-1	-1	-1	+1	1839	1791
10	+1	-1	-1	+1	1941	1660
11	-1	+1	-1	+1	2161	2143
12	+1	+1	-1	+1	1893	1777
13	-1	-1	+1	+1	2874	2671
14	+1	-1	+1	+1	2101	2223
15	-1	+1	+1	+1	2804	3052
16	+1	+1	+1	+1	2927	2763

Table C2 Aluminium extraction (%) for 2^4 full factorial design

Acid leaching conditions: agitation rate 150 rpm. The actual factor levels coded as values of (-1) and (+) in the table are as follows: A (Acid concentration): 4M (-1) and 8M (+1); B (Leaching time): 6hrs (-1) and 10hrs (+1); C (Leaching temp): 45^{o}C (-1) and 75^{o}C (+1); D (Solid: Liquid ratio): 1:3(-1) and 1:5(+1)

Std Runs	Control Factors				Replicate 1	Replicate 2
	A	B	C	D		
1	-1	-1	-1	-1	11.7	11.2
2	+1	-1	-1	-1	10.3	9.8
3	-1	+1	-1	-1	13.5	13.6
4	+1	+1	-1	-1	14.0	11.5
5	-1	-1	+1	-1	16.4	15.2
6	+1	-1	+1	-1	16.2	14.0
7	-1	+1	+1	-1	18.0	19.1
8	+1	+1	+1	-1	20.3	21.5
9	-1	-1	-1	+1	11.4	11.1
10	+1	-1	-1	+1	12.0	10.3
11	-1	+1	-1	+1	13.4	13.3
12	+1	+1	-1	+1	11.7	11.0
13	-1	-1	+1	+1	17.8	16.5
14	+1	-1	+1	+1	13.0	13.7
15	-1	+1	+1	+1	17.3	18.9
16	+1	+1	+1	+1	18.1	17.1

Table C3 Aluminium concentration (ppm) for centre points design

Acid leaching conditions: agitation rate 150 rpm. The actual factor levels coded as values of (0) in the table are centre point values and are as follows: A (Acid concentration): 6M (0); B (Leaching time): 8hrs (0); C (Leaching temp): 60^{o}C (0); D (Solid: Liquid ratio): 1:4(0)

Run	Control Factors					
	A	B	C	D		
1	0	0	0	0	2265	2175
2	0	0	0	0	2468	2405
3	0	0	0	0	2304	2120
4	0	0	0	0	2441	2455
5	0	0	0	0	2229	2249
6	0	0	0	0	2402	2007

Table C4 Aluminium extraction (%) for centre points design

Acid leaching conditions: agitation rate 150 rpm. The actual factor levels coded as values of (0) in the table are centre point values and are as follows: A (Acid concentration): 6M (0); B (Leaching time): 8hrs (0); C (Leaching temp): 60^{o}C (0); D (Solid: Liquid ratio): 1:4(0)

Run	Control Factors				Replicates 1	Replicate 2
	A	B	C	D		
1	0	0	0	0	14.0	13.5
2	0	0	0	0	15.3	14.9
3	0	0	0	0	14.3	13.1
4	0	0	0	0	15.1	15.2
5	0	0	0	0	13.8	13.9
6	0	0	0	0	14.9	12.4

APPENDIX D

OPTIMIZATION OF SIGNIFICANT FACTORS

Table D1 Aluminium concentrations (ppm)
Acid leaching conditions: agitation rate 150 rpm. The actual factor levels coded as values of – λ, -1, 0, +1, + λ were as follows: for temperature, °C (A): 68 (- λ), 70 (-1), 75 (0), 80 (+1), 82 (+ λ); time, hrs (B): 7.34 (- λ), 7.75 (-1), 8.75 (0), 9.75 (+1), 10.16 (+ λ)

Standard Run	Coded		Replicate 1	Replicate 2
	A	B		
1	-1	-1	3244	3263
2	+1	-1	3626	3664
3	-1	+1	3359	3313
4	+1	+1	3784	3695
5	- λ	0	3210	3279
6	+ λ	0	3764	3602
7	0	- λ	3456	3409
8	0	+ λ	3540	3575
9	0	0	3522	3109
10	0	0	3526	3509
11	0	0	3568	3342
12	0	0	3490	3295
13	0	0	3506	3432

Table D2 Aluminium extractions (%)
Acid leaching conditions: agitation rate 150 rpm. The actual factor levels coded as values of – λ, -1, 0, +1, + λ were as follows: for temperature, °C (A): 68 (- λ), 70 (-1), 75 (0), 80 (+1), 82 (+ λ); time, hrs (B): 7.34 (- λ), 7.75 (-1), 8.75 (0), 9.75 (+1), 10.16 (+ λ)

Standard Run	Coded		Replicate 1	Replicate 2
	A	B		
1	-1	-1	20.1	20.2
2	+1	-1	22.5	22.7
3	-1	+1	20.8	20.5
4	+1	+1	23.4	22.9
5	- λ	0	19.9	20.3
6	+ λ	0	23.3	22.3
7	0	- λ	21.4	21.1
8	0	+ λ	21.9	22.1
9	0	0	21.8	19.3
10	0	0	21.8	21.7
11	0	0	22.1	20.7
12	0	0	21.6	20.4
13	0	0	21.7	21.3

Table D3 Confirmatory tests

Acid Leaching conditions: acid concentration 6M, leaching time 10.16hrs, temperature 82°C, solid to liquid ratio 1:4. Agitation rate 150 rpm.

Aluminium concentrations (ppm)

Run	
1	3888
2	4140
3	4063
4	3994

Aluminium extractions (%)

Run	
1	24.1
2	25.5
3	25.1
4	24.6
Avg.	24.8

APPENDIX E

POST-SINTER LEACHING

Table E1 Aluminium concentrations (ppm)

Conditions for post-sinter leaching of CFA:

acid concentration 6M, temperature 82°C, solid to liquid ratio 1:4

Leaching time (hrs)	ppm	ppm
10.2	13623	13350

Table E2 Aluminium extractions (%)

Conditions for post-sinter leaching of CFA:

acid concentration 6M, temperature 82°C, solid to liquid ratio 1:4

Leaching time (hrs)	%	%
10.2	84.3	82.6

CFA - XRD Analysis Results

Table E3 Raw CFA before pre-sinter (first stage) leaching

		AS104
Amorphous	52.9	*1.59*
Hematite	0.8	*0.27*
Magnetite	1.65	*0.21*
Mullite	30.68	*1.29*
Quartz	13.97	*0.84*

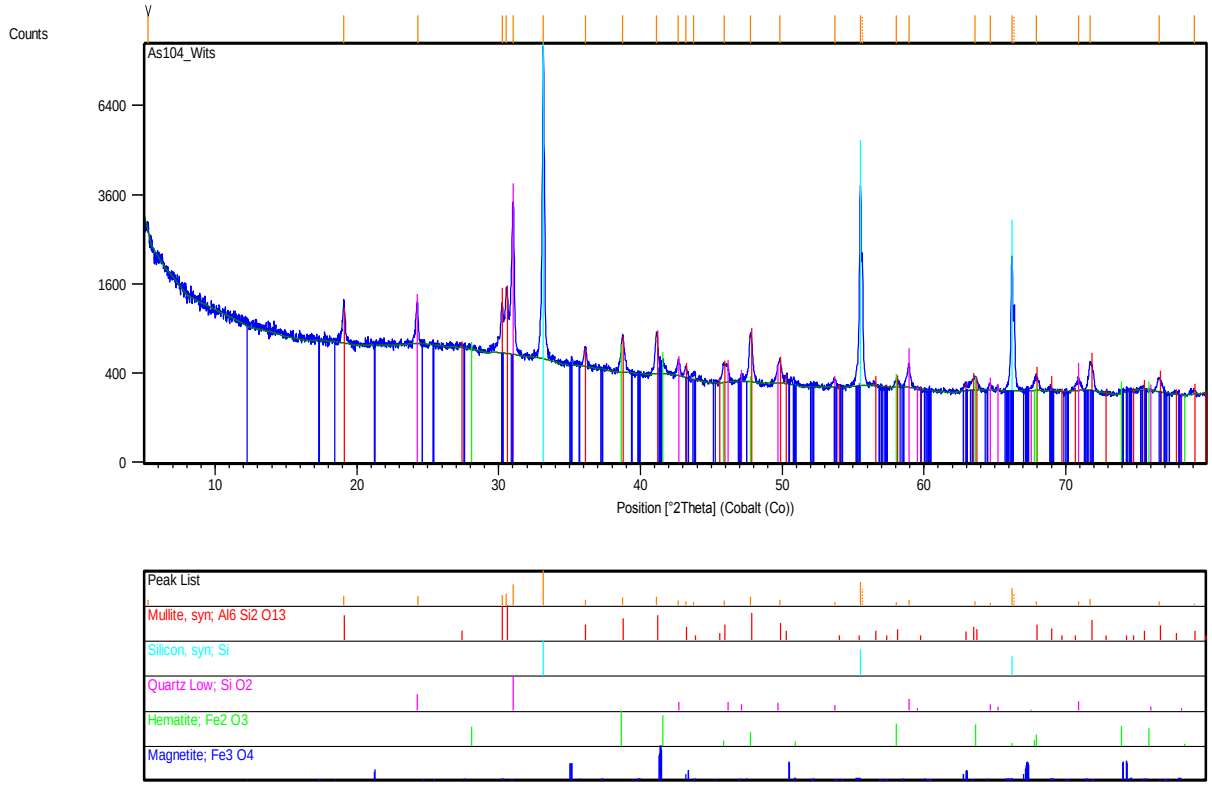

Figure E1. X-Ray Diffractogram of raw-CFA before first stage leaching

Table E4 Raw-CFA after pre-sinter (first stage) leaching

	AS105
Amorphous	58.49
Anhydrite	7.12
Mullite	23.94
Quartz	10.45

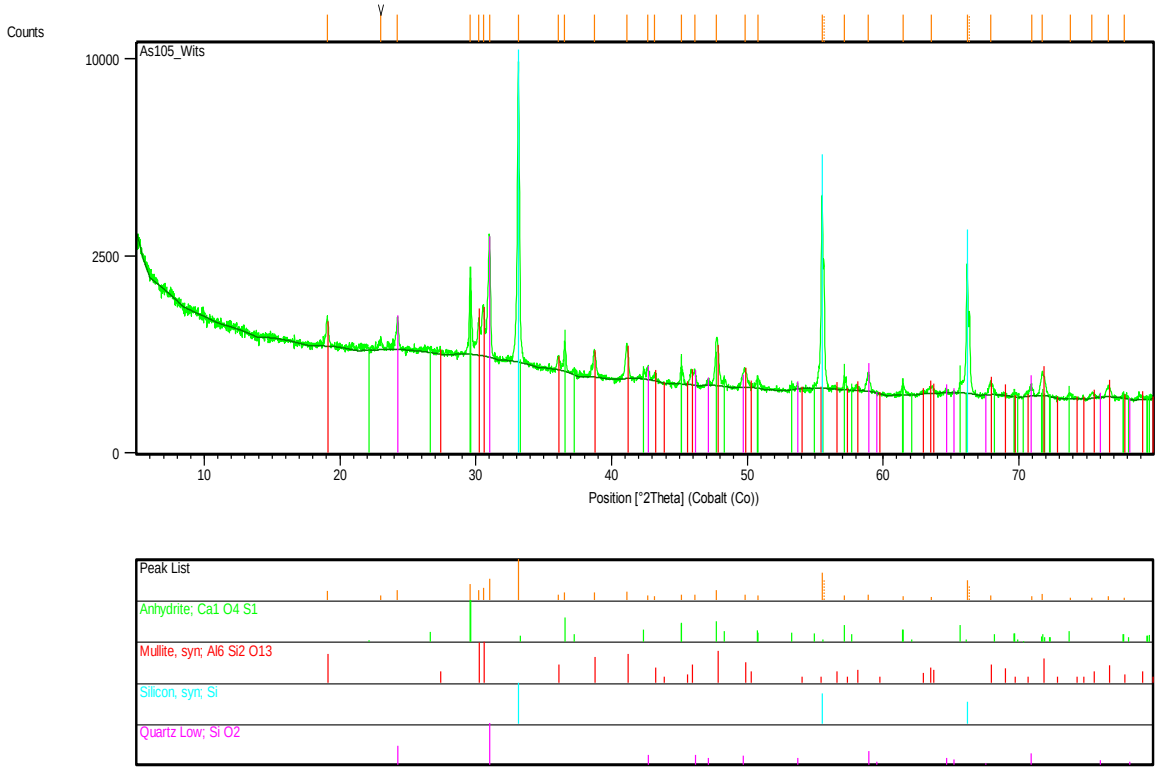

Figure E2. X-Ray Diffractogram of raw-CFA after first stage leaching

Table E5 Sintered residue-CFA Before post-sinter (second stage) leaching

		AS130
Amorphous	23.03	1.89
Anhydrite	0.22	0.1
Cristobalite	8.07	1.41
Mullite	8.02	0.66
Plagioclase	54.07	1.08
Quartz	6.6	0.36

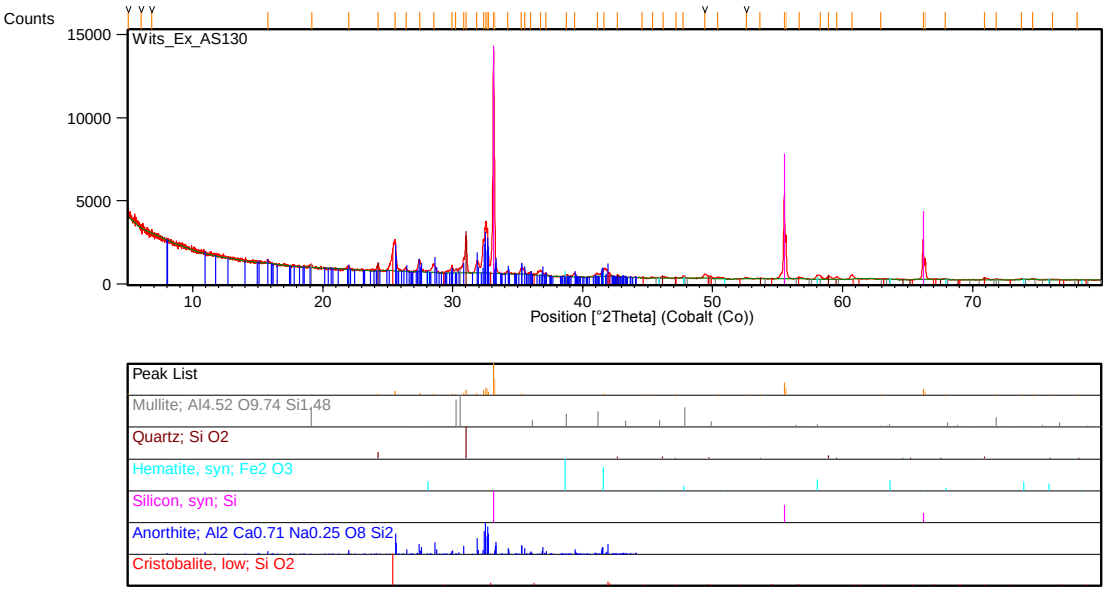

Figure E3. X-Ray Diffractogram of sintered residue-CFA before second stage leaching

Table E6 Sintered residue-CFA after post-sinter (second stage) leaching

	AS129	
Amorphous	52.91	1.11
Anhydrite	23.18	0.42
Calcite	0.26	0.15
Cristobalite	4.68	0.78
Gypsum	2.89	0.28
Mullite	8.98	0.6
Quartz	7.09	0.33

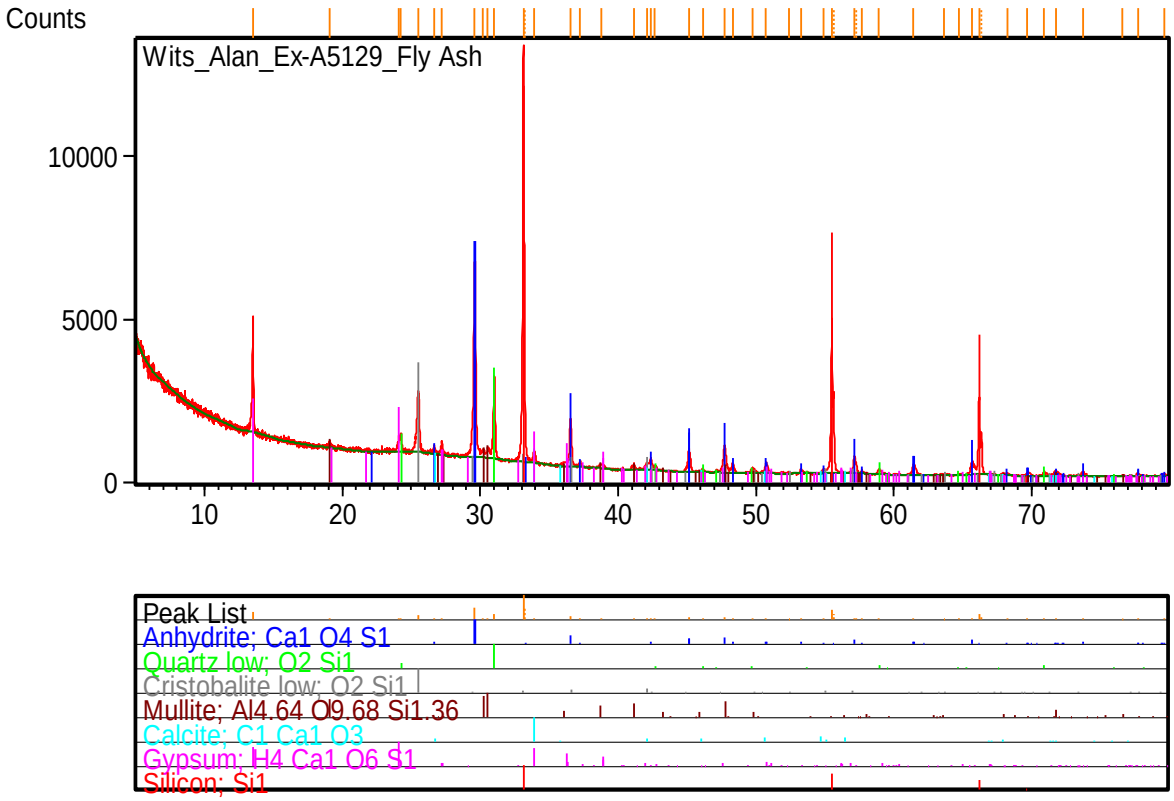

Figure E4. X-Ray Diffractogram of sintered residue-CFA after second stage leaching

Calcium sulphate content in leached raw-CFA (Tables E7 – E12)

Table E7

Ex_AS_367			Ex_AS_369			Ex_AS_384		
Amorphous	48.44	0.93	**Alunogen**	4.51	0.57	**Amorphous**	46.56	0.99
Anhydrite	6.93	0.33	**Amorphous**	44.25	1.11	**Anhydrite**	0.29	0.18
Gypsum	1.56	0.3	**Anhydrite**	6.35	0.3	**Gypsum**	6.33	0.3
Mullite	30.35	0.66	**Gypsum**	0.71	0.22	**Mullite**	33.07	0.78
Quartz	12.72	0.42	**Mullite**	28.95	0.63	**Quartz**	13.75	0.45
			Pyrophyllite	2.88	0.48			
			Quartz	12.36	0.39			

Table E8

Ex_AS_385			Ex_AS_386			Ex_AS_387		
Amorphous	47.44	1.02	**Amorphous**	49.2	0.99	**Amorphous**	45.98	0.99
Anhydrite	2.92	0.33	**Anhydrite**	0.95	0.21	**Anhydrite**	0.5	0.21
Gypsum	2.69	0.24	**Gypsum**	3.72	0.25	**Gypsum**	4.43	0.27
Mullite	32.91	0.75	**Mullite**	31.79	0.75	**Mullite**	34.01	0.78
Quartz	14.05	0.45	**Quartz**	14.34	0.42	**Quartz**	15.08	0.45

Table E9

Ex_AS_388			Ex_AS_431			Ex_AS_432		
Amorphous	48.34	0.9	**Amorphous**	50.36	1.02	**Amorphous**	49.68	0.99
Anhydrite	0.39	0.15	**Anhydrite**	0.14	0.1	**Anhydrite**	0.21	0.14
Gypsum	4.48	0.26	**Gypsum**	5.15	0.28	**Gypsum**	5.46	0.27
Mullite	32.51	0.69	**Mullite**	31.04	0.81	**Mullite**	31.64	0.78
Quartz	14.28	0.42	**Quartz**	13.31	0.48	**Quartz**	13.01	0.45

Table E10

Ex_AS_433			Ex_AS_435			Ex_AS_488		
Amorphous	49.35	1.02	**Amorphous**	45.79	0.96	**Amorphous**	48.2	1.02
Anhydrite	0.18	0.15	**Anhydrite**	2.21	0.19	**Anhydrite**	3.96	0.3
Gypsum	4.55	0.27	**Gypsum**	5.17	0.26	**Gypsum**	3.54	0.24
Mullite	32.14	0.78	**Mullite**	32.53	0.72	**Mullite**	31.11	0.75
Quartz	13.78	0.45	**Quartz**	14.31	0.42	**Quartz**	13.2	0.42

Table E11

Ex_AS_489			Ex_AS_490			Ex_AS_491		
Amorphous	49.43	0.99	**Alunogen**	3.55	0.45	**Amorphous**	52.48	2.97
Anhydrite	4.81	0.33	**Amorphous**	41.21	2.1	**Anhydrite**	5.93	0.36
Gypsum	2.91	0.23	**Anhydrite**	5.56	0.36	**Gypsum**	1.02	2.76
Mullite	30.24	0.72	**Gypsum**	4.36	1.77	**Mullite**	26.19	0.69
Quartz	12.61	0.42	**Mullite**	29.73	0.72	**Pyrophyllite**	4.13	0.66
			Pyrophyllite	3.31	0.45	**Quartz**	10.25	0.42
			Quartz	12.27	0.42			

Table E12

Ex_AS_492		
Alunogen	4.33	0.48
Amorphous	46.5	17.7
Anhydrite	5.5	0.33
Gypsum	1.3	17.7
Mullite	27.53	0.69
Pyrophyllite	3.85	0.6
Quartz	10.95	0.42